ENG 408

408 - Seismic performance evaluations and design of timber-steel hybrid shear wall systems for mid-rise light timber framed buildings (EQC funded project 16/716)

Minghao Li, University of Canterbury

June 2018

ENG 408

Final report for EQC biennial research grant (contract no. 16/716)

Seismic Performance Evaluations and Design of Timber-steel Hybrid Shear Wall Systems for Mid-rise Light Timber Framed Buildings

Minghao Li[1], Wenchen Dong[2], Darren Kho[3], Chin-Long Lee[4], Minjuan He[5], and Zheng Li[6]

Abstract

This project presents seismic performance evaluations and design of a type of timber-steel hybrid shear wall system consisting of steel moment frames infilled with light timber framed shear walls. This hybrid system can be easily incorporated into multi-storey light timber framed (LTF) buildings and the construction materials are readily available in New Zealand. A finite element (FE) model of the hybrid wall system was developed with its critical input parameters calibrated by a connection test database of nailed plywood-timber connections and bolted and screwed timber-steel interface connections. The FE hybrid wall model was validated against existing hybrid wall testing data. The validated model was used to run a parametric study to establish a hysteresis database of the hybrid walls with various design configurations in terms of steel member sizes, nail sizes, and plywood thickness. Aligned with another project funded by National Natural Science Foundation of China, a shake table test on a 4-storey 2/3 scale hybrid structure was conducted to study its dynamic behavior under strong ground shakings including the 2011 Canterbury earthquake. The experimental results showed excellent seismic performance of the timber-steel hybrid structure. Finally, a design example of the hybrid wall systems in a 6-storey LTF building was presented following the displacement-based seismic design flowchart.

Key words: timber-steel hybrid structures; seismic design; timber connections; shear wall modelling, shake table test

[1] Senior Lecturer, University of Canterbury, New Zealand, minghao.li@canterbury.ac.nz
[2] PhD student, University of Canterbury, New Zealand, wenchen.dong@pg.canterbury.ac.nz
[3] M. Eng. student, University of Canterbury, New Zealand, darrenkho09@gmail.com
[4] Senior Lecturer, University of Canterbury, New Zealand, chin-long.lee@canterbury.ac.nz
[5] Professor, Tongji University, China, hemj@tongji.edu.cn
[6] Associate Professor, Tongji University, China, zhengli@tongji.edu.cn

Table of Contents

1. Introduction

In New Zealand, bracing walls sheathed with gypsum plaster boards are typically used to resist wind and seismic loads in low-rise light timber framed (LTF) houses according to NZS3604 (2011). Plywood shear walls are used for cases where high bracing demands are needed, for example, in multi-storey timber buildings. However, plywood shear walls may reach their capacity limitation when seismic loads are high and no sufficient walls can be designed as shear walls. Therefore, timber-steel hybrid structures may provide an alternative solution with enhanced strength and stiffness. In recent years, timber-steel hybrid structures have attracted a lot of research interests in order to overcome the limitation of conventional timber shear wall systems. Dickof et al. (2012) introduced a timber-steel hybrid system consisting of steel frames with infilled cross laminated timber (CLT) panels. He et al. (2014) introduced another type of timber-steel hybrid system consisting of steel moment frames with infilled oriented strand board (OSB) shear walls. Experimental studies and numerical modeling were conducted to study its loading sharing mechanism, critical design parameters and seismic performance (Li, et al. 2014; 2015; and 2017).

This project investigates the seismic performance of a type of timber-steel hybrid solution consisting of steel moment frames infilled with LTF shear walls sheathed by wood-based structural panels such as plywood or oriental strand board (OSB), as shown in Figure 1. A detailed finite element based hybrid wall model is developed with its critical input parameters calibrated by connection component testing of nailed plywood-timber connections and bolted timber-steel interface connections adopted by the hybrid system. The wall model is validated by existing hybrid shear wall test data. The validated model is then used to develop a database of the cyclic response of the hybrid wall systems with various wall configurations and design capacities. The influence of steel member sizes, nail sizes, and plywood thicknesses on the overall hybrid wall performance was investigated. Critical shear wall design properties, such as strength, stiffness, and ductility, are assessed. A shake table test on a 4-storey 2/3 scale hybrid structure was also conducted to study its seismic performance under strong ground shakings including the 2011 Canterbury earthquakes. Finally, a displacement based seismic design methodology and a design example is further presented for the application of the hybrid system in multi-storey timber buildings.

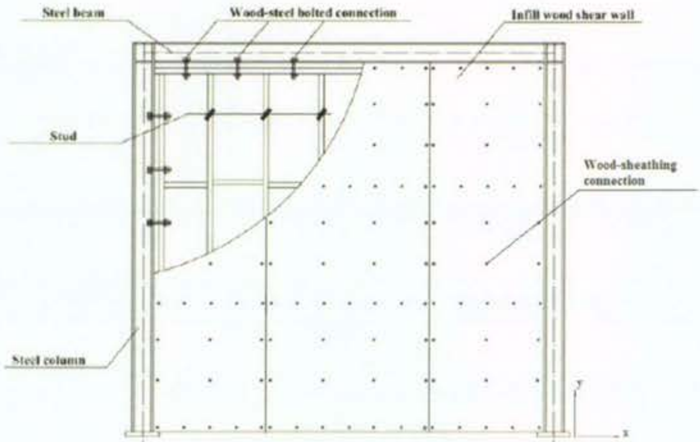

Figure 1: Typical timber-steel hybrid wall configuration

2. Hybrid Wall Modelling & Validation

A detailed FE model of a timber-steel hybrid shear wall structure was developed in ABAQUS software package (ABAQUS SIMULIA, 2011). As shown in Figure 1, it consists of three types of elements to model the components in the hybrid wall system: beam elements for timber and steel framing members, panel elements for plywood/OSB sheathing and spring elements for the timber-sheathing connections and timber-steel interface connections.

2.1 Hybrid wall modelling

Steel and timber framing members were modelled by B21 elements in the ABAQUS element library. Steel properties were assumed to be elastic-perfectly plastic. The steel beam-column joints were modelled as rigid connections so that the steel frames are treated as ductile moment resisting frames (MRF). The column supports were assumed to be semi-rigid with its rotational spring stiffness calibrated by existing experimental data. Wood-based sheathing panels were modelled by CPS4R elements. The in-plane elastic moduli for plywood/OSB were taken for both directions (parallel and perpendicular to face grain). All wood material properties assumed to be elastic.

The nonlinear behavior of the hybrid shear walls is mainly governed by the critical connections (mainly the nailed timber-sheathing connections) and the steel MRF yielding. Therefore, it is important to incorporate robust connection elements. For these connections, user defined nonlinear spring elements were used. Their hysteric behavior was calibrated by an experimental testing program on a group of timber-steel and timber-sheathing connections. Non-critical connections such as the connections between timber framing members were simply assumed as pinned. As shown in Figure 2, Q-pinch hysteretic algorithm, proposed by Folz and Filiatrault (2001), was used to model the hysteretic behavior of the critical connections. The Q-pinch model needs to calibrate a series of K factors to fit the experimental load-slip curves. The loading, unloading, and reloading rules also need to be clearly defined to form the connection hysteresis. For timber shear walls under racking loads, nail fasteners tend to deform along different directions, and will not be restricted to only horizontal or vertical movement. Therefore, the oriented spring pairs proposed by Judd (2005) were used to model the coupling behavior of the nailed connections along the primary slip direction and the perpendicular to the primary slip direction.

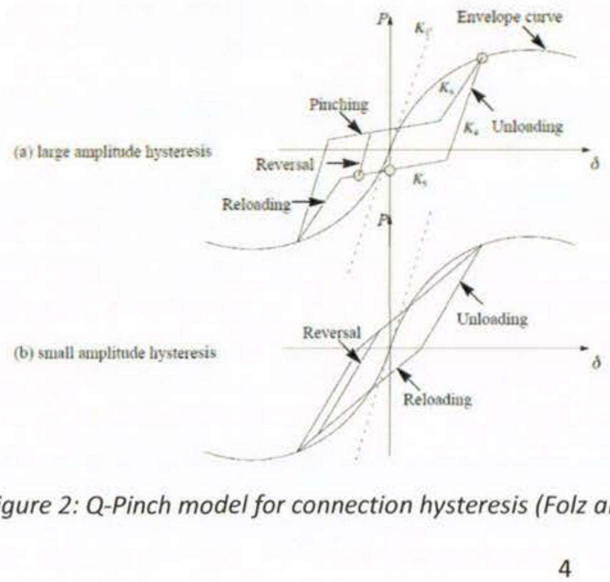

Figure 2: Q-Pinch model for connection hysteresis (Folz and Filiatrault, 2001)

For the bolted timber-steel interface connections, Li et al (2015) suggested that these connections should be strong enough to transfer the loads between the steel frames and the infill walls. Any premature failure should be avoided. These connections only deform in lateral and axial directions. Thus, for simplicity, non-oriented (uncoupled) spring pairs were adopted to represent the connection behavior under shear loading and axial loading. The Q-pinch algorithm was also used to model the behavior under lateral loads. Elastic springs were used to model the connection behavior under axial loads.

2.2 Hybrid wall model validation

Experimental results of a hybrid shear wall consisting of a steel moment frame and an infill OSB shear wall were used to validate the hybrid shear wall model. Detailed information about the hybrid wall testing program was reported by Dong (2017). The model input parameters for the critical connections were also calibrated by the experimental testing of nailed timber-OSB connections, bolted timber-steel interface connections and base connections of the steel columns. Figure 3 shows the tested wall configuration. Figure 4 shows the FE hybrid wall model and the comparison between the experimental load-drift hysteresis and the model simulation results. It can be seen that the model agreed well with the test results.

Figure 3: Hybrid wall test setup (Dong, 2017)

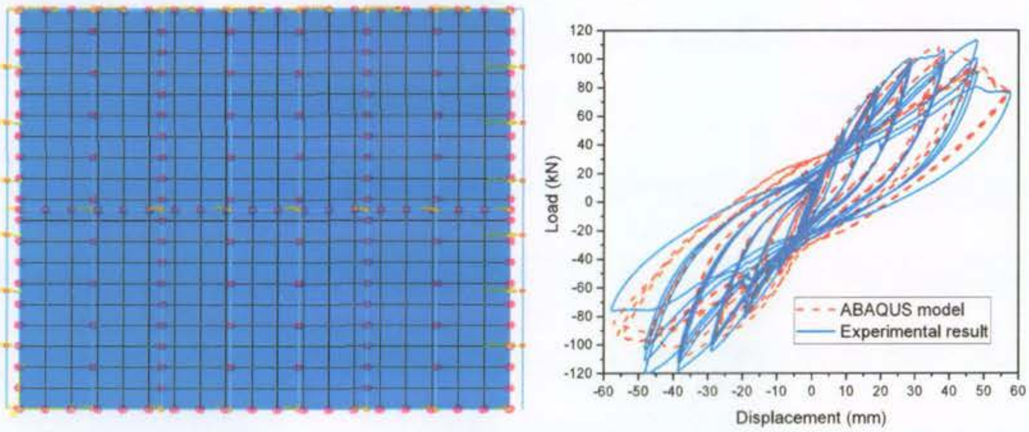

Figure 4: Experimental hysteresis curves vs. ABAQUS model simulation

3. Experimental Testing of Critical Connections

In New Zealand, OSB is not typically used in timber construction. Instead, plasterboards and plywood are commonly used. To apply the hybrid system in New Zealand, there is a need to establish a test database for nailed timber-plywood connections and steel-timber interface connections which are the critical connection types in the timber-steel hybrid walls. Following the ISO16670 (2003) standard, 176 nailed timber-plywood connections, 44 screwed timber-steel interface connections and 44 bolted timber-steel interface connections were tested. All the timber members and plywood were made out of NZ grown Radiata pine and graded following New Zealand standards NZS 1748 (2011) and NZS 2269 (2012). Table 1 and Table 2 give the test matrices in which five replicates were tested under monotonic loading and six were tested under cyclic loading. For the nailed connections, three nail sizes (ϕ2.8x50mm, ϕ3.15x75mm, and ϕ3.55x90mm) and three plywood thicknesses (12mm, 17mm, and 25mm) were considered. Two loading orientations for timber (parallel to grain and perpendicular to grain) were considered as well. For the bolted and screwed timber-steel interface connections, the timber members were loaded parallel to the grain direction with bolts (M10 and M12) and coach screws (M10 and M12) respectively.

Table 1 Test matrix of bolted and screwed timber-steel interface connections.

Fasteners (timber-steel interface)	Thread	Double Studs		Triple Studs	
		Mono	Cyclic	Mono	Cyclic
4.6 Bolts	M10	x5	x6	x5	x6
	M12	x5	x6	x5	x6
4.6 Coach screws	M10	x5	x6	x5	x6
	M12	x5	x6	x5	x6

Table 2 Test matrix of nailed timber-plywood connections

Nail size (diameter x length, mm)	Parallel to grain						Perpendicular to grain					
	Mono			Cyclic			Mono			Cyclic		
	Plywood thickness (mm)			Plywood thickness (mm)			Plywood thickness (mm)			Plywood thickness (mm)		
	12	17	25	12	17	25	12	17	25	12	17	25
ϕ2.8 x 60	x5	x5	n.a.	x6	x6	n.a.	x5	x5	n.a.	x6	x6	n.a.
ϕ3.15 x 75	x5	x5	x5	x6	x6	x6	x5	x5	x5	x6	x6	x6
ϕ3.55 x 90	x5	x5	x5	x6	x6	x6	x5	x5	x5	x6	x6	x6

3.1 Steel-timber Interface Connections

Figure 5 shows the test setup of the timber-steel interface connections. A 10mm thick steel plate was used as the flange of steel H beams or column to connect the boundary timber framing members of the infill wall. The test also considered the influence of the number of the timber studs on the connection behavior. Figure 6 shows the average monotonic load-slip curves of the connections. It was found that the bolted connections had higher capacity and stiffness than the screwed connections under the same test setup due to the rope effect. Figure 7 also shows the typical failure mode. Significant fastener yielding and wood embedment crushing were observed, also indicating good ductility of these interface connections.

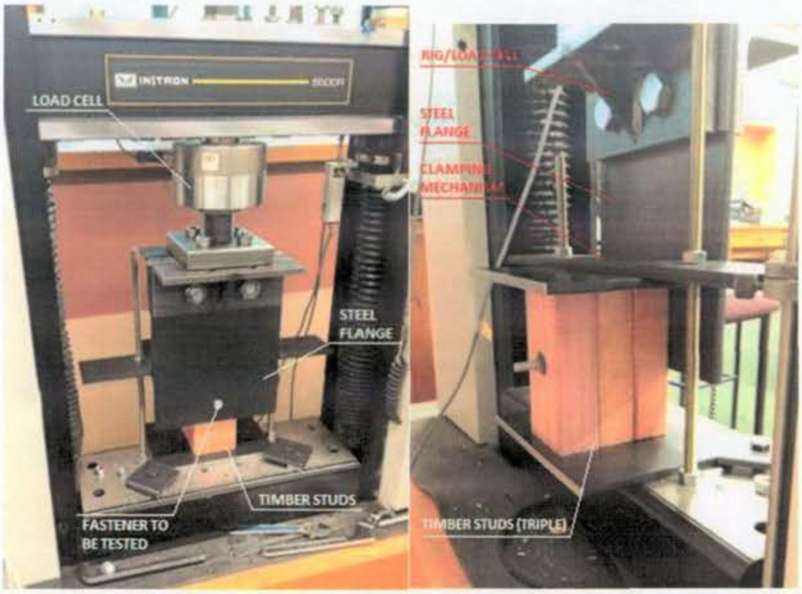

Figure 5: Test setup for Timber-Steel interface connections (front view and side view)

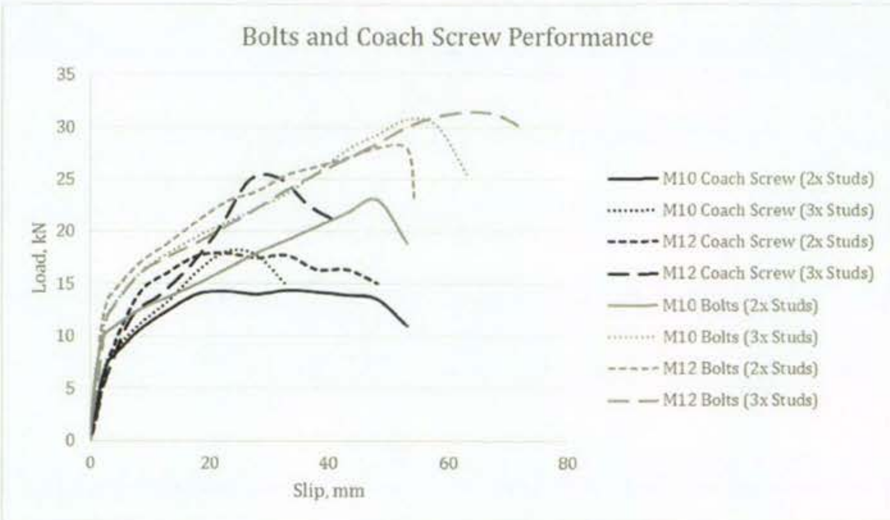

Figure 6: Average monotonic load-slip curves of bolted and screwed interface connections

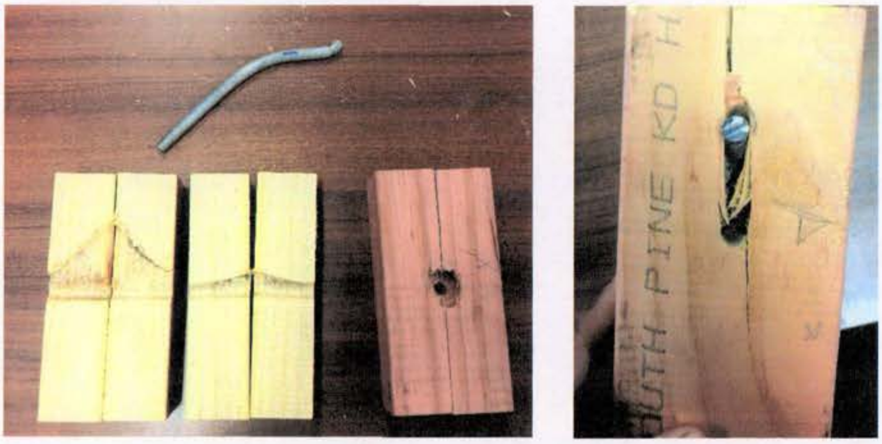

Figure 7: Typical failure mode of the screwed and bolted connections

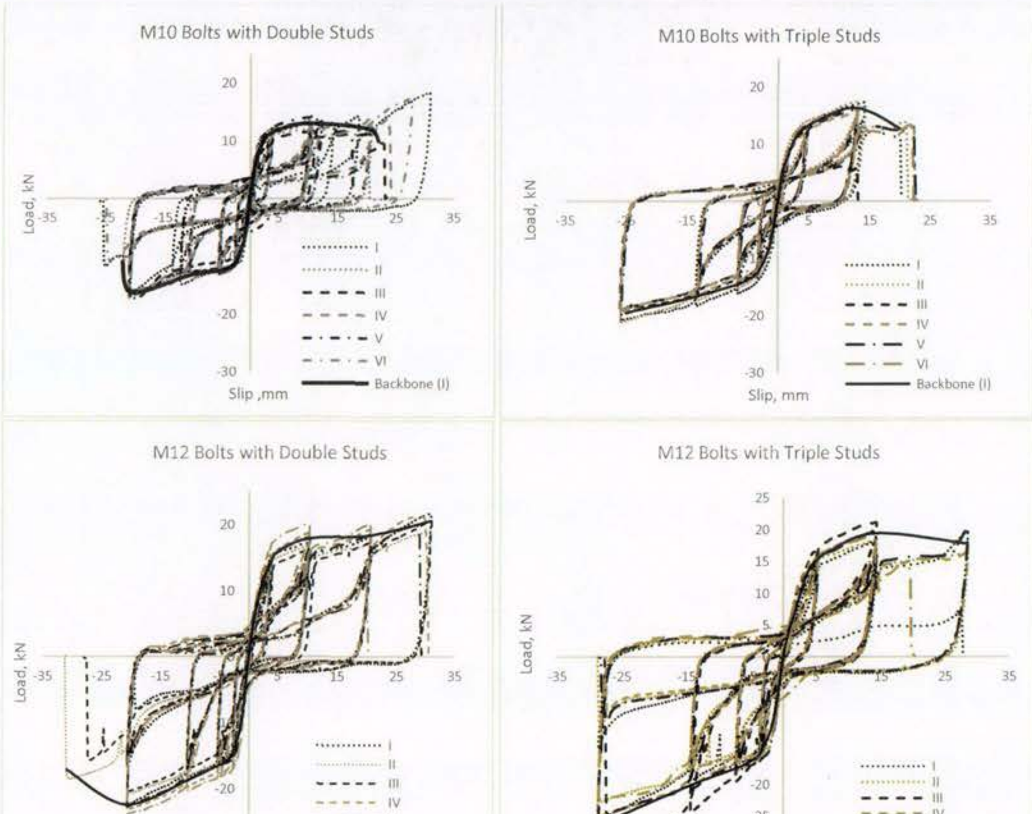

Figure 8: Hysteresis and average backbone curves of bolted connections under cyclic loading

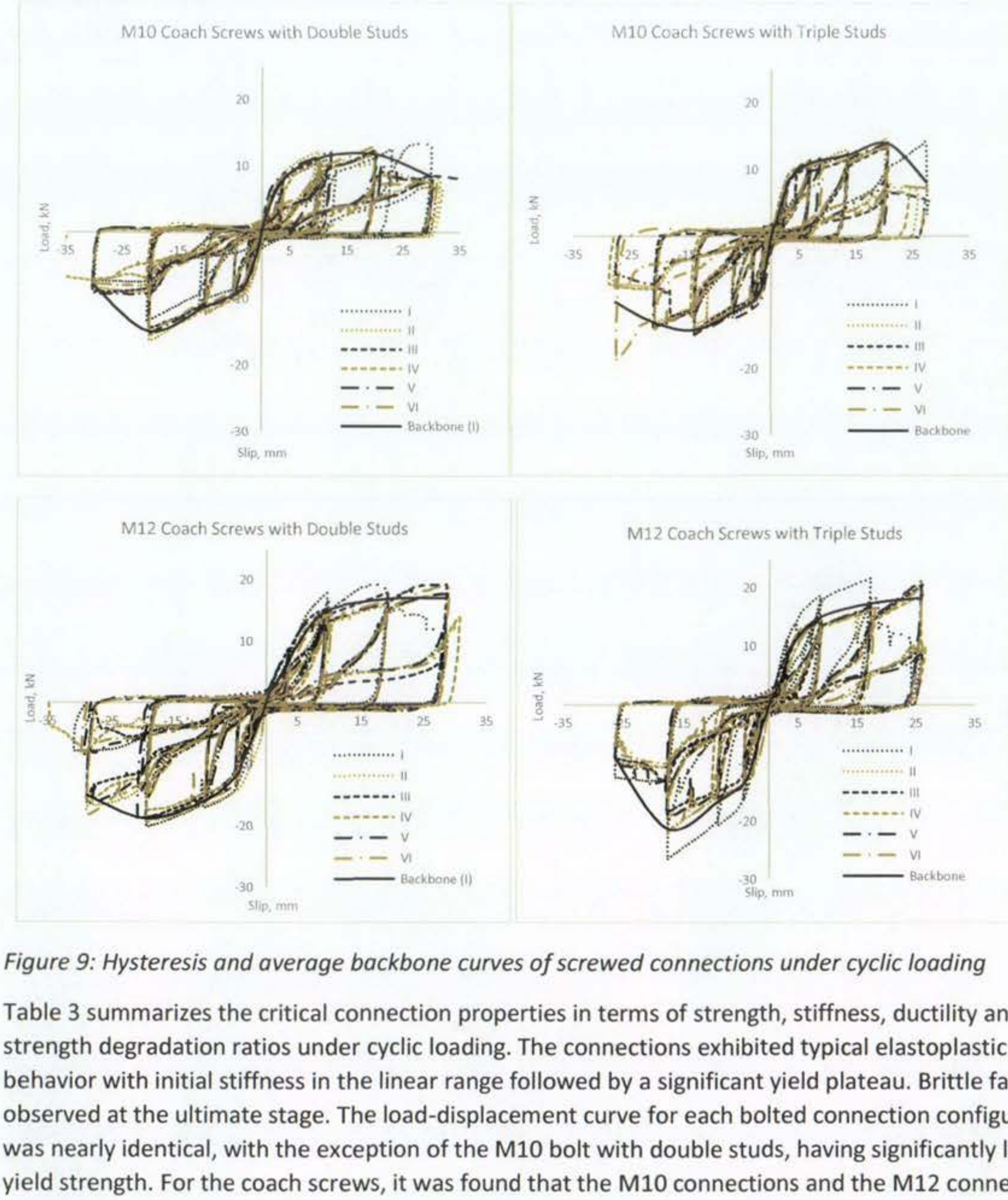

Figure 9: Hysteresis and average backbone curves of screwed connections under cyclic loading

Table 3 summarizes the critical connection properties in terms of strength, stiffness, ductility and strength degradation ratios under cyclic loading. The connections exhibited typical elastoplastic behavior with initial stiffness in the linear range followed by a significant yield plateau. Brittle failure was observed at the ultimate stage. The load-displacement curve for each bolted connection configuration was nearly identical, with the exception of the M10 bolt with double studs, having significantly lower yield strength. For the coach screws, it was found that the M10 connections and the M12 connection had slightly different behavior. The M10 connections showed larger ultimate deformations but lower peak loads.

In the bolted connections, bolt sizes (M10 or M12) showed a positive correlation with the connection capacities. The M12 connections had 11.7 – 40.4% higher peak loads than the M10 connections. Yield displacement (Δ_y), ductilty (μ) and initial stiffness (k_i) of the bolted connection was a function of both bolt size and the number of timber studs. The connections with double studs had 15.6 – 26.7% smaller yield displacements when increasing thread size from M10 to M12. Increasing bolt size from M10 to M12 also reduced the ductility factors by 38.7%. However, for the connections with triple studs, the increased bolt size lead to the increase of the yield displacements by 31.7-34.8% and ductility by 22.5%.

In the coach screwed connections, it was found that the screw size (M10 or M12) and number of timber studs had positive correlation on peak load (F_{max}) and yield displacements (Δ_y). The M12 connections had 18.8 to 56.0% higher peak loads (F_{max}) than the M10 connections, and had 62.0 to 93.9% larger yield displacements (Δ_y). However, the screw size had negative correlation with the connection initial stiffness (k_i), The increase of screw size from M10 to M12 led to substantial drop of the initial stiffness by 22.2-87.5%.

It was also found that under cyclic loading, the connection ductility was significantly lower than the monotonic ductility, indicating the significant influence of the loading protocol on the connection behavior. However, the connection strength values were comparable under cyclic loading and monotonic loading. In general, the bolted connections had higher peak loads, initial stiffness and ductility than the coach screwed connections. Compared with the screwed connections, the bolted connections had 10 - 76% larger peak loads, 6.7 – 107% higher initial stiffness and up to 2.5 times larger ductility factors. Strength degradation properties for bolted and coach screwed connections were very similar. Therefore, the bolted connections performed better and will be able to provide a better option for the steel-timber interface connections.

Table 3 Critical properties of bolted connections

	M10 Bolts				**M12 Bolts**			
	Double Studs		**Triple Studs**		**Double Studs**		**Triple Studs**	
	Mono	**Cyclic**	**Mono**	**Cyclic**	**Mono**	**Cyclic**	**Mono**	**Cyclic**
k_i (kN/mm)	3.8	6.0	3.2	5.3	5.6	6.1	3.1	4.7
F_y (kN)	9.4	9.3	9.5	10.1	13.2	14.0	12.6	13.2
F_{max} (kN)	25.7	15.9	26.8	18.0	28.7	21.4	31.5	22.3
F_{ult} (kN)	22.7	14.3	23.9	15.6	27.1	19.8	29.8	16.9
Δ_y (mm)	3.2	1.6	3.1	2.2	2.7	2.9	3.0	4.1
Δ_{max} (mm)	61.2	21.8	49.7	19.5	46.2	24.6	67.0	24.7
Δ_{ult} (mm)	70.5	23.0	54.3	23.0	51.3	26.0	71.5	27.5
μ	31.0	15.0	20.0	11.0	19.0	9.3	25.8	9.6
$F_{(1-3)}$	-	47.9 - 92.5%	-	56.0 - 73.2%	-	59.7 - 88.3%	-	46.6 - 79.2%

Note: k_i = initial stiffness
F_y = yield strength,
F_{max} = maximum strength,
F_{ult} = ultimate strength, taken as $0.8F_{max}$ or is equal to F_{max} if a brittle failure is observed
Δ_y = yield displacement, corresponding to F_y
Δ_{max} = maximum displacement, corresponding to F_{max}
Δ_{ult} = ultimate displacement corresponding to F_{ult}.
μ = ductility ratio
$F_{(1-3\%)}$ = strength degradation ratio

Table 4 Critical properties of coach screwed connections

	M10 Coach Screws				M12 Coach Screws			
	Double Studs		Triple Studs		Double Studs		Triple Studs	
	Mono	Cyclic	Mono	Cyclic	Mono	Cyclic	Mono	Cyclic
k_i (kN/mm)	3.3	2.8	3.0	3.4	2.7	2.2	1.6	3.2
F_y (kN)	7.5	7.4	8.5	8.0	11.7	12.1	10.1	11.4
F_{max} (kN)	14.6	13.8	18.6	14.5	18.2	18.7	25.8	20.9
F_{ult} (kN)	11.7	8.2	14.9	10.4	14.6	12.4	20.6	10.1
Δ_y (mm)	2.9	2.9	3.3	2.4	4.7	5.8	6.4	3.8
Δ_{max} (mm)	28.6	19.3	24.9	20.0	26.1	23.0	30.5	20.9
Δ_{ult} (mm)	53.9	31.1	33.5	24.9	48.1	28.7	43.3	26.0
μ	19.0	11.8	10.3	11.1	10.4	5.4	7.0	7.2
$F_{(1-3)}$	-	41.4 - 61.7%	-	33.6 - 65.6%	-	29.6 - 74.1%	-	35.1 - 73.1%

Note: k_i = initial stiffness

F_y = yield strength,

F_{max} = maximum strength,

F_{ult} = ultimate strength, taken as $0.8F_{max}$ or is equal to F_{max} if a brittle failure is observed

Δ_y = yield displacement, corresponding to F_y

Δ_{max} = maximum displacement, corresponding to F_{max}

Δ_{ult} = ultimate displacement corresponding to F_{ult}.

μ = ductility ratio

$F_{(1-3\%)}$ = strength degradation ratio

3.2 Nailed Timber-plywood Connections

Figure 10 shows the test setup of the nailed timber-plywood connections. Figure 11 shows the average monotonic load-slip curves. Figure 12 and Figure 13 show the cyclic load-slip curves as well as the positive and negative average envelope (or backbone) curves of the hysteresis loops.

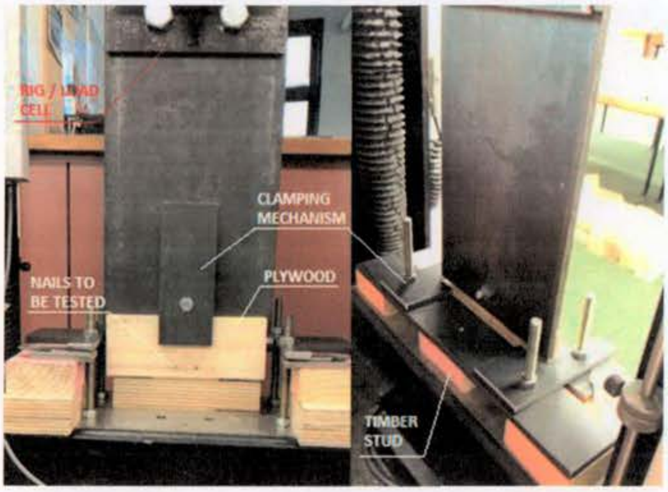

Figure 10: Load-displacement hysteresis of bolted and nailed connections

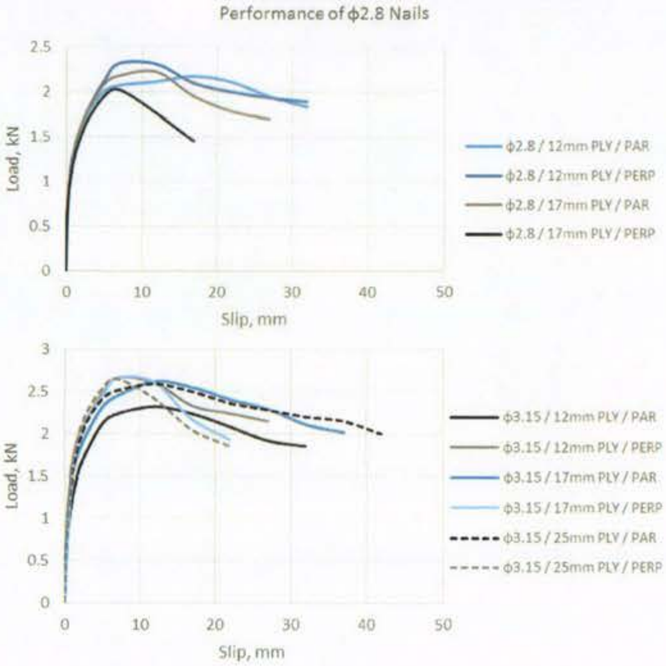

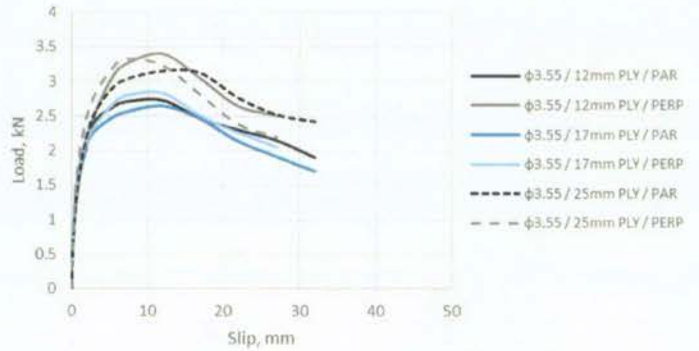

Figure 11: Average monotonic load-slip curves of the nailed connections (with two nails)

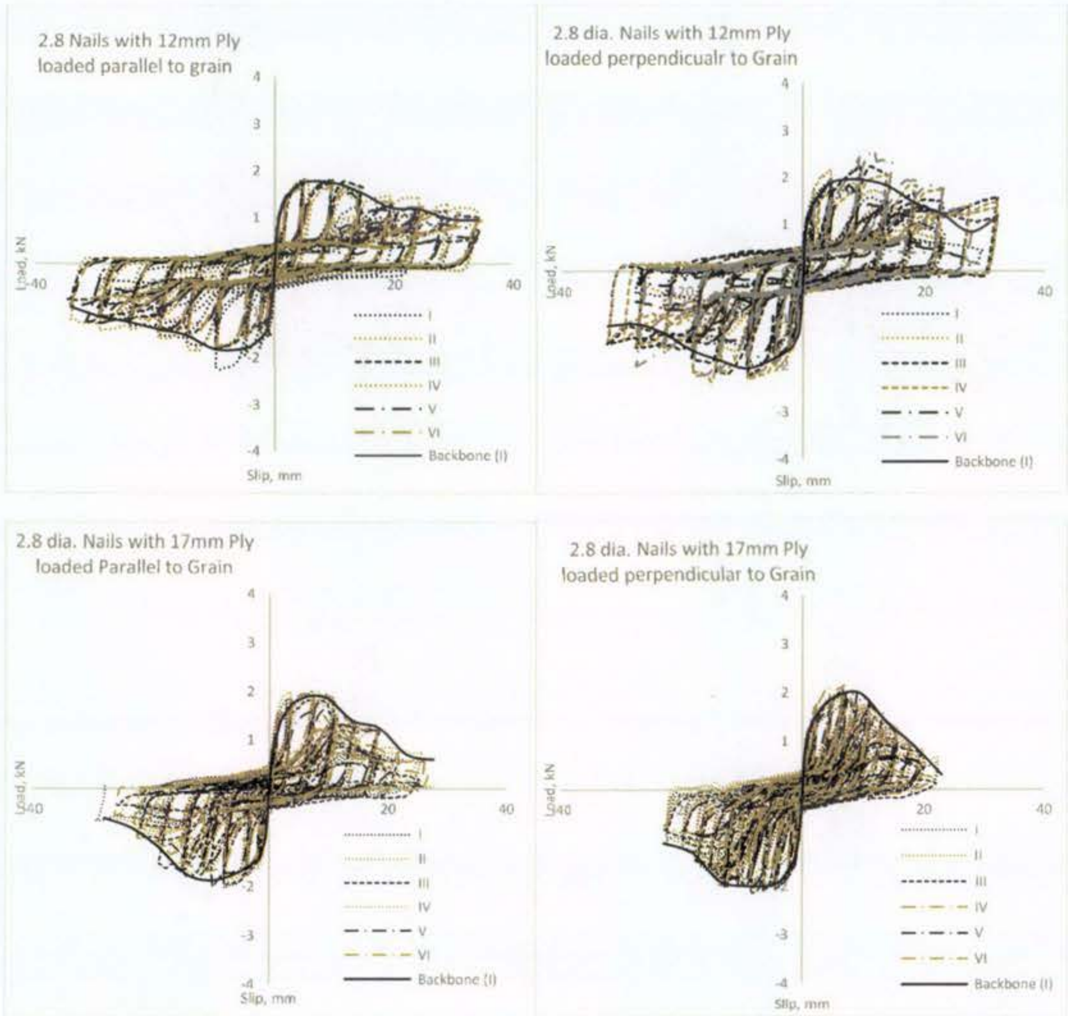

Figure 12: Hysteresis curves for φ2.8 Nails with varying plywood thickness (with two nails)

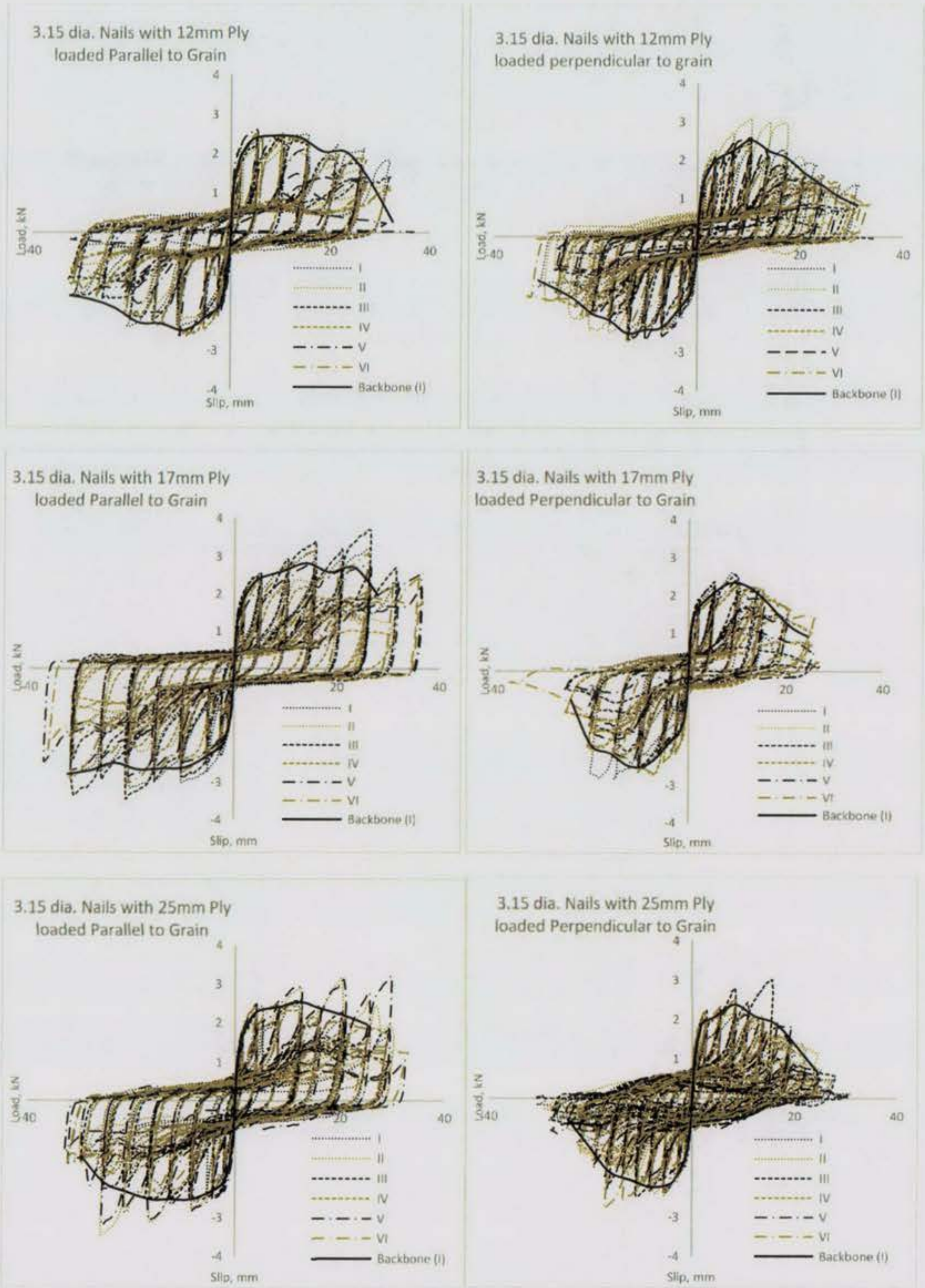

Figure 13: Hysteresis curves for φ3.15 Nails with varying plywood thickness (with two nails)

The connection properties in terms of strength, stiffness, ductility under monotonic and cyclic loading are summarized in Table 5-Table 7. It should be noted that each connection consist of two nail fasteners. All the nailed connections showed very ductile behavior with the monotonic ductility higher than the cyclic one. It was also found the loading orientation with respect to timber grain had no significant influence on the connection behavior. Given plywood thickness, the increase of nail size led to the increase of the connection capacity. However, given nail size, the increase of the plywood thickness did not necessarily lead to the increase of the connection capacity. Overall, the combinations of 17mm plywood with ϕ3.15x75; 25mm plywood with ϕ3.55x90 performed better than other combinations in terms of strength and stiffness.

Table 5 Connection properties for φ2.8 Nailed connections (two nails per connection)

ϕ2.8 NAILS	12mm Ply				17mm Ply			
	Parallel		Perpendicular		Parallel		Perpendicular	
	Mono	Cyclic	Mono	Cyclic	Mono	Cyclic	Mono	Cyclic
k_i (kN/mm)	2.3	1.8	3.3	2.4	2.2	2.5	2.9	1.8
F_y (kN)	1.3	1.3	1.2	1.4	1.2	1.3	0.9	1.2
F_{max} (kN)	2.2	1.8	2.4	2.2	2.3	1.9	2.1	2.2
F_{ult} (kN)	1.8	1.5	2.0	1.7	1.8	1.5	1.7	1.8
Δ_y (mm)	0.9	1.8	0.8	1.2	0.7	1.3	0.4	1.9
Δ_{max} (mm)	14.2	10.4	11.7	8.5	10.8	8.3	6.7	8.2
Δ_{ult} (mm)	27.7	19.4	20.5	16.9	20.3	13.3	13.4	14.8
μ	32.3	11.9	26.5	14.6	29.6	10.6	32.2	12.3
$F_{(1-3)}$	-	21.3 - 46.5%	-	19.7 - 36.3%	-	12.3 - 33.3%	-	6.1 - 13.9%

Note: k_i = initial stiffness

F_y = yield strength,

F_{max} = maximum strength,

F_{ult} = ultimate strength, taken as $0.8F_{max}$ or is equal to F_{max} if a brittle failure is observed

Δ_y = yield displacement, corresponding to F_y

Δ_{max} = maximum displacement, corresponding to F_{max}

Δ_{ult} = ultimate displacement corresponding to F_{ult}.

μ = ductility ratio

$F_{(1-3\%)}$ = strength degradation ratio

Table 6 Connection properties for φ3.15 Nailed connections (two nails per connection)

φ3.15 NAILS	12mm Ply				17mm Ply				25mm Ply			
	Parallel		Perpendicular		Parallel		Perpendicular		Parallel		Perpendicular	
	Mono	Cyclic	Mono	Cyclic	Mono	Cyclic	Mono	Cyclic	Mono	Cyclic	Mono	Cyclic
k_i (kN/mm)	1.7	1.8	2.6	2.1	2.6	2.1	2.1	2.8	2.4	2.8	2.2	3.3
F_y (kN)	1.3	1.7	1.7	1.7	1.5	1.6	1.7	1.5	1.8	1.8	1.7	1.7
F_{max} (kN)	2.4	2.7	2.8	2.7	2.7	2.9	2.8	2.6	2.7	2.8	2.7	2.4
F_{ult} (kN)	1.9	2.1	2.3	2.1	2.1	2.3	2.3	2.1	2.1	2.2	2.2	2.0
Δ_y (mm)	1.1	1.8	1.1	3.2	1.5	1.2	1.4	1.1	1.7	1.3	1.3	3.4
Δ_{max} (mm)	11.5	9.5	10.4	12.7	12.7	15.2	9.3	10.5	15.4	12.7	7.9	8.8
Δ_{ult} (mm)	32.4	22.6	18.4	22.1	31.1	28.4	17.2	17.3	32.5	23.2	14.8	15.4
μ	28.9	14.5	16.2	8.1	21.5	25.8	13.0	15.4	19.7	18.7	11.5	11.3
$F_{(1-3)}$		15.6 - 40.7 %	-	22 - 46.7 %	-	19.9 - 31.2%	-	14.5 - 30.5 %	-	22 - 36.4 %	-	14.6 - 29.5 %

Note: k_i = initial stiffness
F_y = yield strength,
F_{max} = maximum strength,
F_{ult} = ultimate strength, taken as $0.8F_{max}$ or is equal to F_{max} if a brittle failure is observed
Δ_y = yield displacement, corresponding to F_y
Δ_{max} = maximum displacement, corresponding to F_{max}
Δ_{ult} = ultimate displacement corresponding to F_{ult}.
μ = ductility ratio
$F_{(1-3\%)}$ = strength degradation ratio

Table 7 Connection properties for φ3.55 nailed connections (two nails per connection)

ϕ3.55 NAILS	12mm Ply				17mm Ply				25mm Ply			
	Parallel		Perpendicular		Parallel		Perpendicular		Parallel		Perpendicular	
	Mono	Cyclic	Mono	Cyclic	Mono	Cyclic	Mono	Cyclic	Mono	Cyclic	Mono	Cyclic
k_i (kN/mm)	3.4	1.5	2.3	3.2	3.5	2.4	3.5	2.3	2.5	2.4	2.8	3.3
F_y (kN)	1.7	1.9	2.0	1.9	1.8	1.9	1.8	1.8	1.8	2.0	2.0	2.1
F_{max} (kN)	2.8	3.0	3.5	2.8	2.9	2.9	2.9	2.7	3.2	3.1	3.4	3.1
F_{ult} (kN)	2.2	2.4	2.8	2.2	2.3	2.3	2.3	2.2	2.6	2.5	2.7	2.5
Δ_y (mm)	0.9	1.2	1.5	2.2	1.1	1.5	1.1	1.4	1.4	1.6	1.2	1.8
Δ_{max} (mm)	10.5	11.6	10.0	9.1	10.3	12.5	10.3	9.5	14.2	10.0	11.1	9.9
Δ_{ult} (mm)	22.9	22.6	21.1	16.9	20.2	24.0	20.2	17.2	25.7	20.3	18.0	18.2
μ	26.3	19.1	14.4	8.9	19.5	17.1	19.5	12.8	19.9	13.0	16.5	11.4
$F_{(1-3)}$	-	13.8 - 33%	-	14.3 - 27.5%	-	13 - 24.4%	-	12.8 - 24%	-	8 - 15%	-	7.6 - 15.5%

Note: k_i = initial stiffness
F_y = yield strength,
F_{max} = maximum strength,
F_{ult} = ultimate strength, taken as $0.8F_{max}$ or is equal to F_{max} if a brittle failure is observed
Δ_y = yield displacement, corresponding to F_y
Δ_{max} = maximum displacement, corresponding to F_{max}
Δ_{ult} = ultimate displacement corresponding to F_{ult}.
μ = ductility ratio
$F_{(1-3\%)}$ = strength degradation ratio

4. Shake Table Test on a 4-storey Timber-steel Hybrid Building

Aligned with a research project funded by National Natural Science Foundation of China, a 4-storey 2/3 scale timber-steel hybrid structure was tested on a shake table at Tongji University in Shanghai. The objective of the test was to evaluate seismic performance of the hybrid building system under strong ground motions adjusted to three seismic intensity levels. A group of four earthquake ground motions including the 2011 Canterbury earthquake were used for the test.

4.1 Building Specimen

The building specimen was designed as a portion of a prototype four-storey building located in Sichuan Province, a high seismic region in China. It has a floor plan of 34.2 x 12 m and the story height is 3.3m. The plan view and the elevation of the structure are shown in Figure 14. According to Load Code for the Design of Building Structures (GB50009, 2012) and Code for Seismic Design of Buildings (GB50011, 2010), this building was designed on soil type II and the seismic intensity level of 8, leading to the design spectral acceleration of 0.16g under frequent earthquakes with a 50-year return period for the building. The dead load of the floors was about 1.8 kPa and the live load was 2 kPa. One portion of this building was selected to construct the test specimen which was scaled to 2/3 of the original dimensions due to the high overturning moment demand of the building and the capacity limitation of the shake table. Therefore, the shake table test needed to consider an acceleration scale factor (S_a) of 2.0, and a stress scale factor (S_σ) of 1.0, respectively. All the scale factors involved in the specimen design were derived on the basis of the similitude law and are listed in *Table* 8. As shown in Figure 15, the test specimen had a floor plan of 8 x 3.75 m and total height of 8.8 m. The shake table size is 6.25 x 4.25 m and was extended to 8.6 m in one direction by a steel extension frame rigidly connected to the table.

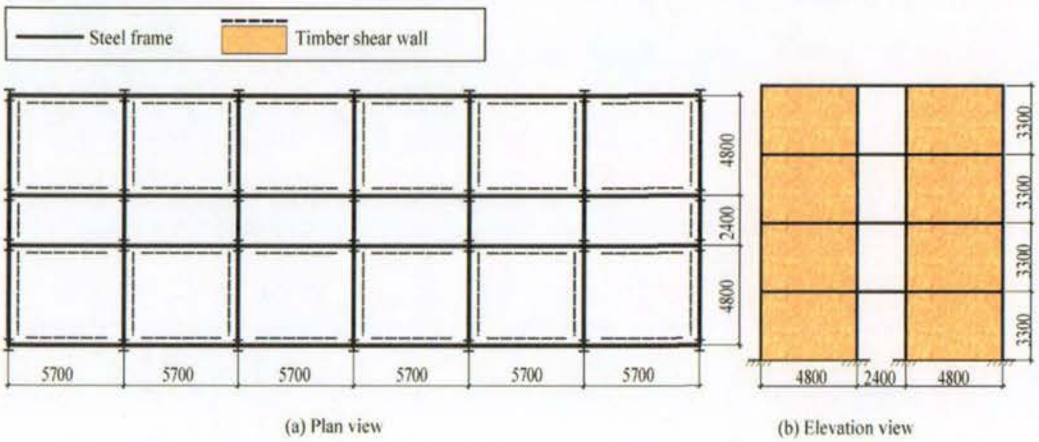

Figure 14: Plan view and elevation of the prototype building (all dimension are in millimeter)

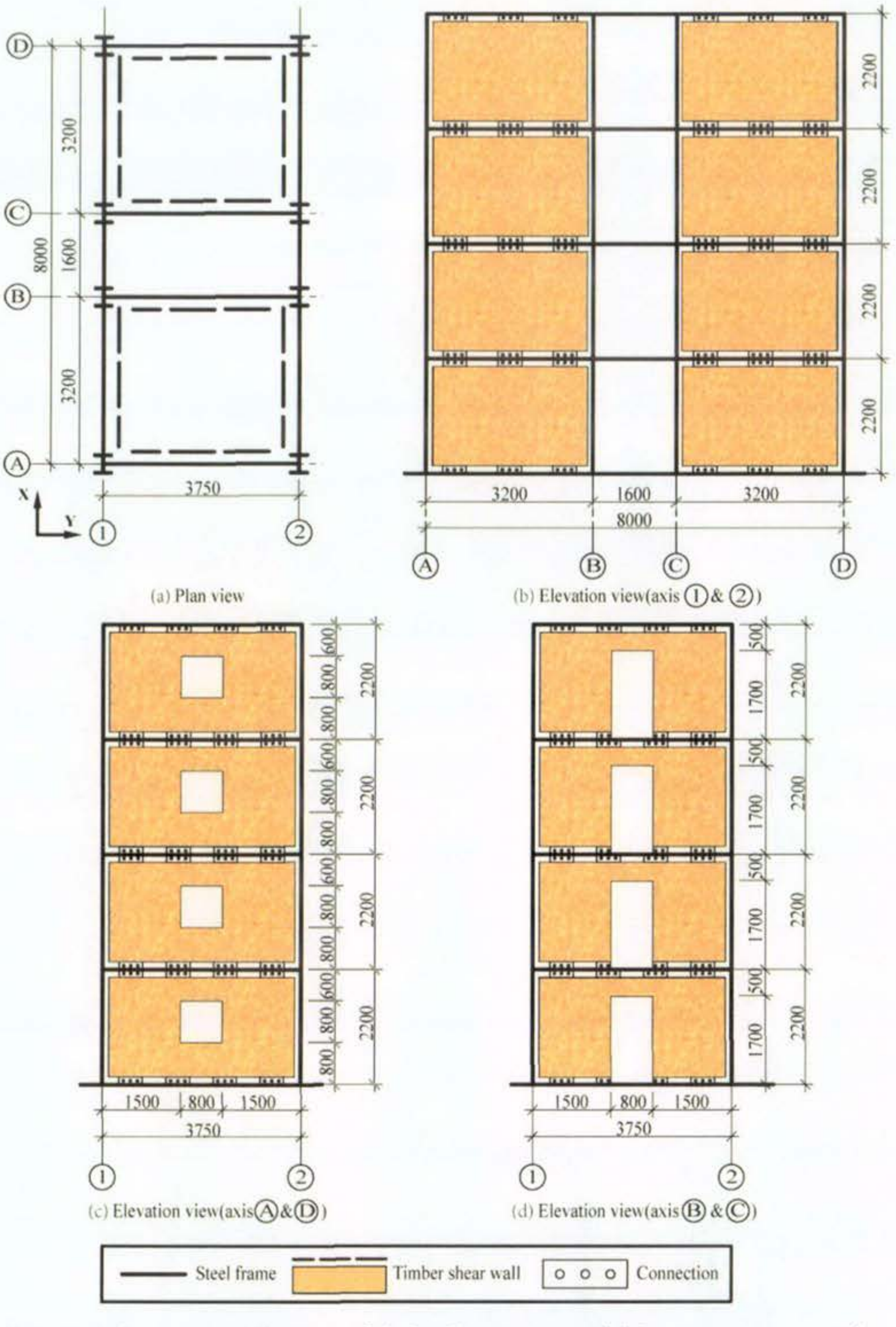

Figure 15: Plan view and elevation of the building specimen (all dimensions are in mm)

Table 8 Similitude scale factors

Parameter	Relation	Scaling factor
Length	S_l	2/3
Linear displacement	$S_\delta = S_l$	2/3
Angular displacement	$S_\phi = S_\sigma / S_E$	1
Strain	$S_\varepsilon = S_\sigma / S_E$	1
MOE	$S_E = S_\sigma$	1
Stress	S_σ	1
Poisson's ratio	S_υ	1
Mass density	$S_\rho = S_\sigma / (S_a \cdot S_l)$	0.75
Mass	$S_m = S_\sigma \cdot S_l^2 / S_a$	0.2222
Force	$S_F = S_\sigma \cdot S_l^2$	0.4444
Linear load	$S_q = S_\sigma \cdot S_l$	0.6667
Area load	$S_p = S_\sigma$	1
Moment	$S_M = S_\sigma \cdot S_l^3$	0.2963
Damping	$S_c = S_\sigma \cdot S_l^{1.5} \cdot S_a^{-0.5}$	0.3849
Period	$S_T = S_l^{0.5} \cdot S_a^{-0.5}$	0.5774
Frequency	$S_f = S_l^{-0.5} \cdot S_a^{0.5}$	1.7321
Velocity	$S_v = (S_l \cdot S_a)^{0.5}$	1.1547
Acceleration	S_a	2

Figure 16 shows the building specimen mounted on the shake table. Hot rolled H-section steel members with Grade Q235 (with yield strength of 235 MPa) were used to manufacture the steel members. The steel sections are listed in *Table* 9. To ensure ductile behavior of the steel frame and good welding quality, welding was mainly performed in the factory. M16 high strength bolts were used to transfer the shear force between the steel frame and the infill shear walls.

Figure 16: Building specimen on the shake table

*Table 9 Sections of steel frame members**

Storey No.	Member	Direction	Steel profile H-a×b×c×d (mm)*
1-3	Column	-	H-150×150×7×10
	Beam	X	H-125×125×6.5×9
		Y	H-125×125×6.5×9
4	Column	-	H-125×125×6.5×9
	Beam	X	H-125×125×6.5×9
		Y	H-100×100×6×8

*Note: H-a×b×c×d represents height a, width b, web thickness c, and flange thickness d.
X and Y are the longer and shorter directions on the building plan, as indicated in Figure 15(a).

The infill LTF shear walls consisted of No. 2 grade Canadian Spruce-Pine-Fir (SPF) timbers (NLGA, 2014) sheathed with OSB panels. All the infill walls were double-side sheathed, except that the walls on the 4th storey along the longer x direction were single-side sheathed. The stud spacing was 406 mm in the x direction and 305 mm in the y direction. The floor diaphragms were composed of joists of 38 mm × 184 mm SPF timbers sheathed with 15 mm thick OSB panels. ϕ3.3 × 82.5 nails were used to attach the OSB panels in the walls and the floors. Table 10 shows the nailing patterns used in the infill walls.

Table 10 Nail layouts for the timber shear walls

Direction	Story	Side with sheathing	Spacing/mm	
			edge	field
X	4	single sided	125	250
	3	double-sided	150	300
	2	double-sided	200/100	200
	1	double-sided	150/75	150
Y	4	double-sided	150	300
	3	double-sided	100	200
	2	double-sided	75	150
	1	double-sided	75	150

4.2 Data Acquisition

The acceleration and displacement responses of the test specimen under seismic excitations were recorded by over 200 sensors. The instrumentation consisted of various types of accelerometers, linear voltage displacement transducers (LVDTs) and strain gages. Accelerometers were installed at the middle of floor to record horizontal accelerations in the X and the Y directions at each story. Four accelerometers were also placed at the corner of the steel extension frame beneath the specimen to measure the vertical acceleration. Six LVDTs provided the displacement measurements at each story.

4.3 Test Program

Earthquake records from Wenchuan earthquake (May 12, 2008), Canterbury earthquake (February 22, 2011), El-Centro earthquake (May 18, 1940) and Kobe earthquake (January 17, 1995) were selected for the test. Table 11 shows the test matrix consisting of uni-directional and bi-directional ground shaking as well as white noise scanning. The changes of the building vibration period due to damage were measured by white noise scanning after each seismic excitation. Figure 17 shows the unscaled spectral accelerations of the input ground motions. To fulfill the similitude requirement, the original records were scaled by S_t=0.5774 in time. After applying an acceleration scale factor (S_a) of 2.0, the peak ground acceleration (PGA) of the unidirectional seismic excitations, as well as the X-component (primary component) of the bidirectional seismic excitations, was scaled to 0.07g, 0.40g, and 0.80g to present three types of earthquakes with return periods of 50-year, 500-year and 2500-year.

Table 11 Test matrix

Sequence	Record	PGA(g)		Sequence	Record	PGA(g)	
		X	Y			X	Y
1	White noise	0.07		21	White noise	0.07	
2	White noise		0.07	22	White noise		0.07
3	Wenchuan	0.14		23	Wenchuan	0.4	
4	Canterbury	0.14		24	Canterbury	0.4	
5	El Centro	0.14		25	El Centro	0.4	
6	KOBE	0.14		26	El Centro	0.4	0.17
7	White noise	0.07		27	KOBE	0.4	
8	Wenchuan	0.4		28	KOBE	0.4	0.17
9	Canterbury	0.4		29	White noise	0.07	
10	El Centro	0.4		30	White noise		0.07
11	KOBE	0.4		31	Wenchuan	0.8	
12[1]	White noise	0.07		32	White noise		
13	White noise	0.07		33	Canterbury	0.8	
14	White noise		0.07	34	White noise	0.07	
15	Wenchuan	0.14		35	El Centro	0.8	
16	Canterbury	0.14		36	White noise	0.07	
17	El Centro	0.14		37	KOBE	0.8[2]	
18	El Centro	0.14	0.0595	38	White noise	0.07	
19	KOBE	0.14		39	KOBE	0.75[2]	
20	KOBE	0.14	0.0595	40	White noise	0.07	

1. The timber shear wall in story 1-2 of X direction was strengthened before sequence 13;
2. PGA of Kobe earthquake on sequence 39 was scaled down because the overturning moment of the specimen on sequence 37 exceeded the capacity limitation of the shake table.

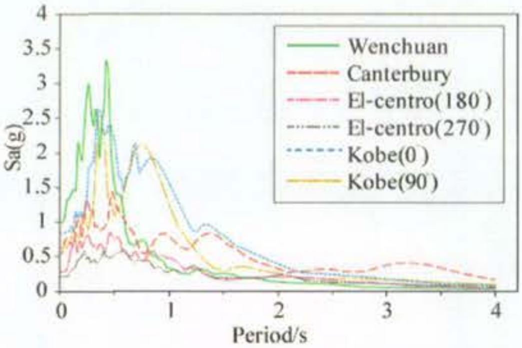

Figure 17: Unscaled spectral acceleration of the input ground motions

4.4 Results and Discussions

The timber-steel hybrid structure had excellent performance under the input seismic excitations scaled to three intensity levels, with PGA ranging from 0.14g to 0.80g. The overall damage to the building specimen was not significant. And there was no visible damage to the steel frames and the timber-steel bolted interface connections through the entire test sequence. Under the frequent earthquake shakings with PGA of 0.14g, no damage was observed in the building. Under the shakings with PGA of 0.4g, due to the narrow gap between adjacent OSB sheathing panels in the infill walls, one panel corner was crushed, as shown in Figure (a). Also, a small number of nailed timber-OSB connection started to fail. When the PGA increased to 0.80g, more nailed connection failures were observed. Nail withdrawal was the most typical connection failure mode, as shown in Figure 18 (b) and (c). In addition, the nailed connections along the edge of the sheathing panels were damaged by nail head pull-through and OSB panel local crushing, as shown in Figure 18(d), (e), and (f), respectively. Most of the failures were observed at the 2nd and the 3rd stories, which had larger inter-storey drifts compared to the 1st and the 4th stories.

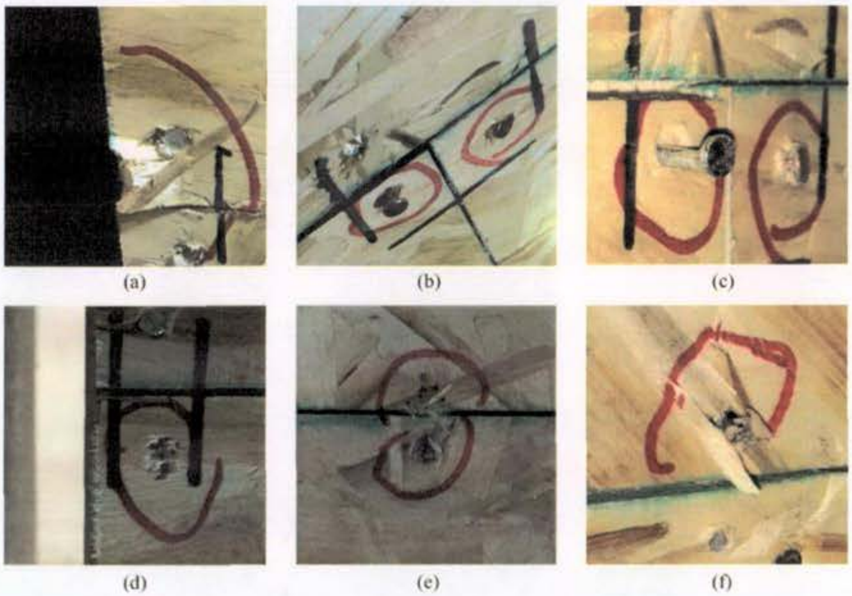

Figure 18: Typical failure modes in infill timber shear wall

Table 12 lists the peak storey drift responses of the building in the test sequence. As an example, Figure 19 shows the time-history response of the roof drift under El Centro earthquake (PGA = 0.80g) and Kobe earthquake (PGA = 0.75g) excitations.

Figure 20(a)-(d) present the inter-storey drift ratios under the unidirectional seismic excitations. The peak inter-storey drift ratios under bidirectional seismic excitations are shown in Figures 20(e) and (f). It was found that the peak inter-storey drift ratios in the X direction had almost the same values with those under unidirectional seismic excitation. In all the test phases, the maximum peak inter-storey drift ratio of 0.85% was recorded under Kobe earthquake with the measured PGA of 0.75g.

Under the uni-directional 2011 Canterbury earthquake (Christchurch Botanic Garden station) with PGA scaled to 0.14g, 0.4g and 0.8g, the peak inter-storey drifts were only 0.15%, 0.4% and 0.6%, respectively. These inter-storey drift levels were well below the drift criteria for normal buildings specified by NZS1170.5 (2004), indicating excellent performance of this building under severe ground shakings.

Table 12 Maximum story displacements

Sequence	**Record**	**PGA(g)**		**Peak drift response at different storeys (mm)**				
		X	**Y**	**4**		**3**	**2**	**1**
3	Wenchuan	0.14			6.3	5.3	3.9	1.9
4	Canterbury	0.14			8.0	6.9	4.9	2.5
5	El Centro	0.14			9.6	8.1	5.8	2.9
6	KOBE	0.14			8.0	6.8	5.1	2.4
8	Wenchuan	0.40			16.2	13.5	9.6	4.5
9	Canterbury	0.40			25.2	21.4	15.9	7.4
10	El Centro	0.40			27.0	23.2	17.4	8.5
11	KOBE	0.40			26.8	23.0	16.6	7.9
15[1]	Wenchuan	0.14			6.7	5.5	3.8	1.7
16	Canterbury	0.14			8.4	7.2	4.8	2.2
17	El Centro	0.14			8.7	7.4	4.8	2.4
18	El Centro	0.14	0.06	X:	8.4	7.1	4.8	2.4
				Y:	3.2	2.6	2.2	1.1
19	KOBE	0.14			8.5	7.3	5.2	2.3
20	KOBE	0.14	0.06	X:	9.0	7.7	5.6	2.4
				Y:	2.5	2.0	1.6	0.9
23	Wenchuan	0.40			17.2	13.9	9.2	4.1
24	Canterbury	0.40			23.4	19.5	13.7	6.3
25	El Centro	0.40			24.3	20.6	15.0	7.3
26	El Centro	0.40	0.17	X:	24.3	20.6	15.2	7.5
				Y:	9.7	8.7	7.0	3.6
27	KOBE	0.40			20.6	17.1	12.3	5.7
28	KOBE	0.40	0.17	X:	21.4	17.6	12.9	6.0
				Y:	7.6	6.2	5.0	2.8
31	Wenchuan	0.80			25.3	20.5	13.1	5.6
33	Canterbury	0.80			42.2	34.6	23.9	10.8
35	El Centro	0.80			50.6	41.6	28.5	12.7
39	KOBE	0.75			57.1	47.8	32.6	14.0

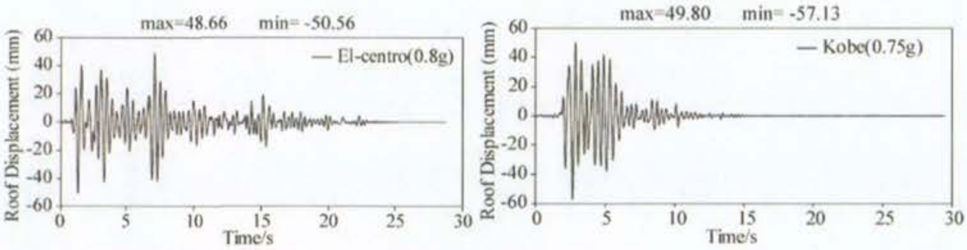

Figure 19: Roof displacement time history curve

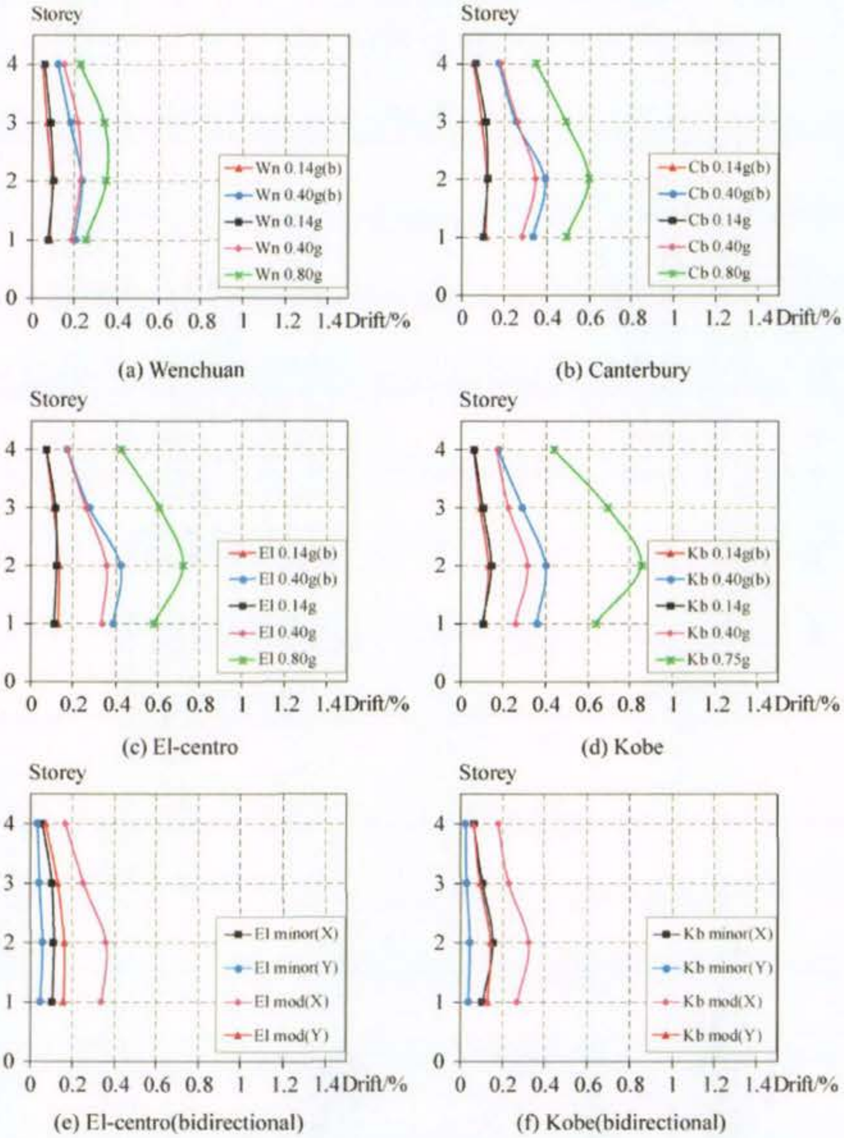

Note: "b" in the legend indicates the seismic excitations were conducted before the specimen was strenghened

Figure 20: Inter-storey drift responses under different ground motions

5. Parametric Study of Hybrid Shear Walls

Experimental studies in laboratories are time-consuming and costly and can only test a limited number of design configurations and loading scenarios. Thus, further parametric studies were conducted by ABAQUS modelling to study the influence of various design parameters on the hybrid wall performance under cyclic loading. Critical wall properties such as strength, stiffness, and ductility were derived according to the load-drift hysteresis of the hybrid walls.

5.1 Description of Benchmark Wall

In Figure 21, a hybrid wall was designed as the benchmark wall configuration for the parametric study. The steel frame was 3.75 m long and 2.475 high. The size of the infill wall was 3.6 m × 2.4 m, fitting three full-size plywood sheets (1.2 m x 2.4 m each). The steel beams and columns were UB250 and UC200 following AS/NZS 3679.1 (2010). Radiata pine timbers with 90 mm x 45 mm were spaced at 400 mm for wall studs. M12 bolts spaced at 250 mm were used to form the timber-steel interface connections. Figure 21 also shows the corresponding ABAQUS FE model. The nail sizes, plywood thickness, and the sizes of bolts and coach screws used in the parametric study were the same as those used in the connection tests. Cyclic displacement loading protocol followed the ISO16670 (2003), as shown in Figure 22. Table 13 lists all the input material properties. Table 14 lists the input Q-Pinch model parameters for the critical nailed connections and bolted timber-steel interface connections. As an example, Figure 23 shows the load-drift hysteresis of the benchmark wall that used 12 mm thick plywood and ϕ3.15x75 nails with 50 mm edge spacing and 300 field spacing. The individual contributions from the steel moment frame and the infill wall were also presented.

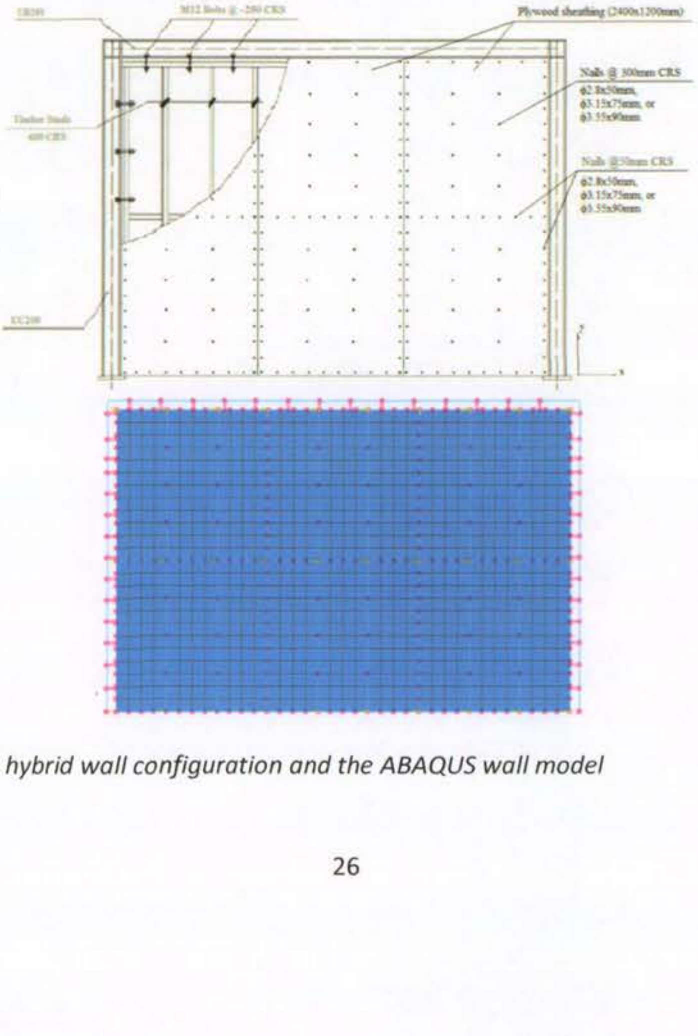

Figure 21 Benchmark hybrid wall configuration and the ABAQUS wall model

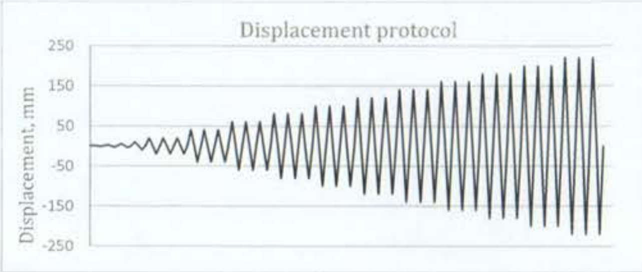

Figure 22: Cyclic displacement protocol

Table 13 Input properties of structural components in hybrid wall modelling

Structural Component	Finite-Element representation (ABAQUS)	Material and Section properties
Steel framing	Beam element: 2-node (B21)	E = 210GPa(a), ρ = 7850 kg/m3, σy = 300MPa, σyp = 301MPa, εp = 0.001(d)
Timber framing	Beam element: 2-node (B21)	E = 8.0GPa ρ = 450 kg/m3 Cross-sectional area = 90x45mm
Sheathing	Solid element: 8-node plain stress, reduced integration (CPS8R)	Ex = 1.9GPa, Ey = 9.1GPa, G = 455MPa, ρ = 650 kg/m3, σy = 300MPa, σyp = 301MPa, εp = 0.001 Plywood thicknesses (tp) = 12mm, 17mm, 25mm
Timber-sheathing connections	User defined element pair: 2-node, non-linear (U1)	Nail sizes = Φ2.8x50mm, Φ3.15x75mm, Φ3.55x90mm Plain shank, Q-Pinch parameters(b)
Timber-steel connections	User defined element pair: 2-node, non-linear (U1)	Q-Pinch parameters(b)
Steel-frame base connections	Spring element: 2-nodes, linear (SPRING2)	krot = 2.0e7 kNm/rad(c)
Timber-frame base connections	Spring element: 2-nodes, linear (SPRING2)	krot = 10, 000 kNm/rad

Table 14: Critical connections tested on and their calibrated parameters

Nail size - plywood thickness	ϕ2.8x50 12mm	ϕ3.15x75 12mm	ϕ3.55x90 12mm	ϕ2.8x50 17mm	ϕ3.15x75 17mm	ϕ3.55x90 17mm	ϕ3.15x75 25mm	ϕ3.55x90 25mm	M12 Bolt
Initial stiffness **k_1, N/mm**	846	625	1243	850	1094	970	1131	1303	7200
Plastic stiffness **k_2, N/mm**	25	20	39	35	25	27	34	53	7400
Degraded stiffness **k_3, N/mm**	38.5	20	33	60	31.5	35	35	50	100000
Unloading stiffness **k_4, N/mm**	920	675	1950	1050	1450	1000	1231	1903	7400
Yield Force **F_0, N**	780	1120	1070	750	1025	1090	935	1175	16500
Pinching Force **F_I, N**	175	250	320	150	220	305	310	280	4200
Δ_y, mm	1.1	2	1.1	1.1	1.6	1.1	1.1	1.1	2.5
Δ_{ult}, mm	9.9	7.3	10	8.2	18.3	12.6	8.2	10	28
Δ_{fail}, mm	16	21	20	14	24	25	15	17	30
Reloading degradation factor, α	0	0	0	0	0	0	0.35	0.2	0.7
Stiffness degradation factor, β	1.1	1.05	1.1	1.1	1.1	1.1	1.1	1.1	1.1

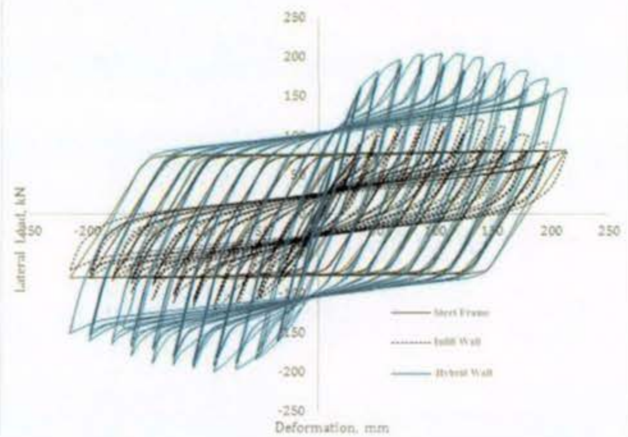

Figure 23: Typical load-drift hysteresis predicted by ABAQUS hybrid wall model

5.2 Effect of Steel Member Sizes

Several steel member sizes were chosen based on the benchmark wall configuration given the nail size of ϕ3.15x75mm with 50/300 nailing pattern and 17mm thick plywood. The envelope curves of the hysteresis loops under different combinations of steel member profiles are shown in Figure 24. The maximum wall strength and initial stiffness are presented in Table 15. It can be seen that the strength and stiffness of the hybrid wall increased with the increase of steel member sizes; however, the change of the ductility was negligible. Because the elasto-plastic steel property was used in the model, the post-peak wall behavior will only be governed by the infill wall.

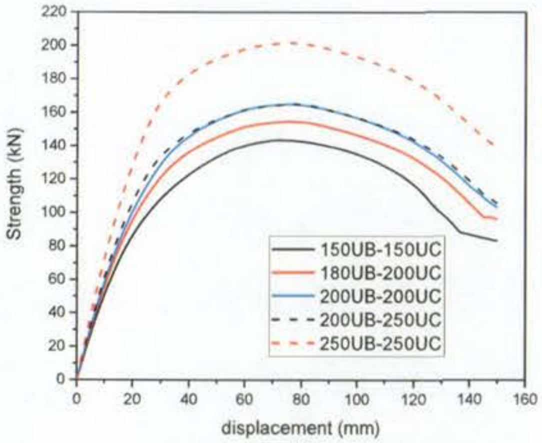

Figure 24: Load-drift envelope curves of hybrid walls with different steel member sizes

Table 15 Influence of steel member sizes on hybrid wall strength and stiffness

Steel beam & column profile	F_{max} (kN)	K_i (kN/mm)
150UB-150UC	143.52	3.12
180UB-200UC	154.54	3.44
200UB-200UC	164.71	3.70
200UB-250UC	165.07	3.75
250UB-250UC	201.49	4.83

5.3 Effect of Nail Size and Plywood Thickness

Four nailing patterns (50/300, 75/300,100/300 and 150/300) and two plywood thickness values (12 mm and 17mm) were adopted to study the effect of nail sizes and plywood thicknesses. Figure 25 shows that the capacity of the hybrid walls is positively correlated with the nail size. Also reduced nail spacing can significantly increase the wall capacity. In Figure 26, given the nail spacing, the influence of the plywood thickness on the wall capacity is not significant for the ϕ3.15x75mm nails. But for the larger ϕ3.55x90mm nail, slightly increase of the wall capacity can be found with increased plywood thickness.

Figure 27 and Figure 28 show the influence of nail sizes and sheathing thickness on the wall stiffness. Given the panel thickness and nail spacing, the influence of nail sizes on the overall hybrid wall stiffness was not significant. It was found that the combinations of ϕ3.15x75mm nails with 17mm plywood and ϕ3.55x90mm nails with 25mm plywood are better choices for high stiffness.

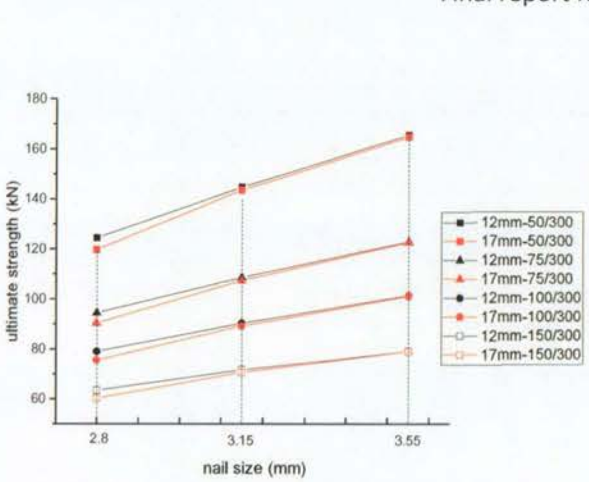

Figure 25: Effect of nail size on wall capacity

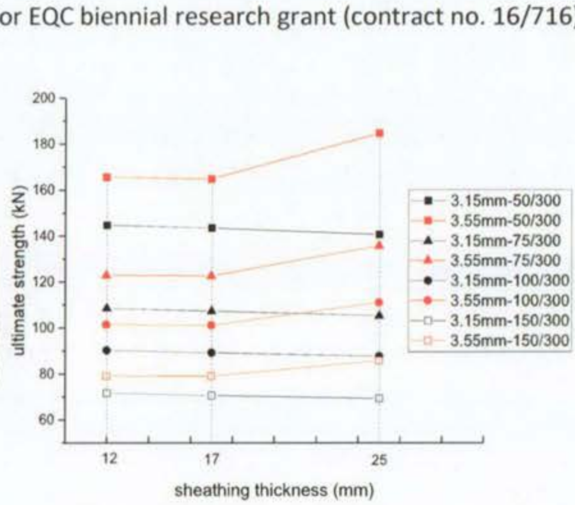

Figure 26: Effect of plywood thickness on wall capacity

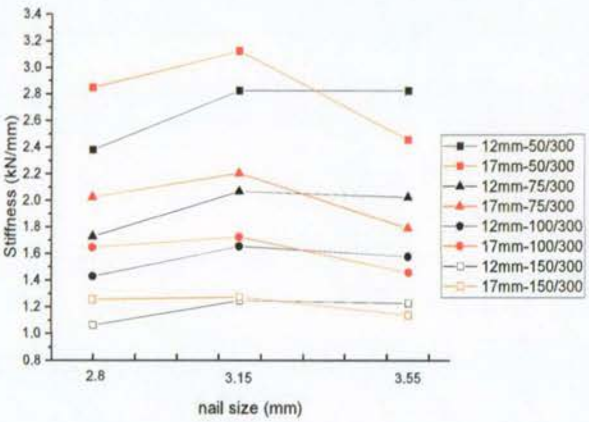

Figure 27: Effect of nail size on wall stiffness

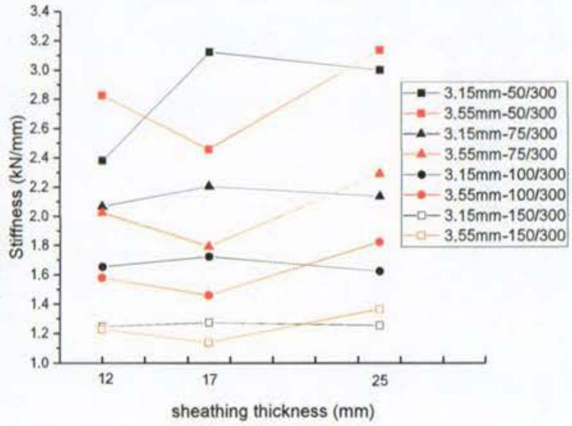

Figure 28: Effect of plywood thickness on wall stiffness

5.4 Load-Sharing and Wall Ductility

The load-sharing mechanism among the steel moment frame and the infill wall has a major impact on the hybrid system performance. A load sharing factor ρ is defined as the ratio between the load carried by the infill wall and the total load carried by the hybrid wall. As an example, Figure 29 demonstrates that the change of the ρ factor with the increasing wall drift. In this wall configuration, 150UB and 150UC were used as the steel beams and columns and three combinations of nail size and plywood thickness (ϕ2.8x50 with 12mm ply; ϕ3.15x75 with 17mm plywood, and ϕ3.55x75 with 25 mm plywood) were considered. The same nailing pattern 100/300 was used. It is shown that the infill wall carried more than 80% of the total load at the early stage and then the percentage will decrease gradually due to nail yielding and damage accumulated with increased wall drift. Meanwhile, a larger portion of load needs to be carried by the steel frame so that the system can achieve a better ductility compared to conventional timber shear walls.

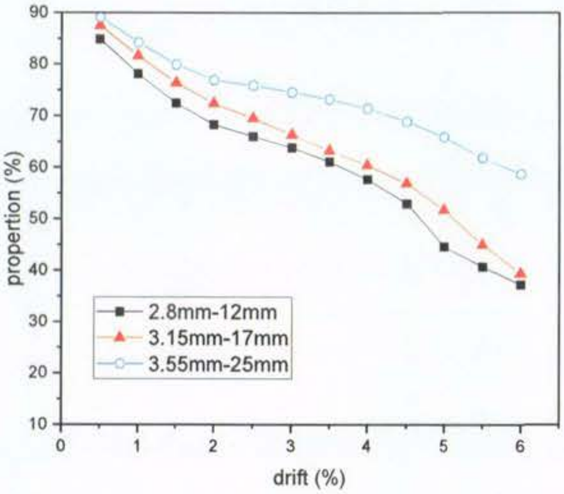

Figure 29: Evolving ρ factor in hybrid wall systems with increased wall drift demand

The hybrid walls with a total of 8 combinations of nail sizes and plywood thickness under the 100/300 nailing patterns were simulated and the ductility ratios are listed in Table 16. It was shown that the system ductility factors ranged from 4.0 to 6.0. It seems that the system consisting of ϕ3.15x75mm with 17mm plywood had the highest system ductility ratio of 6.

Table 16 Ductility factors of hybrid walls with various nail - plywood combinations

Plywood thickness	ϕ2.8x50	ϕ3.15x75	ϕ3.55x90
12 mm	5.07	6.00	5.83
17 mm	4.05	4.59	5.13
25 mm	n. a.	5.82	5.15

6. Displacement-based Seismic Design

6.1 Introduction of Design Method

The performance-based seismic design focusing on the displacement demand/capacity is considered as a better seismic design approach compared with the force based approach because the building displacement responses are directly correlated to the structural/non-structural damage of the buildings. Therefore, in this project, the direct displacement design method for multi-storey building proposed by Priestley et al. (2005) was used to apply the timber-steel hybrid wall systems into multi-storey LTF buildings.

Figure 30 shows the flowchart for this method. The method only requires the hysteretic damping estimation and shear wall design tables instead of detailed FEM model. From the previous parametric study, design tables for the hybrid wall system can be established, as shown in Table 17. Using the benchmark hybrid wall setup, the table shows the wall capacity and secant stiffness at various drift ratios given the combinations of nailing pattern and plywood thickness.

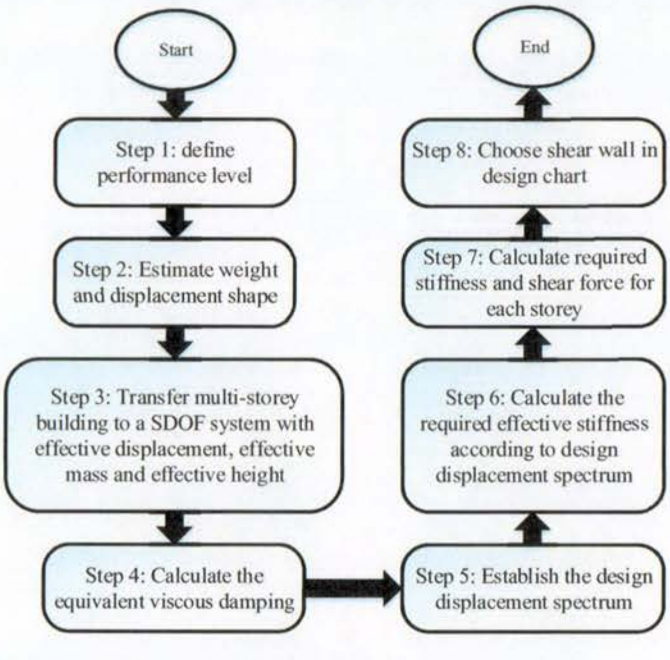

Figure 30: Flow chart for direct displacement design

Table 17 Hybrid shear wall design table

Nailing pattern	Nail size	Plywood thickness	Wall ID		Equivalent secant stiffness @ Various inter-storey drift ratio		
					1%	2.5%	5%
50/300	ϕ2.8x50	12	Wall#1	k_{eq} *(KN/mm)*	3.3	2.0	0.7
				F (kN)	82.7	119.3	81.3
		17	Wall#2	k_{eq} *(KN/mm)*	3.3	2.0	*
				F (kN)	82.7	119.6	*
	ϕ 3.15x75	12	Wall#3	k_{eq} *(KN/mm)*	3.5	2.3	1.2
				F (kN)	86.6	138.8	138.0
		17	Wall#4	k_{eq} *(KN/mm)*	4.0	2.3	1.0
				F (kN)	96.4	140.3	116.8
		25	Wall#5	k_{eq} *(KN/mm)*	3.9	2.3	0.8
				F (kN)	94.2	137.4	100.5
	ϕ 3.55x90	12	Wall#6	k_{eq} *(KN/mm)*	4.3	2.5	1.3
				F (kN)	102.5	152.1	156.0
		17	Wall#7	k_{eq} *(KN/mm)*	4.0	2.4	1.3
				F (kN)	98.6	146.4	161.4
		25	Wall#8	k_{eq} *(KN/mm)*	4.5	2.8	1.3
				F (kN)	111.6	167.0	154.4
100/300	ϕ2.8x50	12	Wall#9	k_{eq} *(KN/mm)*	2.0	1.3	0.6
				F (kN)	51.0	76.0	66.4
		17	Wall#10	k_{eq} *(KN/mm)*	2.0	1.3	0.4
				F (kN)	51.1	75.3	47.1
	ϕ 3.15x75	12	Wall#11	k_{eq} *(KN/mm)*	2.2	1.4	0.7
				F (kN)	54.7	86.5	87.2
		17	Wall#12	k_{eq} *(KN/mm)*	2.4	1.5	0.7
				F (kN)	60.8	87.1	80.2
		25	Wall#13	k_{eq} *(KN/mm)*	2.4	1.4	0.6
				F (kN)	58.1	85.5	76.7
	ϕ 3.55x90	12	Wall#14	k_{eq} *(KN/mm)*	2.6	1.6	0.8
				F (kN)	64.8	94.7	97.3
		17	Wall#15	k_{eq} *(KN/mm)*	2.5	1.5	0.8
				F (kN)	61.4	91.3	99.7
		25	Wall#16	k_{eq} *(KN/mm)*	2.8	1.7	0.9
				F (kN)	69.7	103.7	102.8

6.2 Design Example

A six-story timber-steel hybrid system having plan dimension of 22.5*m* x 9*m* and storey height of 2.5m is selected for the design example, as shown in Figure 31. The building is located in Christchurch, New Zealand with soil class D referring to NZS 1170.5 (2004). The elastic damping ratio ξ_{el} of 3% was assumed for the hybrid wall systems.

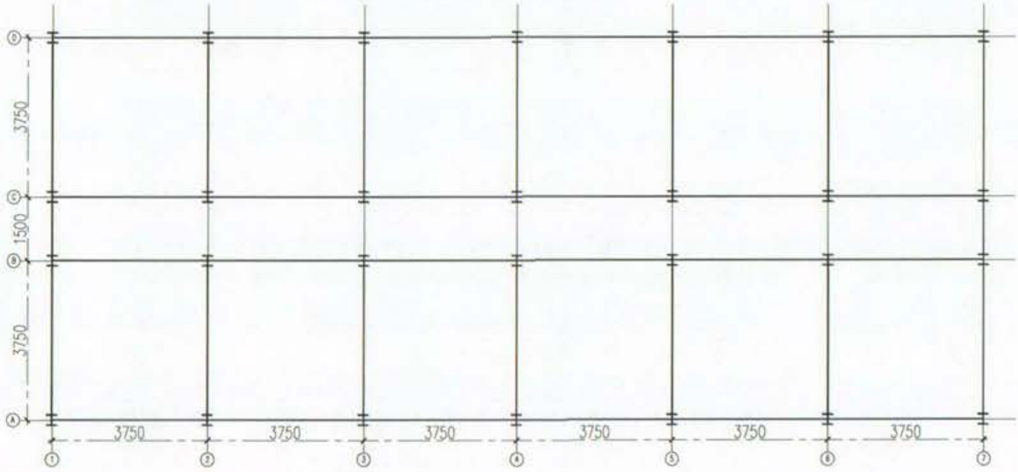

Figure 31: Plan and vertical layouts

- **Performance criteria and design acceleration spectra**

In this study, two performance level, Life Safety (LS) and Collapse prevention (CP) were defined in Table 18. The seismic hazard factor and near fault factor for Christchurch city are shown in Table 19. The LS inter-storey drift criteria is recommended in NZS1170.5 (2004). Because the hybrid systems consists of ductile steel moment frames and infill timber shear walls, the CP criteria under MCE level earthquakes was defined as 5% inter-storey drift ratio.

Table 18 Definition of performance levels

Performance Level	Hazard Level	Return period factor	Inter-storey drift limit
Life safety (LS)	10%/50yrs	1.0	2.5%
Collapse prevention (CP)	2%/50yrs	1.8	5%

Table 19 Seismic design parameters

Design Parameter	symbol	Value
Hazard factor	Z	0.3
Near-fault factor	N	1.0

The design acceleration response spectrum for LS and CP performance levels are defined as Eq. 1. The calculated maximum acceleration S_a are 0.9g and 1.62g respectively according to NZS 1170.5 (2004).

$$C(T) = C_h(T)ZRN(T,D) \qquad \text{Eq.1}$$

- **Conversion to an equivalent SDOF system**

In order to calculate the base shear using the displacement-based approach, the multi-storey building should be substituted by an equivalent single degree of freedom (SDOF) system shown in Figure 32.

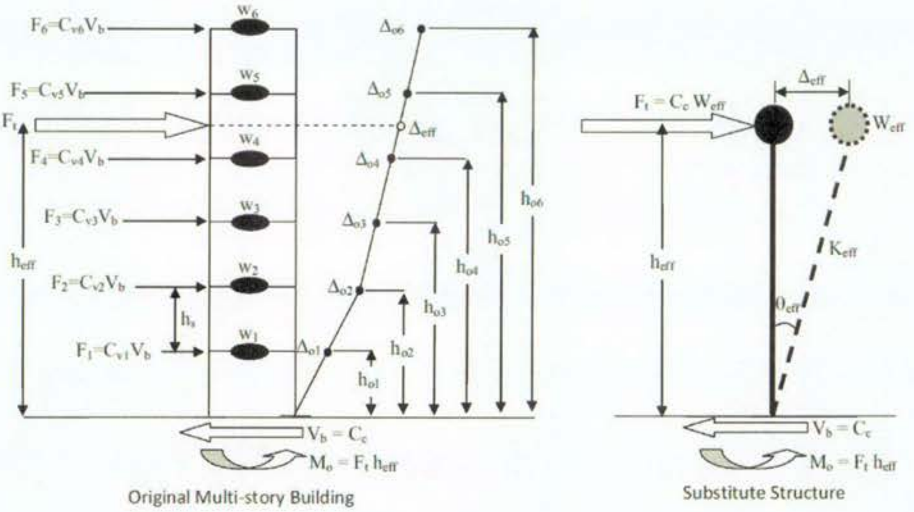

Figure 32: A six-storey building and the equivalent SDOF system (Pang et al., 2010)

The seismic weights for floors and roof are shown in Table 20. A quadratic displacement shape defined as Eq.2 was assumed and the multi-storey building's lateral displacement shape is shown in Figure 33.

Table 20 Seismic weight of roof and floors

	Dead load(kPa)	Imposed load(kPa)	Effective seismic weight
Floor	1.0	2.0	324kN
Roof	0.8	0.5	193kN

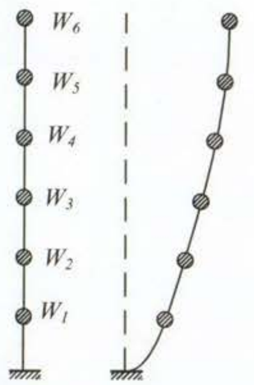

Figure 33: Quadratic displacement shape of the building

The lateral drift of each storey was calculated by

$$\Delta_i = \frac{4}{3} \cdot \left(\frac{H_i}{H_n}\right) \cdot \left(1 - \frac{H_i}{4H_n}\right) \quad \text{Eq.2}$$

Where, H_i is the height of storey *i* and H_n is the total height of the building.

Δ_i has dimensionless value of displacement. The maximum story drift appears on the first floor according to the quadratic displacement shape. The maximum dimensionless inter-storey drift was 0.213 and can be transferred to drift limit. The target equivalent displacement for SDOF system were calculated by Eq. 4 to Eq. 6 and the results are listed in Table 21 and Table 22.

$$\Delta_e = \sum_{i=1}^{6}(W_i\Delta_i^2) \,/\, \sum_{i=1}^{6}(W_i\Delta_i) \quad \text{Eq.3}$$
$$W_e = \sum_{i=1}^{6}(W_i\Delta_i/\Delta_e) \quad \text{Eq.4}$$
$$\mathrm{H}_e = \sum_{i=1}^{6}(W_i\Delta_i H_i) \,/\, \sum_{i=1}^{6}(W_i\Delta_i) \quad \text{Eq.5}$$

Table 21 Conversion to the equivalent SDOF system

Storey	H_i(m)	W_i (kN)	Quadratic Δ_i
1	2.5	324	0.213
2	5	324	0.407
3	7.5	324	0.583
4	10	324	0.741
5	12.5	324	0.880
6	15	193	1.000
$\Delta_e = 0.722$; $\mathrm{W}_e = 1534kN$; $\mathrm{H}_e = 10.02$m			

Table 22 Target displacement for SDOF system

Performanc e level	Drift limit	Inter-storey drift criteria	Drift criteria of the equivalent SDOF system
LS	2.5%	60mm	203.4mm
CP	5%	120mm	406.8mm

- **Equivalent viscous damping**

The effective viscous damping ξ_{eq} is computed as the sum of the hysteretic damping ξ_{hyst} and the elastic damping ξ_{el} as shown in Eq.6. For the timber-steel hybrid system, and the hysteretic is define as Eq.7.

$$\xi_{eq} = \xi_{hyst} + \xi_{el} \quad \text{Eq.6}$$
$$\xi_{hyst} = \frac{1}{2\pi} \cdot \frac{E_D}{k_s\Delta_t^2} \quad \text{Eq.7}$$

Where, E_D and k_s are the energy dissipated per full cycle and the secant stiffness at the target displacement Δ_t respectively. E_D can be calculated by cyclic load-displacement curves of the shear walls. ξ_{hyst} are around 15% and 28% for most of timber-steel hybrid wall at the 2.5% and 5% storey drift based on the parametric studies using the ABAQUS models.

The damping reduction factor, R_{eq} in Eq.8 is used to consider the ductility of the building according to Eurocode 8. R_{eq} are 0.745 and 0.568 for LS and CP performance level.

$$R_{eq} = \left(\frac{0.1}{0.05+\xi_{eq}}\right)^{0.5} \quad \text{Eq.8}$$

- **Design displacement spectra**

The design displacement spectrum $S_d(T)$ at ξ_{eq} can be established by adjusting displacement spectrum $S_d(T)$ at ξ=0.05 based on Eq. 9 and Eq. 10. Figure 34 gives the design displacement spectra with respect to the LS and CP performance levels. The required equivalent period T_{eq} at the inter-storey drift limit 2.5% and 5% were 1.71s and 2.49s, respectively. The equivalent required stiffness were 2113kN/m 997kN/m calculated by Eq.11.

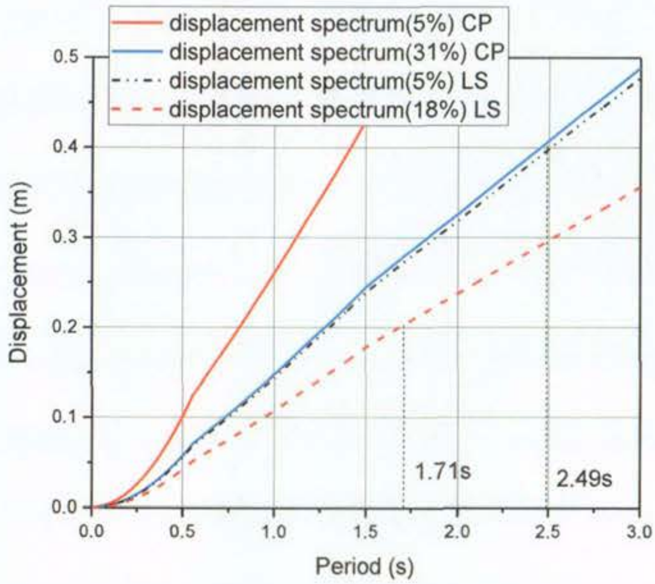

Figure 34: Design displacement spectrum

$$S_d(T) = \frac{T^2}{4\pi} S_a(T) \quad \text{Eq.9}$$

$$S_d(T)_{\xi_{eq}} = R_{eq} S_d(T) \quad \text{Eq.10}$$

$$K_{eq} = (\frac{2\pi}{T_e})^2 \frac{W_e}{g} \quad \text{Eq.11}$$

- **Calculation of load demand and selection of hybrid shear walls**

The total base shear forces were 429kN and 404kN for the LS and CP performance criteria using Eq. 12. By distributing the base shear force up to structure, the floor forces and required floor stiffness can be obtained by Eq.13 considering higher modes of vibration according to NZS 1170.5(2003). The required secant stiffness for each storey can be calculated by Eq. 14.

$$V_b = K_e \Delta_d \quad \text{Eq.12}$$

$$F_i = F_t + 0.92V_b(W_i\Delta_i)/\sum_{i=6}^{6}(W_i\Delta_i) \quad \text{Eq.13}$$

$$k_{req}^{i} = \frac{V_i}{\Delta_i} \quad \text{Eq.14}$$

where the V_i and the Δ_i are the shear force and the assumed drift at *i* storey, respectively.

The design of the hybrid walls was facilitated by simply choosing the type and the number of hybrid walls from Table 17. For this building, the selected wall types and numbers are listed in Table 23. It should be noted that the wall selection was governed by the CP performance criteria because of the significant strength and stiffness degradation of infilled LTF shear walls at the large drift ratio.

Table 23 Selection of wall types and amount

Storey no.	Shear force (kN) (LS)	Shear force (kN) (CP)	K_{req} (kN/mm) (LS)	K_{req} (kN/mm) (CP)	Selection of walls	
					Type	Amount
1	429	404	7.15	6.73	Wall #6	6
2	404	381	7.38	6.95	Wall #6	6
3	357	336	7.21	6.79	Wall #6	6
4	290	273	6.54	6.15	Wall #3	6
5	204	193	5.22	4.92	Wall #16	6
6	103	97	3.03	2.86	Wall #14	4

7. Conclusions

This project presents an experimental and numerical study on hybrid timber-steel shear wall systems suitable for multi-storey LTF buildings. Structural behavior of critical nailed connections and timber-steel interface connections were experimentally tested to establish a connection database for hybrid wall modelling and parametric studies. A 2/3 scale 4-storey hybrid building was tested on a shake table to study its seismic performance at three different seismic intensity levels (earthquakes with 50-year, 500-year and 2500-year return periods). Displacement based seismic design methodology was recommended for designing the hybrid wall systems and its application for a six-storey timber building was presented in a design example.

The main conclusions are summarized as below:

- Form the nailed connection testing and parametric studies of the wall systems, it was found that the increase of nail sizes will generally enhance the wall capacity. Considering the overall strength, stiffness and ductility performance, the hybrid systems with the infill shear walls using ϕ3.15x75mm with 17mm plywood and ϕ3.55x90mm with 25mm plywood performed better than other combinations of the nail size and plywood thickness. And the parametric studies indicated that most of the hybrid walls had high ductility ratios between 4.0 and 6.0.
- The steel frame offsets strength degradation of the infill shear wall at large wall drift demands and provides further strength and ductility. For the hybrid wall system, due to the existence of steel columns, no complicated hold-down design is required because the steel columns normally have sufficient capacity to resist the uplifting forces.
- The shake table tests on a 2/3-scale timber-steel hybrid structure showed that the hybrid system performed excellently with the peak inter-storey drift of 0.85% under severe earthquakes with a return period of 2,500 years. Under the 2011 Canterbury earthquake with PGA scaled up to 0.8g, the peak inter-storey drift was only 0.6%, well below of the drift criteria for the maximum credible earthquakes. It was also found that the damage was mainly limited to the nailed connections in the infill timber shear walls. The steel frames remained intact and the steel-timber interface connections were confirmed to be reliable.
- The displacement based design approach can be easily implemented to design the timber-steel hybrid system for multi-storey timber buildings, as demonstrated by a design example for a six-storey LTF building built in Christchurch New Zealand.

Acknowledgment

The authors would like to acknowledge Earthquake Commission of New Zealand and National Natural Science Foundation of China for providing the research grants.

References

- ABAQUS SIMULIA, 2011, ABAQUS/CAE manual V6.11. Dassault Systems, U.S.
- AS/NZS 1748. 2011. Timber – Solid – Stress-graded for structural purposes. Standards New Zealand.
- AS/NZS 2269. 2012. Plywood – Structural. Standards New Zealand. Standards New Zealand.
- AS/NZS 3679. 2010 Structural steel. Part 1: Hot-rolled bars and sections. Standards New Zealand.
- AS/NZS 1170. Part 5:2011. Structural Design Actions Part 5 Earthquake Actions. Standards New Zealand.
- Dickof C., Stiemer S. F., and Tesfamariam S. 2012. Wood-steel hybrid seismic force resisting systems: seismic ductility. Proc. 12th WCTE, Auckland, New Zealand.
- Dong, W. 2017. Lateral behavior of connections between steel moment-resisting frame and wood-frame shear wall in the hybrid system. Master thesis, Tongji University, China
- Eurocode 8, 2004. Design of structures for earthquake resistance. European Committee for Standardization.
- Folz, B. and Filiatrault, A., 2001. Cyclic analysis of wood shear walls. Journal of Structural Engineering, 127(4), 433-441.
- GB 50009. 2012 Load code for the design of building structures. Ministry of Housing and Urban-Rural Development. Beijing, China.
- GB 50011. 2010 Code for seismic design of buildings. Ministry of Housing and Urban-Rural Development. Beijing, China.
- GB 50017. 2003 Code for design of steel structures. Ministry of Housing and Urban-Rural Development. Beijing, China.
- He M., Li Z., Lam F., Ma R., Ma Z. 2014. Experimental investigation on lateral performance of timber-steel hybrid shear wall systems. Journal of Structural Engineering, 140(6): 04014029-1~12
- ISO16670. 2003. Timber Structures – Joints made with mechanical fasteners – Quasi-static reversed-cyclic test method. The International Organization for Standardization, Geneva.
- Judd, J. P. 2005. Analytical modeling of wood-frame shear walls and diaphragms. Master thesis. Brigham Young University.
- Li Z., He M., Li M., Lam F. 2014. Damage assessment and performance-based seismic design of timber-steel hybrid shear wall systems. Earthquakes and Structures. 7(1): 101-117.
- Li, Z., He, M., Lam, F., and Li, M 2015. Load-sharing mechanism in timber-steel hybrid shear wall systems. Frontiers of Structural and Civil engineering 9(2): 203–214.
- Li, Z. Dong, H., Wang, X., and He, M. 2017. Experimental and numerical investigations into seismic performance of timber-steel hybrid structure with supplemental dampers. Engineering Structures, 151:33-43.
- National Lumber Grading Authority (NLGA). 2017. Standard grading rules for Canadian lumber. Vancouver, Canada.
- NZS3604:2011 – Timber-framed buildings. Standards New Zealand.
- Pang, W., Rosowsky, D. V., Pei, S., & van de Lindt, J. W. 2010. Simplified direct displacement design of six-story woodframe building and pretest seismic performance assessment. Journal of structural engineering, 136(7), 813-825.
- Priestley, M.J.N., Calvi, G.M. and Kowalsky, M.J. 2005. Direct displacement-based seismic design of structures.IUSS Press, Pavia.

16/716

Cyclic behaviour of timber-steel hybrid shear walls

Darren Kho, Wenchen Dong, Minghao Li, and Chin-Long Lee

Department of Civil Engineering and Natural Resources Engineering, University of Canterbury, New Zealand

2018 NZSEE Conference

ABSTRACT: Timber-steel hybrid structures provide a viable solution to strengthen lateral load resisting systems in multi-storey timber residential buildings. This paper investigated cyclic behaviour of one type of timber-steel hybrid shear walls consisting of steel moment resisting frames and plywood infill walls. A detailed finite element model was developed to model the hybrid wall behavior under cyclic loading. The hysteretic parameters of critical connection elements were calibrated by experimental testing results. A parametric study was further conducted to investigate the effect of nail size and plywood thickness on the hybrid wall behavior. Overall, the hybridization of the steel moment frame and the plywood infill walls can provide significantly better performance compared with conventional plywood shear walls. And a combination of ϕ3.15x75mm nails with 17mm thick plywood in the infill wall seems to provide the optimal hybrid wall performance.

1 INTRODUCTION

Due to limited strength and stiffness of sawn timber, conventional light-timber frame (LTF) construction is uncommon to build multi-storey residential buildings in seismic regions such as New Zealand. Currently NZS3604:2011 for timber-framed buildings only allows to build LTF buildings up to a maximum of 2 or 3 storeys. In recent years, research has shown that timber-steel hybrid structures are able to provide high lateral capacity and have the potential to overcome the height restrictions of conventional LTF construction. Dickof et al (2012) introduced a timber-steel hybrid system consisting of steel frames and infill cross laminated timber (CLT) panels. He et al (2014) proposed a timber-steel hybrid system consisting of steel moment frames and oriented strand board (OSB) infill walls. Experimental investigations and numerical studies on these systems have been conducted to better understand the load sharing mechanism, critical design parameters and seismic performance (Li et al. 2014, 2015, and 2017).

The paper presents a numerical study on the cyclic behaviour of one type of timber-steel hybrid shear wall system consisting of steel moment frames and plywood infill walls, as shown in Figure 1. Two critical connections exist in the hybrid system: timber-sheathing connections and timber-steel connections. The timber-sheathing connections are comprised of plywood and timber framing members connected by nail fasteners. These connections provide ductility and energy dissipation for the infill wall via nail yield bending and wood embedment deformation. The timber-steel connections are comprised of timber framing members joined to steel framing members via bolts that can facilitate shear transfer from the steel frame to the infill wall. This study numerically investigates the effect of nail fasteners and plywood sheathing on the hybrid wall performance. Different nail sizes and plywood thicknesses are considered in the finite element (FE) hybrid wall modelling. In addition, experimental testing was conducted to evaluate the critical connection properties and calibrate the input parameters of the connection elements in the FE models. Critical shear wall properties such as strength, stiffness, ductility and energy dissipation are evaluated and compared between various wall configurations according to the FE modelling results.

2 HYBRID WALL MODELLING

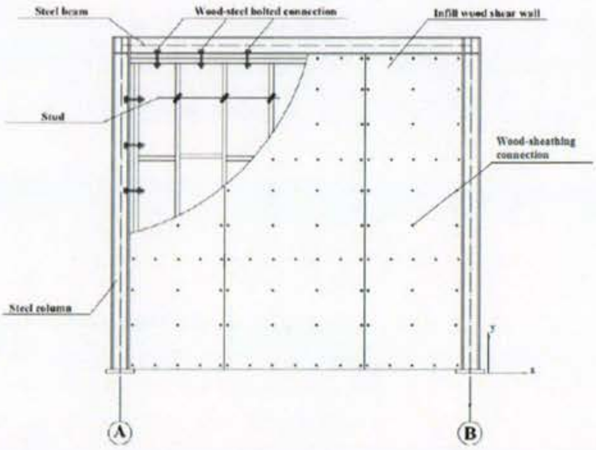

Figure 1: Configuration of a typical timber-steel hybrid shear wall

A detailed FE model of a timber-steel hybrid shear wall structure was developed in a software package called ABAQUS. The model is comprised of three types of elements: beam elements for timber and steel framing members, panel elements for plywood sheathing and spring elements for the timber-sheathing connections and timber-steel interface connections.

2.1 Framing and sheathing elements

Material properties of the steel beam elements (ABAQUS element B21) were defined as elastic-perfectly plastic. Beam-column joints were modelled as rigid connections. Column supports were modelled as rotational linear spring elements with a rotational spring stiffness of 2.015e7 kNm/rad based on previous research conducted by Dong (2017).

Plywood shear walls were modelled using existing plate elements (CPS4R) in ABAQUS. Material properties were taken as elastic. The (in-plane) average elastic modulus for plywood was taken both directions (parallel and perpendicular to face grain).

Timber framing members material properties was taken as elastic. Timber framing supports were modelled as rotational linear springs with a spring stiffness of 10000 kNm/rad. This allowed compression forces in the plywood to be resisted in shear by the supports, and later recorded to determine the force contribution in the plywood shear wall.

2.2 Connection elements

For the critical connections in the system, user defined nonlinear spring elements were used in the model. Their hysteric behavior was calibrated by experimental testing on a group of timber-steel and timber-sheathing connections. Non-critical connections such as the connections between timber framing members were simply assumed as pinned.

2.2.1 Experimental Testing of Connections

Following the ISO16670:2003 test standard monotonic and cyclic tests were conducted on a total of 240 nailed timber-plywood connections and 30 bolted timber-steel connections. The timber specimens were all made of Radiata Pine sourced from NZ. Plywood sheathing was Grade F8 manufactured to AS/NZS2269:2012. Timber studs were Stress Grade 8 (SG8) and manufactured to AS/NZS1748:2011. In the nailed timber-sheathing connections tests, three nail sizes (ϕ2.8x50mm, ϕ3.15x75mm, and ϕ3.55x90mm) and three plywood thickness (12mm, 17mm, and 25mm) were tested. Two loading orientations for timber-sheathing connections were considered – parallel to the timber and the plywood face grain and perpendicular to the timber grain and the plywood face grain. For the bolted timber-steel connections, the timber components were loaded parallel to the grain. Grade 300 M12 bolts were used. Figures 2 shows the test setups and typical load-slip hysteretic curves for the nailed connections and the bolted connections.

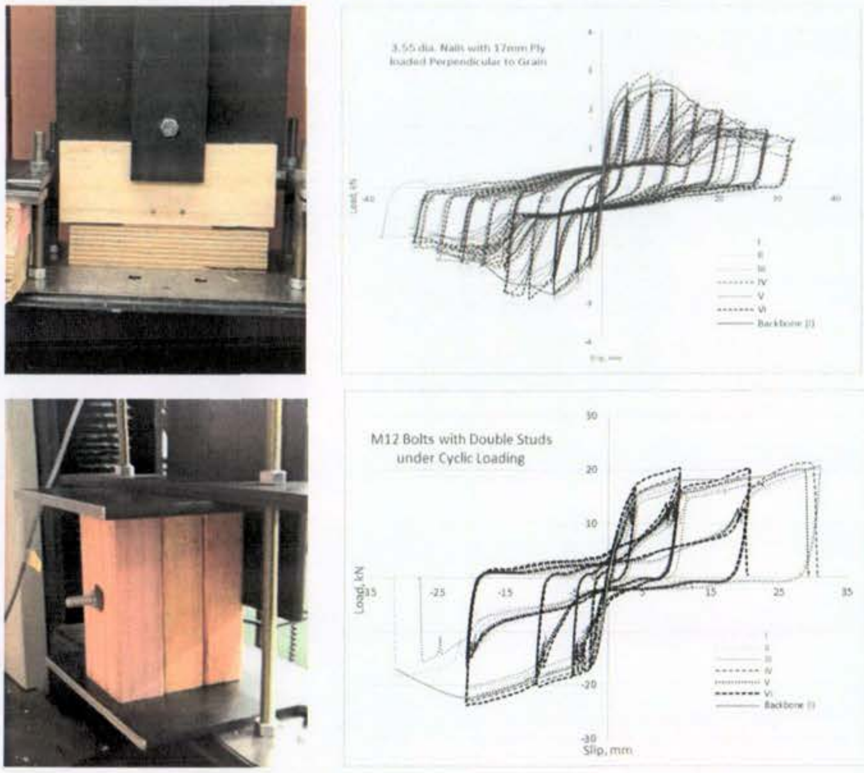

Figure 2 Test setup of nailed connections (left) and bolted connections (right) and typical load-slip hysteretic curves

2.2.2 Modelling of Connections

The nonlinear behavior of the hybrid shear walls is mainly governed by the critical connections and the steel MRF yielding under high loads. Therefore, it is important to incorporate robust connection elements for the hybrid wall model. As shown in Figure 4, Q-pinch hysteretic algorithm, proposed by Folz, et al (2001), was used to model the hysteretic behavior of the critical connections. In timber shear walls under lateral loads, nail fasteners tend to deform along different directions, and will not be restricted to only horizontal or vertical movement. Therefore, the oriented spring pairs proposed by Judd (2005) were also used to model the coupling behavior of the nailed connections along the original motion direction and the perpendicular to the original direction.

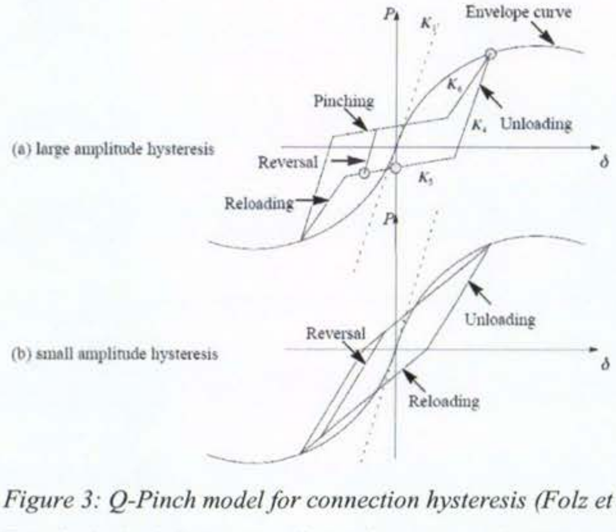

Figure 3: Q-Pinch model for connection hysteresis (Folz et al 2001)

For the bolted timber-steel interface connections, Li et al [6] suggested that these connections should be strong enough and avoid any premature failure before the failure of the infill wall. For these connections, the bolt fasteners are restrained by the flanges of steel members and the timber framing members under lateral loading. Therefore, it was assumed that these connections only deform in lateral and axial directions. Non-oriented (uncoupled) spring pairs were adopted to represent the connection behavior under shear loading and axial loading. The Q-pinch algorithm was used to model the connection behavior under shear loads. Elastic springs were used to model the connection behavior under axial loads.

In this study, the data obtained in experimental tests were used to calibrate the connection parameters. The average parameter values between the perpendicular and parallel to grain loading orientations were taken to represent the nails in the hybrid system. Table 1 lists the calibrated Q-pinch parameters for the nailed connections and the bolted connections under shear loads.

Table 1: Critical connections tested on and their calibrated parameters

Nail size	Plywood thickness	*Initial stiffness,* k_1, N/mm	*Plastic stiffness,* k_2, N/mm	*Degradation stiffness* k_3 N/mm	*Unloading stiffness,* k_4, N/mm	*Yield Force* F_0, N	*Pinching Force* F_1, N	Δ_y, mm	Δ_{ult}, mm	Δ_{fail}, mm	Reloading degradation factor, α	Stiffness degradation factor, β
ϕ2.8x50	12mm	846	25	38.5	920	782.5	175	1.1	9.9	16	0	1.1
ϕ 3.15x75	12mm	625	20	20	675	1120	250	2.0	7.3	21	0	1.05
ϕ 3.55x90	12mm	1243	39	33	1950	1070	320	1.1	10	20	0	1.1
ϕ2.8x50	17mm	850	35	60	1050	750	150	1.1	8.2	14	0	1.1
ϕ 3.15x75	17mm	1094	25	31.5	1450	1025	220	1.6	18.3	24	0	1.1
ϕ 3.55x90	17mm	970	27	35	1000	1090	305	1.1	12.6	25	0	1.1
ϕ 3.15x75	25mm	1131	34	35	1231	935	310	1.1	8.2	15	0.35	1.1
ϕ 3.55x90	25mm	1303	53	50	1903	1175	280	1.1	10	17	0.2	1.1
M12 Bolt	-	7200	7400	100000	7400	16500	4200	2.5	28	30	0.7	1.1

2.3 Validation of Hybrid Wall Models

The FE wall model was validated by experimental results of a hybrid shear wall consisting of a steel moment frame and an OSB infill wall. Detailed information about the experimental testing was reported by Dong (2017). The model input parameters for the critical connections were also calibrated by the experimental testing of the nailed timber-OSB connections and the bolted timber-steel interface connections. Figure 5 shows the tested wall configuration, the FE wall model, and the model predicted load-drift hysteresis compared with the results. It can be seen that the model prediction agreed well with the test results.

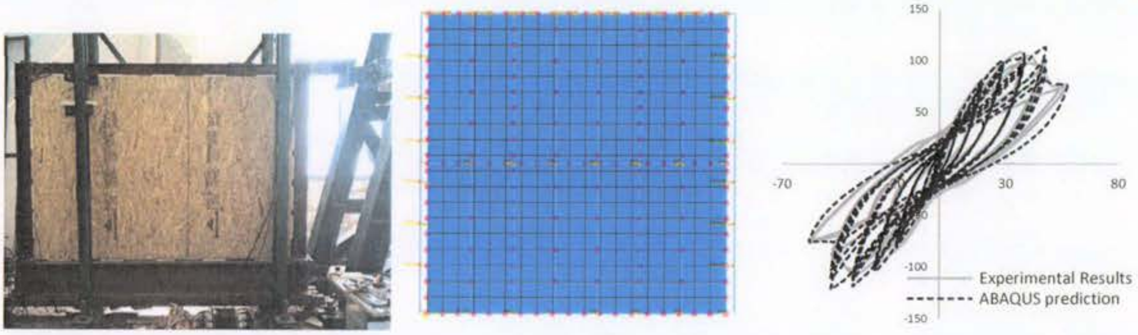

Figure 4: Hybrid wall configuration for model calibration (left). Detailed FE model of hybrid wall experiment (center). Hybrid wall model prediction vs. experimental results (right)

3 PARAMETRIC ANALYSIS

3.1 Wall configuration

Using the validated FE hybrid wall model, a parametric study was carried about on a 3.6m x 2.4m hybrid wall consisting of a steel moment frame and infill plywood shear walls. As shown in Figure 5, the wall configuration was chosen for NZ applications. The types of steel beams and columns, timber members, plywood sheathing, and metal fasteners with the corresponding properties are given in Table 2. The numerical model was subjected to a cyclic loading protocol based on ISO16670:2003. In the parametric study, the configuration of the steel frame was fixed while different combinations of nail fasteners and plywood thickness were considered.

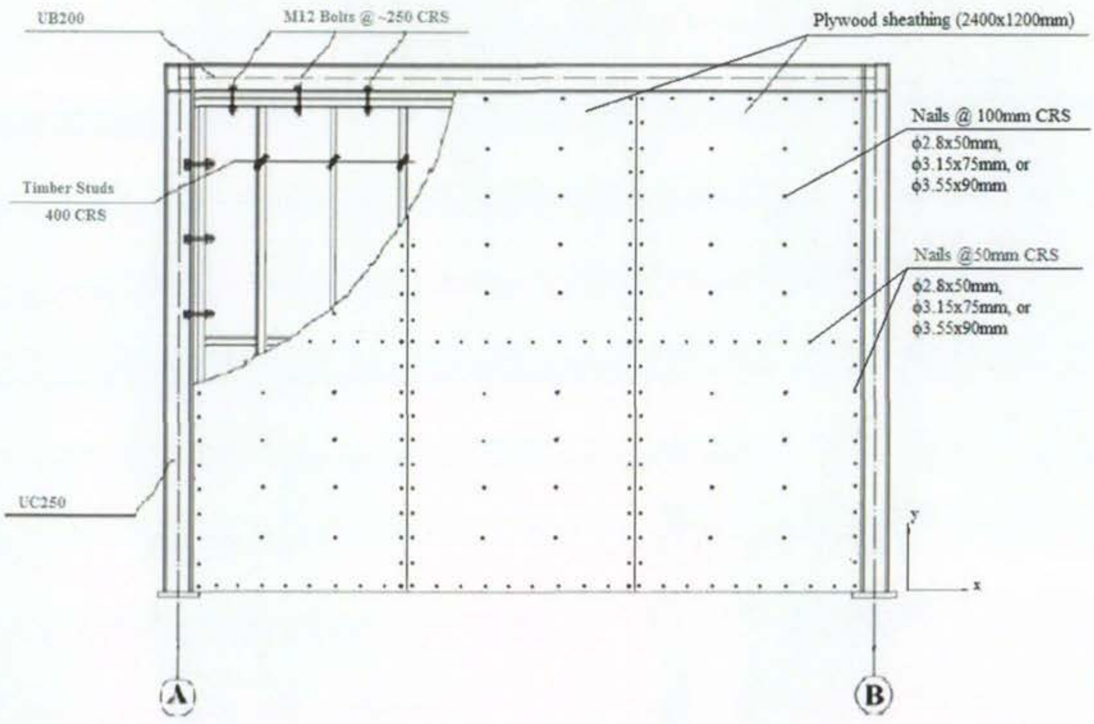

Figure 5: Structural configuration of timber-steel hybrid shear wall

Table 2: Structural properties adopted in the hybrid system

Component	*Size*	ρ	*E (MPa)*	v	*G (MPa)*	σ_y *(MPa)*	σ_p *(MPa)*	ε_p
Steel beam	200UB	7850	210E3	0.3	-	300	301	0.001
Steel column	250UC	7850	210E3	0.3	-	300	301	0.001
Plywood	12, 17, 25mm	650	Ex = Ey = 9100	0.12	455	-	-	-
Timber frame	90x45mm	450	8000	0.3	-	-	-	-
Nails	ϕ2.8x50, ϕ3.15x75, ϕ3.55x90	-	-	-	-	-	-	-

3.2 Results

Table 3 shows the results of the parametric study. Figure 6 shows typical load-drift hysteretic curves of the bare steel frame, the plywood infill wall if working on its own, as well as the hybrid wall system. The wall parameters such as strength, stiffness and ductility ratio μ were evaluated as per ASTM E2126 [13].

Table 3: Summary of parametric study results

Wall #	Nail size	Plywood thick-ness	P_{peak}, kN	$P_{infill, peak}$, kN	k_{hybrid}, kN/m	k_{infill}, kN/m	R	P_{yield}, kN	Δ_y, mm	Δ_{ult}, mm	μ	E_{diss} (kJ)
1	ϕ2.8 x 50	12mm	182	105	4.7	3.0	1.8	151	23.7	142	6.0	12.7
2	ϕ 3.15 x 75	12mm	204	126	4.3	2.7	1.6	171	29.1	195	6.7	28.2
3	ϕ 3.55 x 90	12mm	224	147	5.1	3.6	2.3	176	25.1	180	7.2	26.6
4	ϕ 2.8 x 50	17mm	180	144	5.2	3.6	2.2	146	20.7	102	4.9	12.3
5	ϕ 3.15 x 75	17mm	223	140	5.6	4.0	2.5	182	23.8	216	9.1	35.2
6	ϕ 3.55 x 90	17mm	222	144	5.4	3.8	2.3	182	24.8	180	7.3	28.7
7	ϕ 3.15 x 75	25mm	201	123	6.3	4.7	3.0	165	19.2	142	7.4	20.3
8	ϕ 3.55 x 90	25mm	242	168	6.6	5.1	3.4	192	21.2	160	7.6	24.8
Avg			210	137	5.4	3.8	2.4	171	23.4	165	7.0	23.6

Note: R is defined as k_{infill}/k_{bf}, and k_{infill} is the initial stiffness of plywood infill wall and k_{bf} is the initial stiffness of the bare steel frame; E_{diss} is the total energy dissipation of the shear wall.

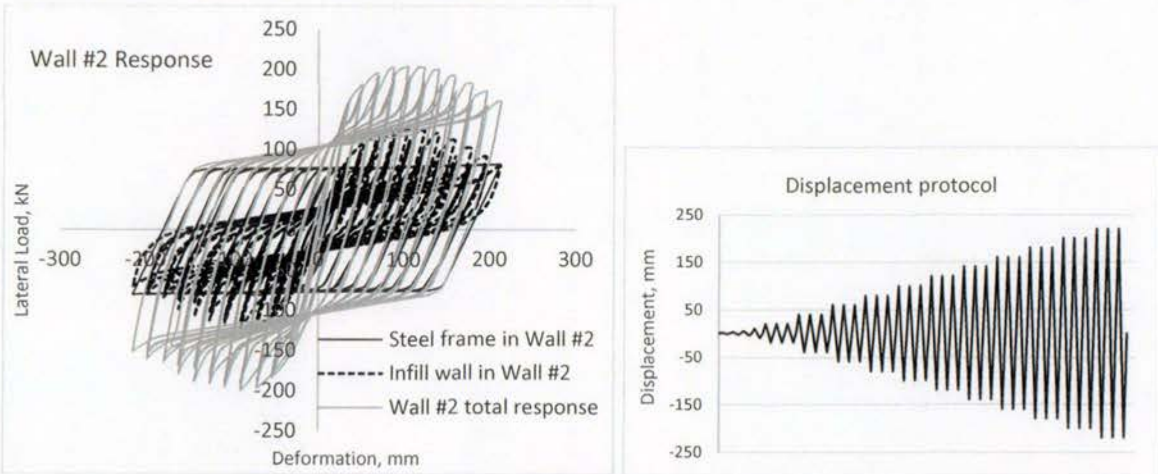

Figure 6: (Left): Typical hybrid shear wall response. Note contributions from steel frame and plywood infill wall. (Right): Cyclic loading protocol as per ISO16670:2003

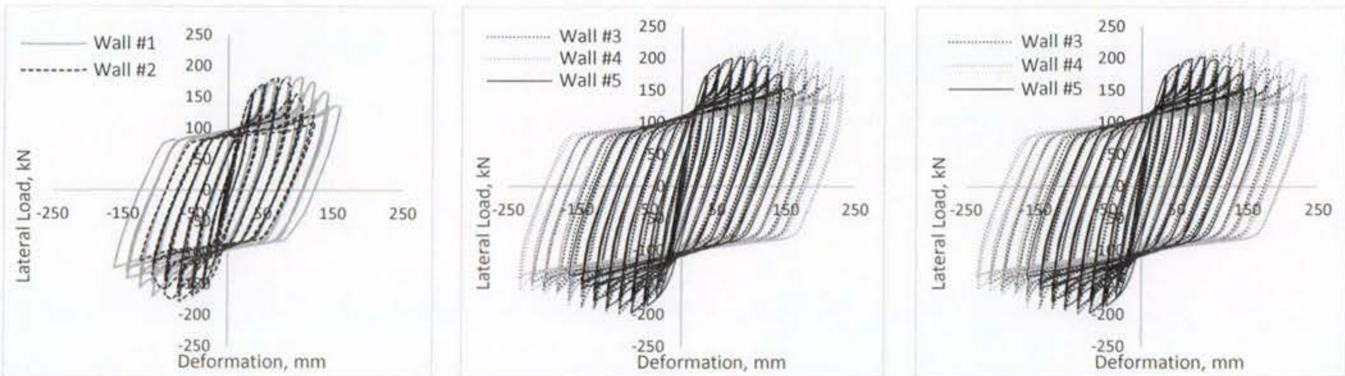

Figure 7: Hysteresis curves of Wall #1 to Wall #8

3.3 **Discussion**

The hybridization of the steel moment frame and infill plywood shear wall significantly increased the wall stiffness and strength compared with plywood shear walls acting independently. Depending on the type of infill wall configurations, the addition of steel moment frame increased the wall stiffness by 32% – 57% and the peak loads by 25% – 73%. It was also found the plywood infill wall carried the majority of the lateral load during initial stages of loading (between 64% – 77%) and dissipated the seismic energy through nailed connections. The ductility ratios of the hybrid walls ranged from 4.9 to 9.1, indicating good ductility of the system.

3.3.1 *Effect of plywood thickness on hybrid system*

Adoption of larger nails and thicker plywood tends to increase the load carrying capacity of the hybrid walls. However, this is not always the case. In the wall configurations using ϕ3.15x75mm nails where the peak load decreased when the plywood thickness increased from 17mm to 25mm. This is because the capacity of the hybrid system is affected by the timber-sheathing connection strength which is dependent upon a number of connection parameters such as nail size, plywood thickness, timber density and nail penetration depth as well. Due to the fact that the penetration length of the nail fastener decreased from 58 mm to 50 mm as plywood thickness increased from 17mm to 25mm, the connection strength drecreased leading to the reduction of the hybrid wall capacity.

The infill wall-to-bare frame stiffness ratio R of the hybrid system has a positive trend with increases in plywood thickness. In this study, R ratios increase between 9% – 56% as plywood thickness is incrementally increased, regardless of the nail size combination. This translates to 9.8% – 30.2% increases in the initial stiffness of the hybrid system. An R ratio greater than 1 will allow the infill walls will carry higher lateral loads than the bare steel frame during the intial stages of loading.

It was also found that the highest ductility factors were provided by the timber-sheathing connections using 17mm thick plywood in combination with larger nails (ϕ3.15x75mm and ϕ3.55x90mm). 17mm thick plywood with smaller nails (ϕ2.8x50mm) is not advised due to insufficent nail penetration length.

3.3.2 *Effect of Nail size*

The parametric study also showed that the nail size inrease (ϕ2.8x50mm, ϕ3.15x75mm, ϕ3.55x90mm) generally increased both the load carrying capacity by 10% – 24%. Increasing nail size also generally increases the ductility. However, in the timber-sheathing connection configurations using 12mm and 17mm plywood, Numerical models of the experimental nail connection data show that ϕ3.55x90mm nails used in combination with 12mm and 17mm ply have smaller ultimate displacements than ϕ3.15x75mm nails used with 12mm and 17mm ply. Results show that using timber-sheathing connections with ϕ3.15x75mm nails in combination with either 12mm or 17mm thick plywood provide the largest ductility factors. Larger nails are recommended to meet requirements for higher peak loads. ϕ3.15x75mm nails seem to provide the greatest ductility while providing comparable strengths to the larger ϕ3.55x90mm nails.

4 CONCLUSION

The hybrid walls consisting of steel moment frames and plywood infill walls had significantly high load carrying capacity and initial stiffness than conventional plywood shear walls, while maintaining good system ductility. In some cases, the load carry capacity and initial stiffness was almost twice of those of the plywood shear walls. This provides great benefits in terms of limiting non-structural damages under serviceability level earthquakes and increased load carrying capacity under major earthquakes.

Increased nail size and plywood thickness tend to increase the load carry capacity and stiffness of the hybrid system. However, proper nail size and plywood thickness should be checked to eliminate the non-ductile nailed connection behavior in the infill walls.

A combination of ϕ3.15x75mm nails with 17mm thick plywood in the infill wall provided the optimal hybrid wall performance in terms of strength, initial stiffness, ductility and energy dissipation.

The parametric study was limited to one type of steel moment frame with a given wall dimension. Further research is needed to consider the influence of the steel frame design on the overall hybrid system behavior.

5 ACKNOWLEDGEMENT

EQC Earthquake Commission is acknowledged for providing a biennial grant to support this research project. Prof. Minjuan He from Tongji University, China is also acknowledged for sharing experimental data of the hybrid shear walls.

6 REFERENCES

AS/NZS1748:2011. "Timber – Solid – Stress-graded for structural purposes." *Standards New Zealand.*

AS/NZS2269:2012. "Plywood – Structural." Standards New Zealand. *Standards New Zealand.*

ASTM E2126:2011 - Standard test methods for cyclic (reversed) load test for shear resistance of vertical element of lateral force resisting systems for buildings". *ASTM International.*

Dickof C., Stiemer S. F., Tesfamariam S. 2012. Wood-steel hybrid seismic force resisting systems: seismic ductility. *Proc. 12th World Conference on Timber Engineering, Auckland, New Zealand.*

Dong, W. 2017. Lateral behavior of connections between steel moment-resisting frame and wood-frame shear wall in the hybrid system. Master's thesis, *Tongji University, Shanghai*

Folz, B. and Filiatrault, A., 2001. Cyclic analysis of wood shear walls. *Journal of Structural Engineering, 127(4), 433-441.*

He M., Li Z., Lam F., Ma R., Ma Z. 2014. Experimental investigation on lateral performance of timber-steel hybrid shear wall systems. *Journal of Structural Engineering, 140(6): 04014029-1~12*

ISO16670. 2003. "Timber Structures – Joints made with mechanical fasteners – Quasi-static reversed-cyclic test method." *The International Organization for Standardization, Geneva.*

Judd, J. P. 2005. Analytical modeling of wood-frame shear walls and diaphragms. Masters of Science thesis. *Brigham Young University.*

Li Z., He M., Li M., Lam F. 2014a. Damage assessment and performance-based seismic design of timber-steel hybrid shear wall systems. *Earthquakes and Structures. 7(1): 101-117.*

Li, Z., He, M., Lam, F., and Li, M 2015. Load-sharing mechanism in timber-steel hybrid shear wall systems. *Front. Struct. Civ. Eng 9(2): 203–214*

Li, Z. Dong, H., Wang, X., and He, M. 2017. Experimental and numerical investigations into seismic performance of timber-steel hybrid structure with supplemental dampers. *Engineering Structures, 151:33-43.*

NZS3604:2011 – "Timber-framed buildings." *Standards New Zealand.*

WCTE 2018
2018 World Conference on Timber Engineering
August 20 - 23, 2018 | Seoul, Republic of Korea

PERFORMANCE OF STEEL-TIMBER HYBRID SHEAR WALL SYSTEMS

Wenchen Dong[1], Darren Kho[2], Minghao Li[3], and Chin-Long Lee[4]

ABSTRACT: This paper studies cyclic behaviour of timber-steel hybrid shear walls consisting of steel moment frames and plywood sheathed infill walls. Connection testing is conducted to study the behaviour of critical nailed plywood connections and timber-steel interface connections in the hybrid system. The influence of steel frames, nail sizes, plywood thicknesses, and timber-steel interface connections on the overall wall performance are investigated by numerical model simulations. This study considers three types of nails, three plywood thicknesses, and two types of interface connections. The experimental data are used to calibrate the input parameters of nonlinear spring elements that are integrated into a detailed finite element model to simulate the hybrid wall responses. The hybrid system's performance is evaluated by a parametric analysis and seismic design recommendations with a case study are also suggested to achieve optimal infill wall design.

KEYWORDS: Nailed connections, plywood, timber-framed shear walls, ductility, cyclic tests

1 INTRODUCTION

In recent years, timber-steel hybrid structures have gained research interests to overcome limitations of conventional timber buildings. For example, Dickof et al. [1] introduced a timber-steel hybrid system consisting of steel frames and infill cross laminated timber (CLT) panels. Another timber-steel hybrid system consisting of steel moment frames and oriented strand board (OSB) sheathed timber infill walls was proposed by He, et al. [2]. Experimental studies and numerical modeling on such a system have been conducted to study loading sharing mechanism, critical design parameters and seismic performance [3-5].

In New Zealand, bracing walls in low-rise timber houses are mostly sheathed with gypsum plaster boards. When higher bracing requirement for wind and seismic loads is required, for example, in multi-storey buildings, plywood shear walls are normally used. Considering high seismicity in New Zealand, the timber-steel hybrid solutions are suitable to provide a cost-effective lateral force resisting system for multi-storey residential buildings due to enhanced strength and stiffness.

This paper presents a parametric study on cyclic behaviour of timber-steel hybrid wall systems consisting of steel moment frames and plywood infill walls, as shown in Figure 1. The study aims to understand the influence of nail sizes, plywood thicknesses, and timber-steel interface connections on the overall hybrid wall performance by numerical model simulations. The model input for critical connection behaviour in the hybrid walls is calibrated by experimental data of nailed timber-plywood connections and timber-steel interface connections. Critical design properties such as strength, stiffness, and ductility will be evaluated and compared between various wall configurations according to model simulation results. Methodology and technical considerations will also be given for multi-storey buildings.

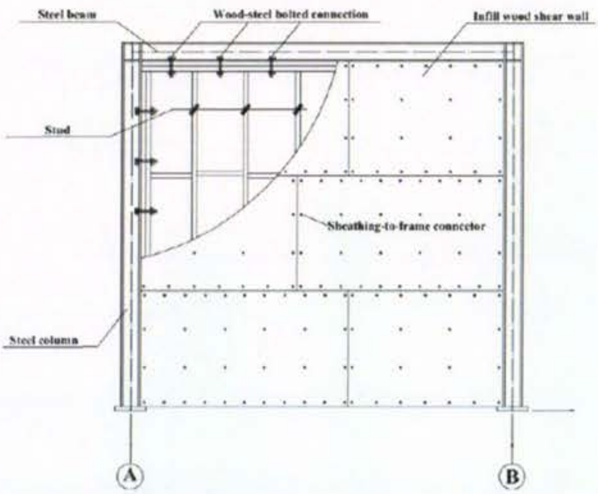

Figure 1: Typical timber-steel hybrid wall configuration

2 METHODS

2.1 EXPERIMENTAL TESTING

Cyclic testing following the ISO16670 test standard [6] was conducted on a total of 160 nailed timber-plywood connections, 40 screwed connections and 40 bolted

[1] wenchen.dong@pg.canterbury.ac.nz, Civil & Natural Resources Engineering, University of Canterbury, New Zealand
[2] darren.kho@pg.canterbury.ac.nz, Civil & Natural Resources Engineering, University of Canterbury, New Zealand
[3] minghao.li@canterbury.ac.nz, Civil & Natural Resources Engineering, University of Canterbury, New Zealand
[4] chin-long.lee@canterbury.ac.nz, Civil & Natural Resources Engineering, University of Canterbury, New Zealand

connections. In the test specimens, timber members and plywood panels were all made out of NZ grown Radiata pine. In the nailed connection tests, three nail sizes (ϕ2.8x50mm, ϕ3.15x75mm, and ϕ3.55x90mm) and three plywood thicknesses (12mm, 17mm, and 25mm) were considered. Two loading orientations for timber (parallel to grain and perpendicular to grain) were considered as well. For the bolted/screwed timber-steel interface connections, the timber members were loaded parallel to the grain direction with bolts (M10, M12 and M14) and coach screws (M10 and M12) respectively. Figure 2 and 3 show the test setups and typical test results in terms of load-displacement curves. Six specimens were tested for each type of connection.

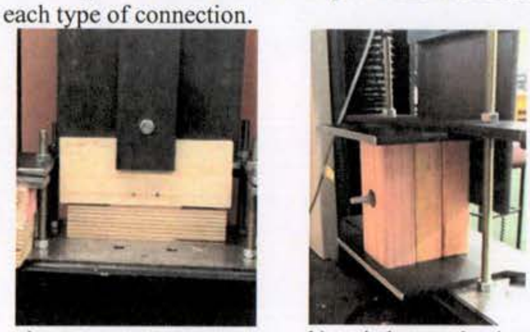

a) Test setup of nailed connections b) timber-steel interface connections

Figure 2 experimental test layouts

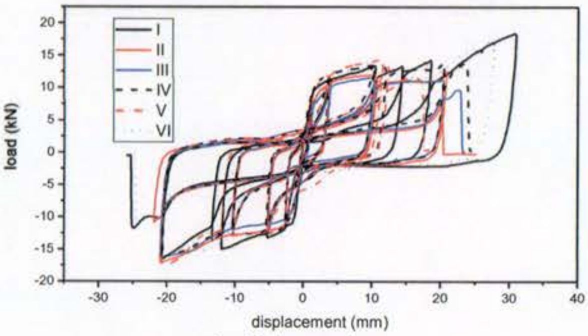

a) Bolt connections

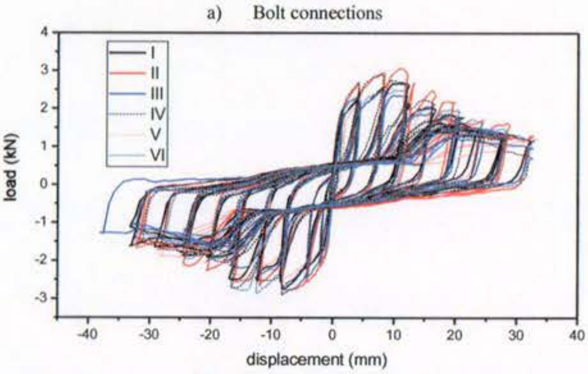

b) Nailed connections

Figure 3 Load-displacement hysteresis of bolted and nailed connections

2.2 Connection modelling

There are two major types of connections in the timber-steel hybrid wall systems: nailed connection and timber-steel interface connection.

2.2.1 Nailed connection modelling

The nonlinear characteristics of timber-steel hybrid shear walls are primarily from nails in the sheathing-to-frame connections. An exponential envelope curve and a hysteretic algorithm (Q-pinch) proposed by Folz,et al[7] and Johhn[8] respectively are utilized to represent the behaviour of nailed connections. Figure 4 illustrates typical constitutive relationships of modelling the connections. In this study, the data obtained in experimental tests were used to calibrate the nailed connection parameters and all parameters required to define constitutive relationships are listed in Table 1. Figure 5 presents one of the curve-fitting results. During the curve-fitting process, average strength extracted from data parallel and perpendicular to grain were employed to estimate the strength. The fitted curve demonstrates a good agreement with the experimental one.

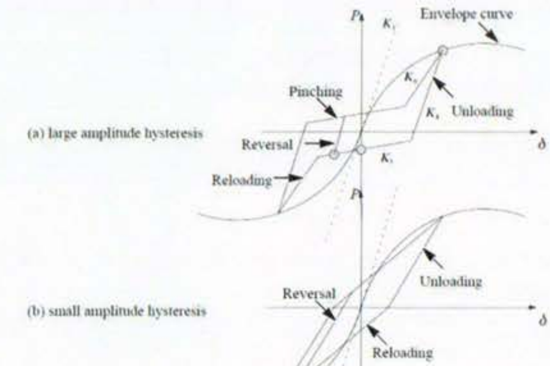

Figure 4 Constitutive relation of sheathing-to-frame connector[8]

Table 1 parameters for Q-pinch model

parameters	stiffness				force		displacement		α	β
	k_1	k_2	k_3	k_4	F_0	F_1	Δ_y	Δ_u		
2.8-12	846	25	38.5	850	782.5	175	1.2	9.9	0	0.95
2.8-17	850	35	60	950	750	150	0.7	8.2	0	1.1
3.15-12	625	20	20	625	1120	250	1.2	7.3	0	1.05
3.15-17	1094	25	31.5	1250	1025	220	1.55	18.25	0.7	1.05
3.15-25	1131	20	25	1131	1110	280	1.1	8.5	0.8	1.05
3.55-12	1243	39	33	1250	1070	320	1.1	10	0.7	1.05
3.55-17	970	27	35	970	1090	305	1.1	12.6	0.52	1.05
3.55-25	1303	53	50	1303	1175	280	1.1	10	0.8	1.05

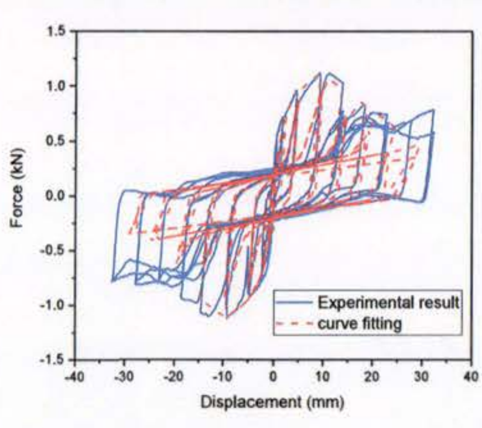

Figure 5 Curve fitting between experiments and simulations

When nails are installed from the sheathing into studs, they tend to deform in various directions instead of only the horizontal or vertical direction. In order to consider this, oriented spring pairs are assumed in a local coordinate system with local directions $\boldsymbol{u}$ and $\boldsymbol{v}$. Figure 6 shows an oriented spring pair, which is established by rotating the horizontal direction by the angle ϕ. Direction $\boldsymbol{u}$ is established as the **nail's initial** direction of motion and the direction $\boldsymbol{v}$ is perpendicular to it.

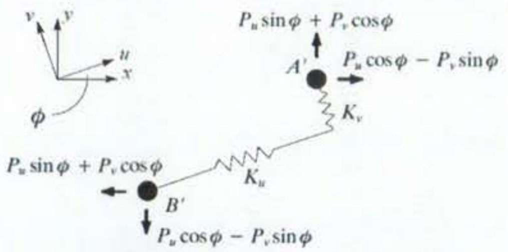

Figure 6 Oriented spring pair[8]

2.2.2 Timber-steel interface connection modelling

The timber-steel interface connections help to transfer loads from the steel frame to the infill timber shear wall so that two subsystems have compatible deformations.

The same constitutive relationship model assumptions used for the nailed connections are used for connections in the shear direction of bolts/screws. However, bolt/coach connections are much stronger than nailed connections, **thus, the parameters' values** for bolt/coach connections are different from nailed connections.

For timber-steel interface connections, bolts/screws are restrained by flanges of the steel beam and column and studs of the infill shear wall. Therefore, assumption that bolts/screws only deform in horizontal and vertical directions is applied to this model. Consequently, non-oriented spring pair shown in Figure 7 is adopted. Experimental tests shown in Fig 2b provided the load-displacement curves parallel to grain. In the direction perpendicular to grain, load transfer is assumed through bearing along the entire length of the studs. Thus an elastic constitutive relationship is used.

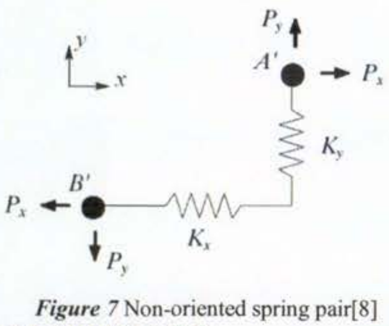

Figure 7 Non-oriented spring pair[8]

2.3 WALL MODELLING

Numerical simulations of the hybrid walls were carried out in a commercial software package ABAQUS[9]. User defined elements were employed to model the nailed connections and the interface connections as well. A bilinear property was induced for the steel frame and the timber members and plywood panels were assumed to remain linear elastic during the whole process. The nailed connections and the timber-steel interface connections were modelled as nonlinear springs with the load-displacement relationship calibrated by the test results. The hybrid shear wall model was validated by the hybrid shear wall testing results presented in literature [10]. As seen in Figure 8, the predicted load-displacement relationship agrees well with experimental result.

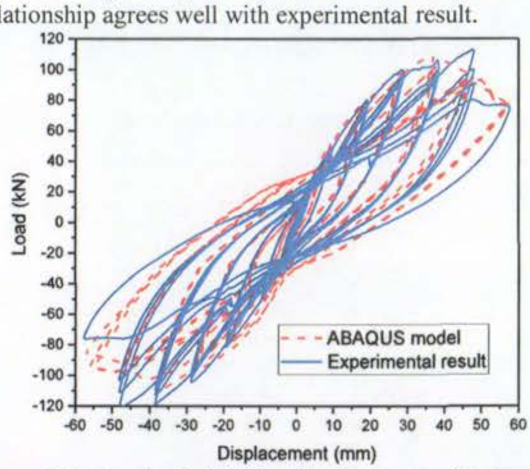

Figure 8 Hysteresis of a hybrid wall vs. hysteresis of a plywood shear wall[10]

3 Discussion

3.1 Model general description

Figure 9 shows a benchmark detailed 2D timber-steel hybrid shear walls model built in ABAQUS. The span and height of steel frame is 3750mm and 2475mm. The size of infill shear wall is 3600mm×2400mm. Cross sections chosen from AS/NZS 3679.1:2016[11] are applied for the beam and column. Radiata pine 90×45mm sawn timbers are used as framing members for infill walls. The diameter and length of nails, thicknesses of plywood panels and diameters of bolts and coach screws used in model are the same with specimen tests. Table 2 represents property of all materials input in ABAQUS.

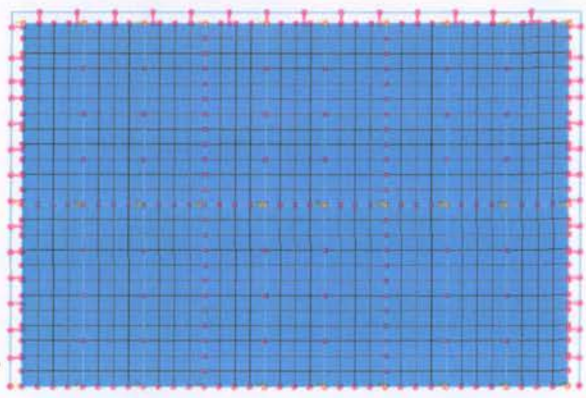

Figure 9 Detailed 2D hybrid shear wall model

Table 2 property of materials

	ABAQUS element	Element property
Frame studs	B21	E=9700MPa =450kg/m³
plywood	CPS4R	E1=E2=E3=9100MPa G12=455Mpa =450kg/m³

Nails between studs	CONN2D2	join
Steel frame	B21	E=210000MPa $f_y = 300Mpa$

Ultimate strength F_{max} is defined as the highest strength the hybrid system can achieve during loading. And initial stiffness $K_{initial}$ in ISO16670[12] is induced by Eq. 1 to evaluate strength and stiffness. $\Delta_{0.4}$ and $\Delta_{0.1}$ are displacement at 40% and 10% of F_{max}.

$$K_{initial} = (0.4F_{max} - 0.1F_{max})/(\Delta_{0.4} - \Delta_{0.1}) \qquad \text{Eq.1}$$

3.2 Timber-steel interface connections

As mentioned in Section 2.2.2, it is required to have enough connections such that the two subsystems have loading sharing effect through compatible deformations. In this model, 14 connections on each side were used to make sure that the connections are the strongest part of hybrid system. Because the experiments of bolts and screws provided different load-displacement curves in shear direction, these parameters were changed in the analysis below.

Five different types of timber-steel interface connections (M10, M12 and M14 for Bolts and M10 and M12 for screws) were investigated in the same configuration shear walls with ϕ3.15x75mm nails, 17mm plywood and 100/300 nail spacing, which means interior nail spacing is 100mm and exterior one is 300mm for a panel. The results are presented in Table 3 which shows that if enough number of connections are configured, all of the shear walls can reach the same initial stiffness and ultimate strength. Thus, all connection types are efficient for hybrid system and the distinction of interface connection types can be neglected.

Table 3 Results for different interface connections

	F_{max} (kN)	$K_{initial}$ (kN/mm)
M10 Bolt	89.17	1.72
M12 Bolt	89.20	1.72
M14 Bolt	89.22	1.72
M10 Coach	88.91	1.71
M12 Coach	89.02	1.72

To consider the influence of the interface connections on the overall system behavior, connection strengths in the shear force direction of bolts/screws were investigated. Five same configuration shear walls consisting of ϕ3.15x75mm, 17mm plywood and 100/300 nail spacing were used. The strength of connections was scaled down to 80%, 60%, 40% and 20% of experimental strength respectively in the shear direction. Figure 10 illustrates that strength degradation in the shear wall direction **won't** have an obvious impact on hybrid system as less than 1% decrease was observed. The initial stiffness can decrease slightly by at most 7%. The reason that both strength and **stiffness didn't decrease** significantly is that the steel frame restrained the vertical motion of the infill shear wall, which is the considered shear force direction above. Most load was transferred by bearing compression between the steel column and side studs. It is also seen that connections between interfaces are important to keep two subsystems contact tightly so that load can be transferred by bearing. This bearing effect is beneficial to the hybrid system because it reduces the shear forces between interfaces and the uplift forces in the shear wall. As a consequence, hold-down installments can be avoided and erections on site will be more convenient.

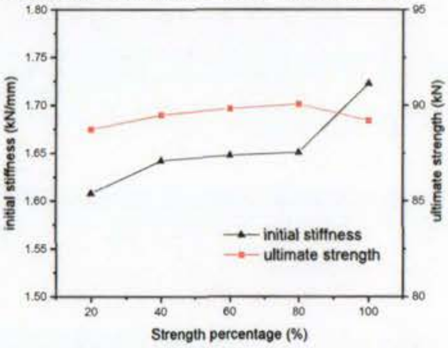

Figure 10 Strength and stiffness for different interface connections

3.3 Steel frame

Several sizes of steel frames were chosen in models with ϕ3.15x75mm, 17mm plywood and 50/300 nail spacing. Their loading curves in one specific path are shown in Figure 11. Also, ultimate strength and initial stiffness are presented in Table 4. Figure 11 shows that the steel frame's **cross section** will increase the strength and stiffness; however, the ductility remains unchanged. Because a bilinear plastic model for steel is used in modelling, the decreasing in strength will only be governed by infill shear wall. It is also noticed that similar beam and column cross sections can achieve a higher strength as the plastic hinges of beam edges restrain the strength increase. In terms of economic design, similar beam and column sections and smaller steel frames are recommended.

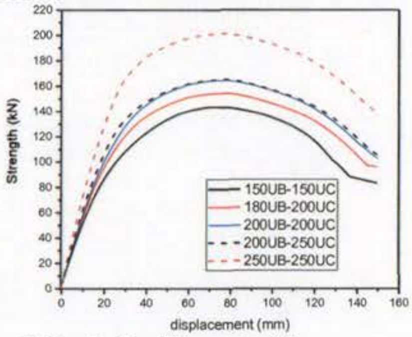

Figure 11 Results for different steel frame cross sections

Table 4 Result for different steel frame cross sections

Beam-Column size	F_{max} (kN)	$K_{initial}$ (kN/mm)
150UB-150UC	143.52	3.12
180UB-200UC	154.54	3.44
200UB-200UC	164.71	3.70
200UB-250UC	165.07	3.75
250UB-250UC	201.49	4.83

3.4 Nail sizes and Plywood thicknesses

It is observed from experiments that the nail sizes and plywood thicknesses contribute to strength and stiffness together. In order to collect more combinations, 50/300, 75/300,100/300 and 150/300 nail spacing configurations were adopted to compare the effect of nail sizes and plywood thicknesses.

12mm and 17mm plywood were used for all three types of nails in the experiments, thus these combinations were used in modelling. Figure 12 presents that the ultimate strength of hybrid system is approximately linear with nail size. The slope of trend line is mainly relative to nail spacing.

For the nails, ϕ3.15x75mm, and ϕ3.55x90mm sizes were experimentally tested with all sizes of sheathing panels. Therefore, they were utilized to observe the effect of plywood thickness. As seen in Figure 13, plywood thickness's influence on strength is neligible for ϕ3.15x75mm with all nails spacing but for ϕ3.55x90mm, slightly increase can be found. According to Figure 12 and 13, plywood thickness has limited attribution to bigger size nail in term of strength. For smaller size nails, the strength is mainly governed by nail size. As a result, ϕ3.15x75mm, and ϕ3.55x90mm nails are recommended.

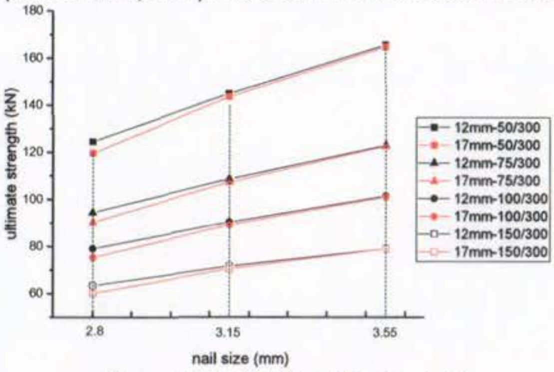

Figure 12 Strength for different nail sizes

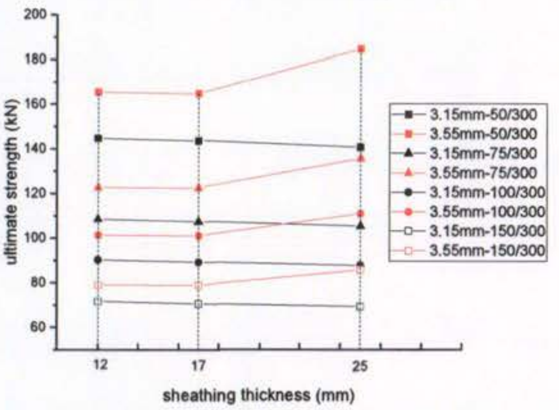

Figure 13 Strength for different plywood thickness

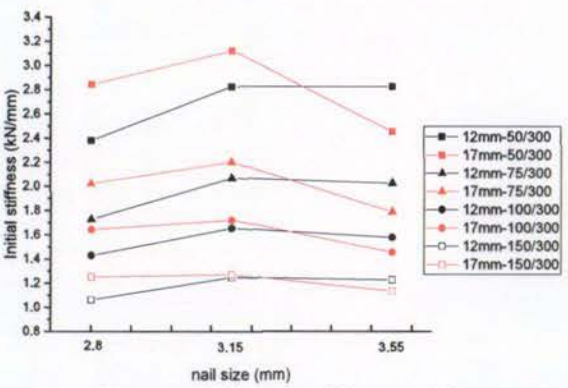

Figure 14 Stiffness for different nail sizes

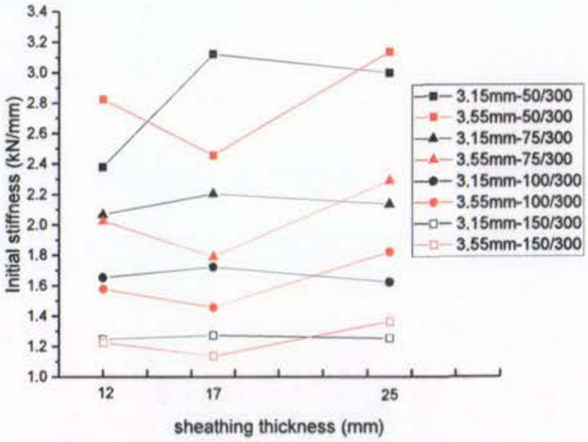

Figure 15 Stiffness for different plywood thickness

Regarding initial stiffness, Figure 14 and 15 shows the results for different nail size and plywood thickness. Initial stiffness fluctuated with nail size and plywood thickness. The initial stiffness mainly depends on the combination of nail sizes and plywood thicknesses. ϕ3.15x75mm with 17mm plywood and ϕ3.55x90mm with 25mm plywood are better choices for high initial stiffness.

3.5 Lateral performance and ductility

The distributions of lateral shear forces have a major impact on this hybrid system's performance and consequently, causes ductility differences. Ratio ρ of lateral forces defined in Eq.2 is considered as an index to describe the distribution. $V_{shearwall}$ is the shear force carried by the shear wall and V_{total} is the total shear force carried by the hybrid system. Figure 16 demonstrates that the shear wall's sharing shear force percentage changed with drift. 150UB and 150UC were set as beam and column in all models with nail spacing 100/300. It is shown that the shear wall tends to carry most (more than 80%) of lateral load initially and then the percentage will decrease gradually due to nails' yielding. With the development of plasticity, a larger ratio of shear forces will be transferred to the steel frame so that the system can achieve a better ductility compared to traditional timber walls, whose allowable drift is only 2.5% in NZS1170.5:2004[13].

$$\rho = \frac{V_{shearwall}}{V_{total}} \qquad \text{Eq.2}$$

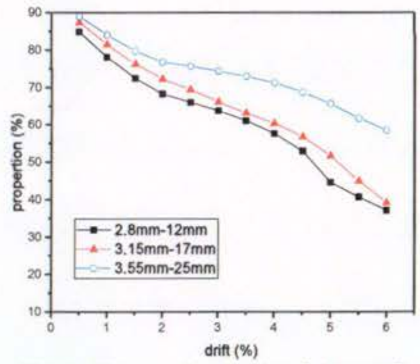

Figure 16 proportional ratio of shear wall

Ductility of the hybrid system can be measured by a ductility factor μ defined as Eq.3. U_{max} is considered as maximum displacement the hybrid system can reach or 6% drift. U_y is the displacement at 80% of ultimate strength. Variations in nail size and plywood thickness combinations with 100/300 nail spacing were measured and the results are listed in Table 5. Table 5 shows that **hybrid system's ductility factor ranges from 1.48 to 1.87**. The system consisting of ϕ3.15x75mm with 17mm plywood has the best ductile performance.

$$\mu = \frac{U_{max}}{U_y} \qquad \text{Eq.3}$$

Table 5 Ductility factor for hybrid system

Plywood thickness \ nail size	ϕ 2.8x50	ϕ 3.15x75	ϕ 3.55x90
12	1.64	1.74	1.65
17	1.48	1.87	1.48
25		1.73	1.58

4 Seismic Design methodology

4.1 Direct displacement Design

Due to the highly nonlinear characteristics of timber shear walls, performance-based seismic design (PBSD) has been proven to be a better design method instead of force-based design. For timber-steel hybrid system, the timber shear wall carries a high proportion of loads and the hybrid system shows nonlinearity. Therefore, PBSD is appropriate method in hybrid system design. Weichiang[14] proposed a direct displacement procedure as shown in Figure 17 based on experimental researches. The method only requires normalized modal analysis and shear wall design tables instead of detailed FEM model. Thus, it is quite convenient for design. As previous parameter analysis, design tables for timber-steel hybrid system can also be produced and are shown in Table 6. As a result, direct displacement design can be established for the hybrid system.

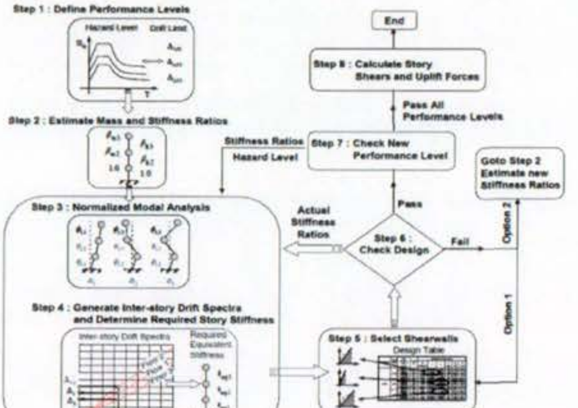

Figure 17 Flow chart for direct displacement design[14]

Table 6 Hybrid shearwall design table

Nail spacing	nail size	sheathing thickness	wall ID		equivalent stiffness(kN/mm) at target drift					
					drift(% of storey height)					
					0.50	1.00	1.50	2.00	2.50	3.00
50/300	2.80	12	p1	keq	4.61	3.93	3.41	2.98	2.66	2.40
		F		F	52.65	82.33	99.78	111.99	120.31	124.07
		17	p2		4.61	3.93	3.41	3.00	2.68	2.38
		F			52.59	82.30	100.42	113.59	119.61	106.54
	3.15	12	p3		4.21	3.82	3.51	3.20	2.92	2.66
		F			49.62	86.05	112.16	129.77	139.80	144.18
		17	p4		5.27	4.59	4.03	3.54	3.15	2.84
		F			61.00	98.16	119.40	133.00	142.10	148.73
		25	p5		5.28	4.55	3.95	3.46	3.08	2.77
		F			60.79	95.88	115.97	129.68	138.15	140.53
	3.55	12	p6		5.56	4.87	4.28	3.77	3.37	3.05
		F			64.54	104.39	127.54	142.79	153.40	161.21
		17	p7		5.07	4.50	4.01	3.57	3.20	2.90
		F			59.16	98.12	122.19	137.50	147.58	154.96
		25	p8		5.72	5.08	4.53	4.04	3.63	3.30
		F			66.92	111.07	138.15	155.96	168.53	178.73
100/300	2.8	12	p9		3.06	2.5	2.14	1.87	1.67	1.51
					33.84	50.8	61.85	70.74	76.57	79.04
		17	p10		3.06	2.5	2.14	1.88	1.68	1.5
					33.78	50.85	62.36	71.8	75.41	73.11
	3.15	12	p11		2.8	2.48	2.23	2.02	1.84	1.67
					32.5	54.43	69.93	81.1	87.03	89.65
		17	p12		3.6	2.97	2.54	2.21	1.97	1.78
					40.16	60.6	73.1	82.58	88.86	93.1
		25	p13		3.6	2.93	2.48	2.16	1.92	1.73
					39.74	59	71.18	80.86	86.04	87.6
	3.55	12	p14		3.84	3.17	2.71	2.36	2.11	1.9
					42.89	64.59	78.07	88.49	95.58	99.62
		17	p15		3.45	2.92	2.54	2.24	2.01	1.82
					39.11	61.18	75.08	85.34	92.05	96.65
		25	p16		4	3.35	2.89	2.54	2.28	2.06
					45.11	69.45	84.81	96.55	104.67	109.48

4.2 Case Study

4.2.1 Description of a six-story hybrid building

A six-story timber-steel hybrid system having plan dimension of 22.5mx9m and storey height of 2.5m is selected as a study case. The plan layouts is shown as Figure 18. The building is located in Christchurch, New Zealand with site subsoil class D referring to NZS

1070.5:2004[13]. 5% damping ratio is adopted. Other defined design parameters are collected in Table 7 and spectral shape factor is presented in Eq. 4.

$$C_h = \begin{cases} 1.12 & T=0 \\ 1.12+1.18(T/0.1) & 0<T<0.1 \\ 3.0 & 0.1<T<0.56 \\ 2.4(0.75/T)^{0.75} & 0.56 \le T \le 1.5 \\ 2.14/T & 1.5<T\le 3 \\ 6.42/T^2 & T>3 \end{cases} \qquad \text{Eq. 4}$$

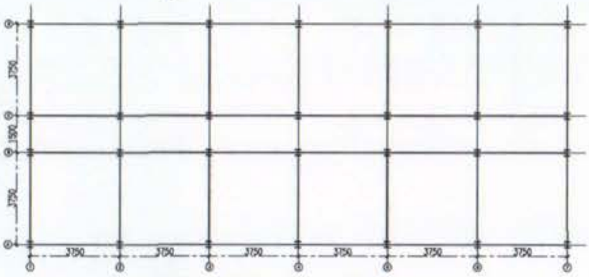

Figure 18 Plan and vertical layouts

Table 7 Seismic design parameters

Parameter name	symbol	Value
Hazard factor	Z	0.3
Return period factor	R	1.8
Near-fault factor	N	1.0

4.2.2 Define performance levels and response spectrum

Because steel frames have a better ductile performance than infill timber shear walls, a design performance level of 3% interstory drift can be defined for 2%/50 years seismic hazard as **Weichiang's paper**[14], which is also defined as collapse prevention(CP) performance level in FEMA 356[15]. Instead of MCE in ASCE 7-05, New Zealand Building code provides design seismic acceleration based on 10%/50 years and return period factor R will be used to amplify the seismic loading.

The design acceleration response spectrum for CP performance level is defined as Eq. 5. The maximum acceleration S_d is 1.62g as shown in Figure 19.

$$C(T) = C_h(T)ZRN(T,D) \qquad \text{Eq.5}$$

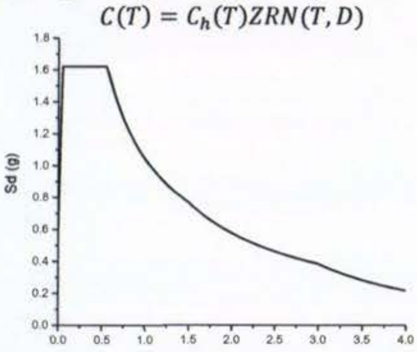

Figure 19 Design acceleration response spectrum

4.2.3 Establish interstory Drift Spectrum

The effective seismic weights for floors and roof are shown in Table 8. The storey stiffness is estimated by design experience. Consequently, mass and stiffness ratio can be defined as Eq.5. By modal analysis, the interstory drift spectrum can be established. From Figure 20, the required period is 0.145s when interstory drift reaches to 3%.

Table 8 Loading and seismic weight

	Dead load(kPa)	Imposed load(kPa)	Effective seismic weight
Floor	1.0	2.0	324kN
Roof	0.8	0.5	193kN

$$\beta_m = [1.0\ 1.0\ 1.0\ 1.0\ 1.0\ 0.59]^T$$
$$\beta_{ke} = [1.0\ 0.92\ 0.82\ 0.62\ 0.54\ 0.37]^T \qquad \text{Eq.5}$$

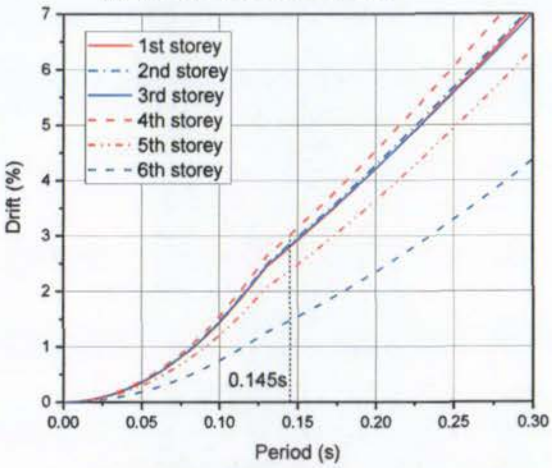

Figure 13 Design acceleration response spectrum

4.2.4 Choose hybrid shearwalls from design tables and check by real stiffness

The required stiffness of each storey can be extracted by using Eq.6. In Eq.6 m is the **first storey's seismic mass.** According to the required stiffness, the required number and layout of shearwalls can be chosen from Table 6 based on **hybrid shear walls' stiffness at the drift of 3%.** The required number of walls and configurations are presented in Table 8. For first storey, 18 shear walls with wall ID p8 are required. After layouts of shear walls are decided, actual stiffness ratio of designed building can be nailed down. Instead of estimated stiffness ratio β_{ke}, the actual stiffness ratio β_{ka} will be used to decide actual required stiffness of the system. Verification is necessary to make sure the actual required stiffness is less than actual interstorey stiffness. Table 8 shows that the designed configurations satisfy defined performance level.

$$k_{req} = \left(\frac{2\pi}{T_{req}}\right)^2 \beta_k m \qquad \text{Eq.6}$$

Table 8 Shearwall configuration results and verification

storey no	K_{req} (kN/mm)	Configuration	K_{real}	K_{req} based on K_{real}
1	56.85	18xp8	59.4	56.85
2	52.3	18xp7	54.9	52.53
3	46.61	16xp7	48.8	46.73
4	35.25	12xp7	36.6	35.01
5	30.7	12xp3	31.92	30.53
6	21.03	12xp15	21.84	20.9

5 CONCLUSIONS

This paper presents parametric analysis of hybrid timber-steel shear walls based on experimental results. PBSD methodology is also adopted for this hybrid system. Conclusions are summarized as below:

- All types of timber-steel interface connections are efficient to transfer load between the steel frame and the shear wall. The effect among different connections is negligible if enough numbers of connections are provided.
- Bigger sizes of steel frames increase the system's ultimate strength but have no impact on the initial stiffness. Similar sizes of column and beam cross sections are recommended regarding better ultimate strength.
- Nail sizes are proportional to ultimate strength but plywood thicknesses' influence on strength is negligible. The systems consisting of ϕ3.15x75mm with 17mm plywood and ϕ3.55x90mm with 25mm plywood are better choices.
- The steel frame offsets strength degradation of the infill shear wall and provides support for it. Further, hold-downs are not required in hybrid system and ductile lateral performance is obtained, which is much higher than building code's requirement.
- Design tables for hybrid system are formed and direct displacement design is used for design. The study case shows that in 2%/50 years seismic hazard, hybrid system can provide good seismic performance up to 3% drift ratio. It is a feasible alternative for multi-storey buildings in high seismicity region.

ACKNOWLEDGEMENT

The authors would like to acknowledge Earthquake Commission of New Zealand to fund the project under a biennial research grant.

REFERENCES

[1] Dickof C., Stiemer S. F., Tesfamariam S. 2012. "Wood-steel hybrid seismic force resisting systems: seismic ductility". Proc. 12th World Conference on Timber Engineering, Auckland, New Zealand

[2] He M., Li Z., Lam F., Ma R., Ma Z. 2014. "Experimental investigation on lateral performance of timber-steel hybrid shear wall systems". Journal of Structural Engineering, 140(6): 04014029-1~12

[3] Li Z., He M., Li M., Lam F. 2014a. "Damage assessment and performance-based seismic design of timber-steel hybrid shear wall systems" Earthquakes and Structures. 7(1): 101-117.

[4] Li, Z., He, M., Lam, F., and Li, M 2015 "Load-sharing mechanism in timber-steel hybrid shear wall systems." Front. Struct. Civ. Eng 9(2): 203–214

[5] Li, Z. Dong, H., Wang, X., and He, M. 2017 "Experimental and numerical investigations into seismic performance of timber-steel hybrid structure with supplemental dampers" Engineering Structures, 151:33-43.

[6] ISO16670. 2003. "Timber Structures – Joints made with mechanical fasteners – Quasi-static reversed-cyclic test method." The International Organization for Standardization, Geneva.

[7] Folz, B. and Filiatrault, A., 2001. "Cyclic analysis of wood shear walls". Journal of Structural Engineering, 127(4), 433-441.

[8] Judd, J. P. 2005. "Analytical modeling of wood-frame shear walls and diaphragms". Brigham Young University.

[9] Hibbitt, Karlsson, & Sorensen. 2001. "ABAQUS/Standard user's manual (Vol. 1) ". Hibbitt, Karlsson & Sorensen.

[10] Wenchen,D. 2017. "Lateral behavior of connection between steel moment-resisting frame and wood-frame shear wall in the hybrid system". Master thesis,Tongji University, Shanghai, China.

[11] Standard.2016. "AS/NZS 3679.1:2016 Structural Steel – part 1: Hot-rolled bar and sections". Sydney/Wellington, Australia/New Zealand: Standards Australia/Standards New Zealand.

[12] International Organization for Standardization (ISO).2003. "Timber structures – Joints made with mechanical fasteners – Quasi-static reversedcyclic test method". ISO 16670, Geneva, Switzerland.

[13] Standard,N.Z.2004. "NZS 1170.5:2004 Structural Design Actions – part 5: Earthquake actions-New Zealand". Wellington, New Zealand: Standards New Zealand.

[14] Pang, W., & Rosowsky, D. V. 2010. "Direct displacement procedure for performance-based seismic design of multistory woodframe structures". MCEER.

[15] Prestandard, F. E. M. A. 2000. "commentary for the seismic rehabilitation of buildings (FEMA356) ". Washington, DC: Federal Emergency Management Agency, 7.

Seismic performance evaluation of timber-steel hybrid structure through large-scale shaking table tests

Minjuan He[1], Qi Luo[1], Zheng Li[1,*], Hanlin Dong[1], Minghao Li[2]

[1] *Department of Structural Engineering, Tongji University, Shanghai, China*

[2] *Department of Civil & Natural Resources Engineering, University of Canterbury, Christchurch, New Zealand*

Abstract

This paper presents the results of shaking table tests on a two-thirds scale four-story timber-steel hybrid structure. The hybrid structural system, developed recently, consists of prefabricated infill timber shear walls and steel moment-resisting frames serving as two structural subassemblies to resist seismic loads together. The hybrid structure was subjected to earthquake ground motions at three different hazard levels with peak ground accelerations scaled to 0.14g, 0.40g, and 0.80g, respectively. Over 200 sensors were used to measure the responses of the structure in terms of acceleration, inter-story drift, roof displacement, load sharing between the steel frames and wood infill walls, etc. The proportion of the shear force resisted by the infill timber shear walls was assessed by peak shear force ratio (*R*), and the results showed that the infill walls significantly contributed to the lateral resistance of the hybrid structure. The structure performed very well with little damage observed after severe earthquake excitations corresponding to the maximum credible earthquake

shaking with a return period of 2450 years.

Keywords: Shaking table test; Timber-steel hybrid; Multi-story building; Seismic performance; Load-sharing effect

1. Introduction

As a building material, wood is gaining more popularities due to its renewability and sustainability. Numerous publications have highlighted the smaller environmental footprint of wood over other construction materials [1]. Wood buildings are able to store carbon during the life cycles and reduce greenhouse gas emission significantly. As a building material, wood has much lower density compared with other conventional building materials, meaning lower seismic load demand and reduced foundation cost. Over the past two decades, a significant breakthrough has been made in the research field of multi-story timber and timber hybrid buildings, focusing on innovative structural systems, seismic performance, fire safety, acoustic effect, etc. Timber Frame 2000 project (TP 2000 project), initiated by the Building Research Establishment (BRE) in U.K., was carried out to investigate the performance and economic prospects of multi-story timber frame buildings. The TP2000 project offered a safe and uncomplicated means to ensure the good performance of mid-rise timber structures and helped to open up a new market for timber buildings up to 7 stories [2], [3]. In 1999, researchers in Japan launched a project focusing on hybrid timber solutions [4]. A series of shaking table tests on three timber-reinforced concrete structures were carried out [5], and performance evaluation methods and design guidelines for such timber-based hybrid structures were proposed [6]. In Europe, SOFIE project was launched to investigate the performance of prefabricated cross-laminated timber (CLT) structures [7]-[9]. Shaking table tests were conducted on a full-scale seven-story CLT building, and the test results showed superior seismic performance of the building [10]-[12]. An advanced finite element (FE) model was further developed to model the building and validated against the shaking table test results [13]. Upon the trend of building taller wood buildings, two multi-institutional research projects were launched in North America. The NEESWood project in the U.S. focused on the development of performance-based design procedures for multi-story light timber frame buildings. In 2009, a full-scale mid-rise light frame apartment building was tested under a series of earthquakes [14]. No significant structural damage to the building was observed even under the maximum considered earthquake (MCE) shaking. The developed performance-based design procedure was shown to be quite effective to ensure life safety [15]-[17]. The Newbuilds project in Canada seeks to explore new opportunities for multi-story and high-rise timber buildings. A hybrid solution with a steel moment frame and CLT infilled shear walls was proposed by Tesfamariam et al [18], [19]. Experimental tests at component levels were carried out to study the performance of connections between the infilled CLT panel and the steel frame [20], and a displacement-based design methodology was developed for this type of structures [21]-[23].

Timber-based hybrid structures represent one of the most effective solutions of using more sustainable construction materials in built environment. An innovative timber-steel hybrid structural system was proposed by He et al. [24] and Li et al. [25]. Such a timber-steel hybrid structure incorporates conventional infilled light timber frame shear walls within steel moment-resisting frames (Fig. 1). The hybridization can increase the structural efficiency and lead to a higher prefabrication level and reduce overall construction cost. Monotonic and reversed cyclic tests were carried out on single-story timber-steel hybrid structures to investigate the lateral performance [24], [25], and parametric analyses were conducted to investigate the loading resisting mechanism, mainly the load-sharing effect between the infill system and the steel frame [26]-[28]. This paper presents the capstone phase of the experimental studies on the proposed timber-steel hybrid structural system. A series of shaking table tests were conducted on a four-story 8.8 m tall timber-steel hybrid structure. The building was tested under a series of earthquake ground motions scaled to three seismic intensity levels. The seismic performance of the hybrid structure was assessed comprehensively. The building response in terms of accelerations, inter-story drifts, roof displacements, load sharing between the steel frames and wood infill walls were carefully monitored with over 200 sensors.

2. Test Specimen

2.1 Building dimensions

The building specimen was designed as a portion of a prototype office building located in Sichuan Province, a high seismic region across China. The prototype building has a floor plan of 3-bay by 6-bay along two directions, and the story height is 3.3m. The plan view and the elevation of the structure are shown in Fig. 2. According to Chinese Load Code for the Design of Building Structures [29] and the Code for Seismic Design of Buildings [30], the prototype building was designed with the soil type II and the seismic precautionary intensity level of 8, which is corresponding to the design spectral acceleration of 0.16 g under frequent earthquakes with a return period of 50 years. The dead and live loads used for the design are listed in Table 1.

One bay of the prototype building was selected to construct the test specimen, and the test specimen was further scaled to 2/3 of the original size due to the capacity limitation of the shaking table subjected to high overturning moment demand on a four-story building. Therefore, the specimen needed to consider an acceleration scale factor (S_a) of 2.0, and a stress scale factor (S_σ) of 1.0, respectively. Other scale factors involved in the specimen design were derived on the basis of the similitude law and are listed in Table 2. As shown in Fig. 3, the test specimen had a total height of 8.8 m, and the floor plan was 8 m by 3.75 m. The dimensions of the shaking table are 6.25 m by 4.25 m and was extended to 8.60 m in one direction by mounting an additional steel extension frame.

2.2 Design of the test specimen

Light frame timber shear walls were used as infill walls in the steel moment-resisting frame. The timber shear walls consisted of No. 2 grade (according to NLGA 2014 [31]) Spruce-Pine-Fir (SPF) dimension lumber studs with the cross section of 38 mm × 89 mm, and 12 mm - thick oriented strand boards (OSBs) were used as shear wall sheathings. The timber shear wall located from the 1st to the 3rd stories were double-side sheathed, while the timber shear walls in the X direction in the 4th story were single-side sheathed. The stud spacing was set as 406 mm in the X direction and 305 mm in the Y direction. The timber diaphragms were composed of joists of 38 mm × 184 mm SPF dimension lumber with 15 mm - thick OSB sheathing panels. The OSB sheathings for both the timber shear walls and the timber slabs were attached to the wooden framing via ϕ 3.3 × 82.5 nails. The nail spacing of the timber shear walls are given in Table 3

The steel frame was manufactured with Q235 steel, commonly used low carbon structural steel with yield strength of 235 MPa according to Chinese Code for Design of Steel Structures [32]. The elastic modulus of Q235 steel is 1.99×10^5 N/mm^2, determined through tensile coupon tests. The sections of the steel frame members are listed in Table 4. To prevent brittle failure at the beam-column connections, a "column-tree" system was adopted. As shown in Fig. 4, the column-trees were fabricated by welding a stub beam, with a length of 630 mm (suggest to indicate the distance in Fig. 4), to the column. As such, welding was mainly performed in the factory to ensure good quality. The rest of the beams were spliced to the stub beams by high-strength bolts after the column trees were erected on site. This could effectively speed up the erection. One 6 mm - thick steel doubler plate was welded at each panel zone of the corner columns and two 6 mm - thick doubler plates were welded at both sides of every panel zone elsewhere to avoid premature shear yielding of the panel zone.

Two types of connections (referred to as Connection A and Connection B, see Fig. 1) were designed to connect the timber shear walls to the steel frames. Connection A was used at the top of the wood wall, while Connection B was used at the bottom of the wood wall. As shown in Fig.5, Connection A consisted of an L-shaped steel connector and a Y-shaped steel connector. The L-shaped connector was connected to the flange of the steel beam by high strength bolts, and the Y-shaped connector was fastened to the timber shear wall by ϕ 3.5 × 60 mm self-tapping screws. Three M16 high strength bolts were used to connect the two connectors and transfer the shear force between the steel frame and the timber shear wall. Likewise, Connection B was connected to the steel frame by bolts and connected to the timber shear wall by self-tapping screws

In order to consider the imposed loads and the self-weight of non-structural members, a total of 7.955 ton additional mass was uniformly attached on the floors at 1st to 3rd story, and 5.115 ton additional mass was attached on the roof.

2.3 Data acquisition

The acceleration and displacement responses of the test specimen under seismic excitations were recorded by over 200 sensors. The instrumentation consisted of various types of accelerometers, linear voltage displacement transducers (LVDTs) and strain gages. As shown in Fig. 6, accelerometers were installed at the middle of the beams to monitor the horizontal accelerations in the X and the Y directions at each story. Four accelerometers were placed at the corner of the steel extension frame beneath the specimen to measure the vertical acceleration. Six LVDTs provided the displacement measurements at each story. The horizontal and vertical displacements of the steel extension beam were recorded by the other eight LVDTs.

The lateral force applied on the timber-steel hybrid system is resisted by the timber shear wall and the steel moment-resisting frame, thus the load-sharing mechanism in the hybrid structure has also been considered in this investigation. The total shear force resisted by the k^{th} story, Q_k, can be obtained by Eq. (1):

$$Q_k = \sum_{i=k}^{4} m_i a_i \tag{1}$$

where m_i and a_i are the mass and acceleration of the i^{th} story, respectively. A calculation procedure was carried out to acquire the portion of shear force resisted by the steel columns. As shown in Fig. 7, the strain gages $S_{kA,1}$ to $S_{kA,8}$ and $S_{kB,1}$ to $S_{kB,8}$, located at 600 mm and 1400 mm height of the steel column, were used to calculate the shear force transferred in the steel column, Q_k^c. On the basis of a previous numerical analysis, the segment of this 800 mm long steel column was close to the point of contraflexture and remained elastic during the tests. Eq. (2) was used to calculate the shear force in one of the steel columns:

$$Q_k^c = \frac{M_t + M_b}{L} = \frac{EW(\varepsilon_{t\max} + \varepsilon_{t\min} + \varepsilon_{b\max} + \varepsilon_{b\min})}{2L} \tag{2}$$

As shown in Fig. 8 and Eq. (2), N is the axial force in the steel column; M_t and M_b are the bending moments measured by the upper strain gages and the lower strain gages, respectively; $\varepsilon_{t\max}$ and $\varepsilon_{t\min}$ are the maximum and minimum measurements by the upper strain gages; $\varepsilon_{b\max}$ and $\varepsilon_{b\min}$ are the maximum and minimum measurements by the lower strain gages; L is the vertical distance between these two sets of the strain gages; W is the section modulus of the steel column; and E is the elastic modulus of steel [24]. Using Eq. (2), the total shear force $\sum Q_k^c$ resisted by the steel columns at k^{th} story can be calculated by summing up all the shear forces in the steel columns. Accordingly, the shear resistance contributed by the timber shear walls for the k^{th} story can be calculated by Eq (3).

$$\sum Q_k^w = Q_k - \sum Q_k^c \qquad \text{Eq. (3)}$$

2.4 Test program

Wenchuan earthquake (May 12, 2008), Canterbury earthquake (February 22, 2011), El-centro earthquake (May 18, 1940) and Kobe earthquake (January 17, 1995) were selected as seismic excitations for the shaking table tests. Fig. 10 shows the unscaled spectral accelerations of the input ground motions. To fulfill the similitude requirement, the original records were scaled by S_t=0.5774 in time. During the tests, some of the ground motions were unidirectional while others were bidirectional. After applying an acceleration scale factor (S_a) of 2.0, the peak ground acceleration (PGA) of the unidirectional seismic excitations, as well as the X-component (primary component) of the bidirectional seismic excitations, was scaled to 0.07g, 0.40g, and 0.80g in accordance with the Chinese Code for Seismic Design of Buildings [30]. When determining the scale factors of the Y-component (secondary component) of the bidirectional seismic excitations, more details should be taken into consideration. Firstly, the PGA ratio between the secondary component and the primary component is 0.85 according to the Chinese Code for Seismic Design of Buildings [30]. Secondly, in the transverse direction of the prototype, the tributary area of the sub-structure covered two bays of the prototype equivalently, the area indicated by the red dotted lines in Fig. 9. However, in the longitudinal direction, the tributary area of the sub-structure was one bay of the prototype. Therefore, the corresponding equivalent mass in the longitudinal direction was half of the mass in transverse direction. In order to consider this effect, the PGA of the secondary component of the bidirectional seismic excitations was further reduced by half. Consequently, when bidirectional seismic excitations were conducted, the ratio of secondary component PGA to primary component PGA is $0.85 \times 0.5 = 0.425$.

The test program is given in Table 5 . To investigate the seismic performance of the hybrid structure influenced by different timber shear wall stiffness, the infill shear walls in the X direction at the 1st and 2nd stories were strengthened after the 12th test. The changes of building natural frequency was obtained by white noise scanning after each seismic excitation. The completed building specimen on the shaking table is shown in Fig. 11.

3. Results and discussions

3.1 Dynamic identification

The identification of dynamic characteristics of the test specimen was obtained by white noise excitations. Fig. 12(a) shows the change of fundamental frequencies of the specimen in the X direction and the corresponding damping ratios after each seismic excitation. As the intensity of the ground motions increased, the frequency decreased and the damping ratio increased gradually, indicating the progressive stiffness degradation of the test specimen, and this was mainly due to the damage accumulation in the timber shear walls. (Suggest to remove the overlapped parts in

Fig. 12) From Test 12 to Test 13, the frequency increased by 6.7% and the damping ratios decreased by 26.6% because the timber shear walls were strengthened after Test 12, as mentioned before. When the tests were completed, the fundamental frequency of the specimen dropped to 3.531 Hz but the damping ratio increased to 0.119. Fig. 12(b) shows the measurements after each seismic excitation of major seismic events. It is noted that the decrease of fundamental frequency and the increase of damping were primarily caused by the El-centro and Kobe earthquake excitations, indicating that considerable damages had occurred in the structure under these two seismic excitations. However, the fundamental frequency in the minor direction, i.e., the Y direction remained about 3.875 Hz with no significant changes throughout the entire test sequence.

3.2 Acceleration response

High floor acceleration responses in a building during earthquakes may cause non-structural damage and discomfort or even injury to occupants. The acceleration amplification factors β, defined as the ratio of the peak floor acceleration to the PGA, are provided in Fig. 13. The β factors of the test specimen varied from 0.67 to 3.35. The β factors before and after the test specimen was strengthened under unidirectional seismic excitations with different intensity levels are compared in Fig. 13 (a) - (d). Generally, β factors decreased slightly after the test specimen was strengthened. The β factors under the moderate earthquake shaking were obviously smaller than those under the minor earthquake shaking. However, when the PGA of the seismic excitations increased to 0.80g, the reduction of β was only observed during the

Wenchuan earthquake shaking and the Canterbury earthquake shaking. The magnitude of β increased with the height of the structure and the distributions of the β varied with different earthquake ground shaking. The β factors of the test specimen under the bidirectional X and Y ground motions are given in Fig. 13 (e) and (f). The β factors in the X direction were almost the same as those measured under the unidirectional ground motions.

3.3 Displacement response

The peak inter-story drift responses of the test specimen in different tests are shown in Fig. 14. Peak inter-story drift ratio of 0.85% was recorded under the Kobe earthquake with the measured input PGA of 0.75g, indicating sufficient lateral capacity to resist high seismic loads. Generally, the peak inter-story drift response was observed at the 2^{nd} story meaning the 2^{nd} storey could be more flexible than the other stories. Fig. 14 (a) - (d) presents the inter-story drift ratios under the unidirectional seismic excitations with different seismic hazard levels. After the reinforcement of the specimen (i.e. Test 12), the peak inter-story drift ratios of the 1^{st} and 2^{nd} stories slightly decreased, while the peak inter-storey drift ratios of the 3^{rd} and 4^{th} stories did not change much. The peak inter-story drift ratios under bidirectional seismic excitations are shown in Fig. 14 (e) and (f). It was found that the peak inter-story drift ratios in the X direction had almost the same values with those under unidirectional seismic excitation. The maximum lateral displacements for each story under different earthquake levels are summarized in Table 6. As examples, the time history response of the roof displacement under El-centro earthquake (PGA = 0.80g) and Kobe earthquake (PGA = 0.75g) are shown in Fig. 15.

3.4 Load sharing between the timber infill walls and the steel moment frames

The total shear force carried by all the timber shear walls and the shear force for each story can be calculated by Eq (1) through Eq. (3). According to Fig. 14 (d), the maximum inter-story drift was obtained at the 2nd story under the Kobe earthquake with PGA of 0.75g. The corresponding time-history responses of the shear force carried by the 2nd story infill timber walls and the time-history response of the total shear force carried by the hybrid system at the 2nd story are given in Fig. 16. To quantify the contribution of the timber shear walls, R is defined to evaluate the proportion of the inter-story shear force resisted by the infill walls at each story. For the k^{th} story, R can be calculated by Eq. (4):

$$R=(R^{+}+R^{-})/2 \tag{4}$$

$$R^{+}=\sum Q_k^{w,peak+} / Q_k^{peak+} \times 100\% \tag{5}$$

$$R^{-}=\left|\sum Q_k^{w,peak-}\right| / \left|Q_k^{peak-}\right| \times 100\% \tag{6}$$

where R^{+} is the shear force ratio at positive peak inter-story shear force and R^{-} is the shear force ratio at negative peak inter-story shear force, $\sum Q_k^{w,peak+}$ and $\sum Q_k^{w,peak-}$ are the positive and negative peak shear forces in the timber shear walls at the k^{th} story, Q_k^{peak+} and Q_k^{peak-} are the positive and negative peak inter-story shear forces at the k^{th} story.

As shown in Fig. 16, the negative peak shear force in the timber shear walls was -186.48kN and the negative peak inter-story shear force was -391.08kN. The positive peak shear force in the timber walls was 149.3 kN and the positive peak inter-storey shear force was 346.71 kN. Accordingly, R^- and R^+ can be determined as 47.7% and 43.1%, respectively. Thus, R is calculated as 45.4%, the average of R^+ and R^-.

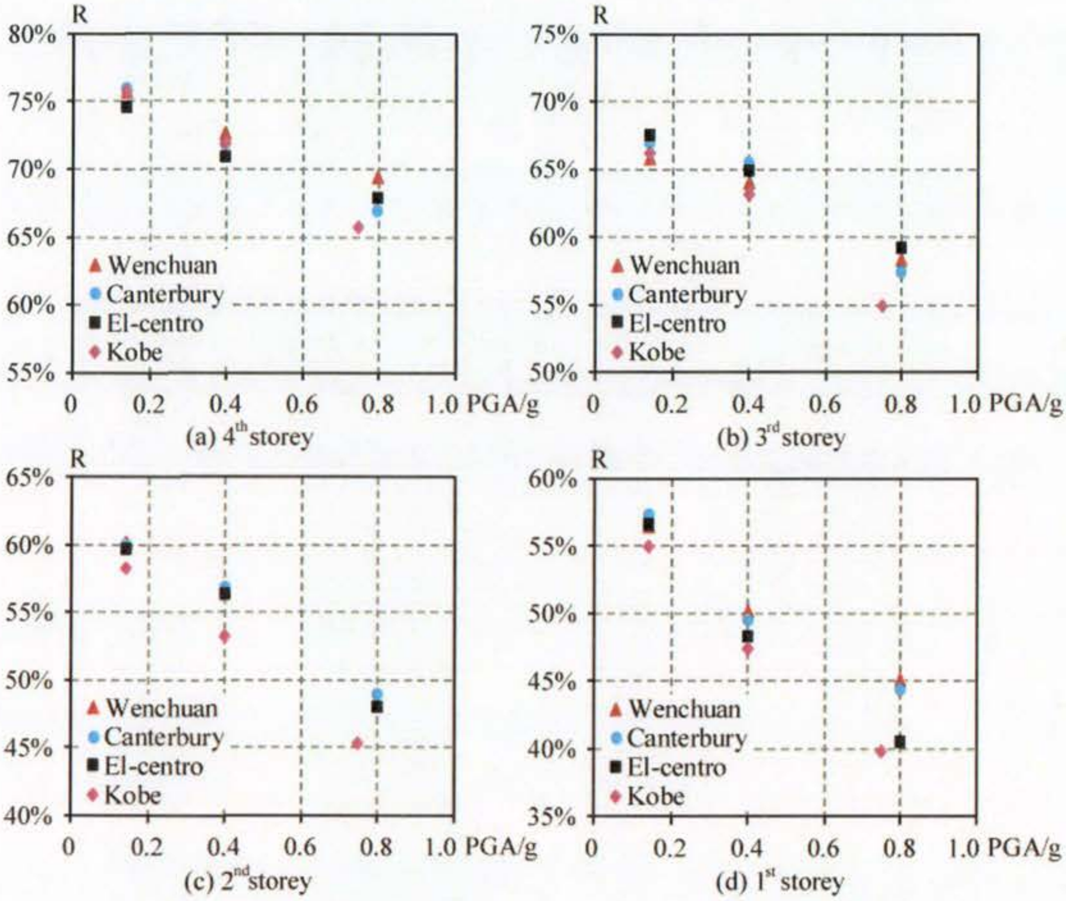

Fig. 17 shows the R values under different ground motion shaking and intensities. The R values varied between 55.1% and 75.9% under minor earthquakes, and between 47.5% and 72.6% under moderate earthquakes. The minimum R value for the 1st story is 39.9% under the Kobe earthquake with PGA of 0.75g. The inter-story shear forces increased from top story to bottom story, and the R values decreased. For each story, the R values had an approximately linear decrease with the increase of the seismic intensity. It should be noted that the R values for the 1st story dropped the most rapidly. The results indicated that the infill timber shear walls were able to resist significant proportion of the shear force in the hybrid structure, and the stiffness of the timber shear walls degraded with the increase of the earthquake induced shear force.

3.5 Damage inspection

The timber-steel hybrid structure had excellent performance under a series of seismic excitations scaled to different intensity levels, with PGA ranging from 0.14g to 0.80g. The damage to the test specimen was not significant. And there was no visible damage to the steel frames and the steel-timber interface connections, while a number of nailed connection failures between OSB sheathing and the timber framing members in the timber shear walls were observed. Due to the narrow gap between adjacent OSB sheathing panels, one panel corner was crushed under the seismic excitations with the PGA of 0.40g, as shown in Fig. 18(a). With the PGA of the seismic excitation increased to 0.80g, more nailed connection failures were observed. Nail withdrawal was the most typical connection failure mode, as shown in Fig. 18 (b) and (c). In general, 2 mm to 5 mm nail withdrawal was observed on the edges of the sheathing panels, and the maximum length of nail withdrawal was 10 mm. In addition, the nailed connections along the edge of the sheathing panels were damaged by the nail head pull-through, local crushing and flake debonding, as shown in Fig. 18 (d), Fig. 18 (e), and Fig. 18 (f), respectively. Almost all the sheathing failures occurred when the PGA of the seismic excitations exceeded 0.4g, and most of them located at the 2nd and the 3rd stories, which had larger inter-story drifts compared to the 1st and the 4th stories.

4. Conclusions

A series of shake table tests on a 2/3-scaled timber-steel hybrid structure were conducted. The hybrid structure performed excellently with the peak inter-story drift of 0.85 % under major earthquakes. Limited structural damage was observed on the infill timber shear wall and the steel moment frames remained intact. According to the test results, the following conclusions can be drawn:

(1) The fundamental frequency decreased by 11% throughout the shake table tests with the PGA of 0.80g. The fundamental frequency increased by 6% after strengthening of the infill timber shear walls was applied. It was found that no significant stiffness degradation occurred under the minor and moderate earthquakes.

(2) Desirable seismic performance of the timber-steel hybrid structure was confirmed. The maximum inter-story drift was 0.85% and the maximum roof displacement was 57.13 mm under the major earthquakes.

(3) The structural was limited to the infill timber shear walls. The steel frames remained intact and the steel-timber interface connections were confirmed to be reliable. Nailed sheathing-timber connection failure was the main damage mode. The damage level and the quantity of the failed nailed connections were closely related to the magnitude of the inter-story drift.

(4) The seismic responses of the specimen under bidirectional excitations showed no significant difference compared with those under unidirectional excitations, which indicates that there was little torsional effect on the specimen due to the symmetrical layout and even distribution of the seismic mass.

(5) Peak shear force ratio R was defined to evaluate the proportion of the inter-story shear force resisted by the timber shear walls. The minimum R value is 39.9% under major earthquakes, indicating that the infill timber shear walls contributed significantly to the lateral resistance of the hybrid structure. However, due to stiffness degradation, the proportion of shear resistance provided by the infill walls decreased with the increase of the seismic intensity.

Acknowledgment

The authors gratefully acknowledge the National Natural Science Foundation of China for supporting this work with a research grant (Grant No. 51378382) and Earthquake Commission of New Zealand with a biennial grant.

References

[1] Green M, Karsh J E. The case for tall wood buildings. In: Canadian Wood Council on behalf of the Wood Enterprise Coalition by Forestry Innovation Investment, North Vancouver, BC, Canada; 2012.

[2] Lennon T, Bullock M J, Enjily V. The fire resistance of medium-rise timber frame buildings. In: World Conference on Timber Engineering; 2000.

[3] Ellis B R, Bougard A J. Dynamic testing and stiffness evaluation of a six-story timber framed building during construction. Eng Struct 2001; 23(10):1232-1242.

[4] Sakamoto I, Okada H, Kawai N, et al. A research and development project on hybrid timber building structures. In: IABSE Symposium Report. International Association for Bridge and Structural Engineering 2001; 85(7): 1-6.

[5] Isoda H, Kawai N, Koshihara M, et al. Timber - reinforced concrete core hybrid system: shake table experimental test. J Struct Eng 2016; 04016152.

[6] Sakamoto I. Final report of a research and development project on timber-based hybrid building structures. In: Proceedings of 8th World Conference on Timber Engineering 2004; 2: 53-64.

[7] Ceccotti A, Follesa M, Lauriola M P, et al. Sofie project–test results on the lateral resistance of cross-laminated wooden panels. In: Proceedings of the First European

Conference on Earthquake Engineering and Seismicity, 2006, 3.

[8] Gavric I, Fragiacomo M, Ceccotti A. Strength and deformation characteristics of typical X-lam connections. In: Proceedings of WCTE, 2012.

[9] Gavric I, Fragiacomo M, Ceccotti A. Cyclic behavior of CLT wall systems: experimental tests and analytical prediction models. J Struct Eng 2015; 141(11):04015034.

[10]Ceccotti A. New technologies for construction of medium-rise buildings in seismic regions: the XLAM case. Struct Eng Int 2008; 18(2):156-165.

[11]Ceccotti A, Sandhaas C, Okabe M, et al. SOFIE project - 3D shaking table test on a seven-story full-scale cross-laminated timber building. Earthq Eng Struct Dyn 2013; 42(13):2003-2021.

[12]Ceccotti A, Follesa M. Seismic behaviour of multi-story X-lam buildings. In: Proc. International Workshop on" Earthquake Engineering on Timber Structures" Coimbra, Portugal; 2006.

[13]Rinaldin G, Fragiacomo M. Non-linear simulation of shaking-table tests on 3- and 7-story X-Lam timber buildings. Eng Struct 2016; 113:133-148.

[14]Lindt J W V D, Pei S, Pryor S E. Construction and experimental seismic performance of a full-scale six-story light-frame wood building. Procedia Engineering 2011; 14:1599-1605.

[15]Lindt J W V D, Pei S, Pryor S E, et al. Experimental seismic response of a full-scale six-story wood apartment building. In: 11th World Conference on Timber Engineering 2010, WCTE 2010 2010; 4: 3158-3165.

[16]Filiatrault A, Christovasilis I P, Wanitkorkul A, et al. Experimental seismic response of a full-Scale light-frame wood building. J Struct Eng 2009; 136(10):1262-1272.

[17]Lindt J W V D, Pryor S E, Pei S. Shake table testing of a full-scale seven-story steel-wood apartment building. Eng Struct 2011; 33(3):757-766.

[18]Dickof C, Stiemer S F, Tesfamariam S. Wood-steel hybrid seismic force resisting systems: Seismic ductility. In: proceedings of the 12th World Conference for Timber Engineering, Auckland, New Zealand; 2012.

[19]Dickof C, Stiemer S F, Bezabeh M A, et al. CLT–steel hybrid system: ductility and overstrength values based on static pushover analysis. J Perform Constr Facil 2014; 28(6):A4014012.

[20]Schneider J. Connections in cross-laminated-timber shear walls considering the behaviour under monotonic and cyclic lateral loading. MASc Thesis, University of Stuttgart, Germany; 2009.

[21]Bezabeh M A, Tesfamariam S, Stiemer S F. Equivalent viscous damping for steel moment-resisting frames with cross-laminated timber infill walls. J Struct Eng 2015; 142(1): 04015080.

[22]Tesfamariam S, Stiemer S F, Bezabeh M, et al. Force based design guideline for timber-steel hybrid structures: steel moment resisting frames with CLT infill walls. Technical Report, University of British Columbia, Canada, 2016.

[23]Bezabeh M A, Tesfamariam S, Stiemer S F, et al. Direct displacement-based design of a novel hybrid structure: steel moment-resisting frames with

cross-laminated timber infill walls. Earthq Spectra 2016; 32(3): 1565-1585.

[24]He M, Li Z, Lam F, Ma R, Ma Z. Experimental investigation on lateral performance of timber-steel hybrid shear wall systems. J Struct Eng ASCE 2014; 140(6): 04014029-1-12.

[25]Li Z, He M, Ma Z, Wang K, Ma R. In-plane behavior of timber-steel hybrid floor diaphragms: experimental testing and numerical simulation. J Struct Eng ASCE 2016; 142(12): 04016119-1-14.

[26]Li Z, He M, Lam F, Li M, Ma R, Ma Z. Finite element modeling and parametric analysis of timber-steel hybrid structures. Struct Des Tall Spec 2014; 23(14): 1045-1063.

[27]Li Z, He M, Lam F, Li M. Load-sharing mechanism in timber-steel hybrid shear wall systems. Front Struct Civ Eng 2015; 9(2): 203-214.

[28]Li, Z, He M, Li, Li M, Lam, F. Damage assessment and performance-based seismic design of timber-steel hybrid shear wall systems. Earthq Struct 2014; 7(1): 101-117.

[29]Ministry of Housing and Urban-Rural Development of the People's Republic of China. GB 50009 – 2012 Load code for the design of building structures. Architecture & Building Press, Beijing, China; 2012 [English version].

[30]Ministry of Housing and Urban-Rural Development of the People's Republic of China. GB 50011-2010 Code for seismic design of buildings. Architecture & Building Press, Beijing, China; 2010 [English version].

[31]National Lumber Grading Authority (NLGA). Standard grading rules for Canadian lumber. 2014; Vancouver, Canada.

[32]Ministry of Construction of the People's Republic of China. GB 50017-2003 Code for design of steel structures. China Planning Press, Beijing, China; 2003 [English version].

List of Tables

Table 1 Loads used for structural design

Load Type	Location	Unit	Value
Dead Load	Floor	kN/m^2	1.9
	Roof	kN/m^2	1.8
	Outer wood wall	kN/m	1.9
	Inner wood wall	kN/m	1.8
Live Load	Office room	kN/m^2	2.0
	Corridor	kN/m^2	2.5
	Roof	kN/m^2	0.5
	Snow	kN/m^2	0.5

Table 2 similitude scale factors

Parameter	Relation	Scaling factor
Length	S_l	2/3
Linear displacement	$S_\delta = S_l$	2/3
Angular displacement	$S_\varphi = S_\sigma / S_E$	1
Strain	$S_\varepsilon = S_\sigma / S_E$	1
MOE	$S_E = S_\sigma$	1
Stress	S_σ	1
Poisson's ratio	S_υ	1
Mass density	$S_\rho = S_\sigma / (S_a \cdot S_l)$	0.75
Mass	$S_m = S_\sigma \cdot S_l^2 / S_a$	0.2222
Force	$S_F = S_\sigma \cdot S_l^2$	0.4444
Linear load	$S_q = S_\sigma \cdot S_l$	0.6667
Area load	$S_p = S_\sigma$	1
Moment	$S_M = S_\sigma \cdot S_l^3$	0.2963
Damping	$S_c = S_\sigma \cdot S_l^{1.5} \cdot S_a^{-0.5}$	0.3849
Period	$S_T = S_l^{0.5} \cdot S_a^{-0.5}$	0.5774
Frequency	$S_f = S_l^{-0.5} \cdot S_a^{0.5}$	1.7321
Velocity	$S_v = (S_l \cdot S_a)^{0.5}$	1.1547
Acceleration	S_a	2

Table 3 Nail layouts for the timber shear walls

Direction	Story	Side with sheathing	Spacing/mm	
			edge	elsewhere
X	4	outside	125	250
	3	both sides	150	300
	2	both sides	200/100[1]	200
	1	both sides	150/75[1]	150
Y	4	both sides	150	300
	3	both sides	100	200
	2	both sides	75	150
	1	both sides	75	150

1. The nail spacing of timber shear wall before/after strengthened.

Table 4 Sections of steel frame members*

Story No.	Member	Direction	Section
1-3	Column	-	H-150×150×7×10
	Beam	X	H-125×125×6.5×9
		Y	H-125×125×6.5×9
4	Column	-	H-125×125×6.5×9
	Beam	X	H-125×125×6.5×9
		Y	H-100×100×6×8

*Note: The members are all hot rolled H-section steel members. H-$a\times b\times c\times d$ indicates the section has a height of a and a width of b. The web thickness is c, and the flange thickness is d. (all dimensions are in millimeter)

Table 5 Test program

Sequence	Record	PGA(g)		Sequence	Record	PGA(g)	
		X	Y			X	Y
1	White noise	0.07		21	White noise	0.07	
2	White noise		0.07	22	White noise		0.07
3	Wenchuan	0.14		23	Wenchuan	0.4	
4	Canterbury	0.14		24	Canterbury	0.4	
5	El Centro	0.14		25	El Centro	0.4	
6	KOBE	0.14		26	El Centro	0.4	0.17
7	White noise	0.07		27	KOBE	0.4	
8	Wenchuan	0.4		28	KOBE	0.4	0.17
9	Canterbury	0.4		29	White noise	0.07	
10	El Centro	0.4		30	White noise		0.07
11	KOBE	0.4		31	Wenchuan	0.8	
12[1]	White noise	0.07		32	White noise		
13	White noise	0.07		33	Canterbury	0.8	
14	White noise		0.07	34	White noise	0.07	
15	Wenchuan	0.14		35	El Centro	0.8	
16	Canterbury	0.14		36	White noise	0.07	
17	El Centro	0.14		37	KOBE	0.8[2]	
18	El Centro	0.14	0.0595	38	White noise	0.07	
19	KOBE	0.14		39	KOBE	0.75[2]	
20	KOBE	0.14	0.0595	40	White noise	0.07	

1. The timber shear wall in story 1-2 of X direction was strengthened before sequence 13

2. The PGA of the Kobe earthquake on sequence 39 was scaled down because the overturning moment of the specimen on sequence 37 exceeded the limitation of the shake table

Table 6 Maximum story displacements

Sequence	Record	PGA(g)		Displacement/mm				
		X	Y		4	3	2	1
3	Wenchuan	0.14			6.273	5.297	3.876	1.872
4	Canterbury	0.14			7.969	6.919	4.934	2.462
5	El Centro	0.14			9.566	8.126	5.775	2.883
6	KOBE	0.14			7.999	6.772	5.085	2.397
8	Wenchuan	0.40			16.204	13.539	9.626	4.502
9	Canterbury	0.40			25.183	21.428	15.866	7.423
10	El Centro	0.40			27.034	23.235	17.435	8.540
11	KOBE	0.40			26.848	23.030	16.644	7.934
15[1]	Wenchuan	0.14			6.729	5.532	3.769	1.679
16	Canterbury	0.14			8.412	7.225	4.821	2.206
17	El Centro	0.14			8.725	7.384	4.842	2.419
18	El Centro	0.14	0.06	X:	8.370	7.088	4.780	2.355
				Y:	3.229	2.636	2.224	1.113
19	KOBE	0.14			8.528	7.258	5.225	2.253
20	KOBE	0.14	0.06	X:	9.042	7.682	5.594	2.362
				Y:	2.538	2.039	1.598	0.867
23	Wenchuan	0.40			17.213	13.936	9.191	4.149
24	Canterbury	0.40			23.406	19.453	13.728	6.271
25	El Centro	0.40			24.321	20.571	14.975	7.338
26	El Centro	0.40	0.17	X:	24.266	20.564	15.234	7.478
				Y:	9.736	8.677	6.954	3.619
27	KOBE	0.40			20.636	17.112	12.343	5.686
28	KOBE	0.40	0.17	X:	21.432	17.588	12.860	6.002
				Y:	7.586	6.224	5.038	2.842
31	Wenchuan	0.80			25.321	20.509	13.085	5.599
33	Canterbury	0.80			42.151	34.565	23.865	10.765
35	El Centro	0.80			50.560	41.566	28.458	12.711
39	KOBE	0.75			57.130	47.843	32.626	13.954

1. The timber shear wall in story 1-2 of X direction was strengthened before sequence 13

List of Figures:

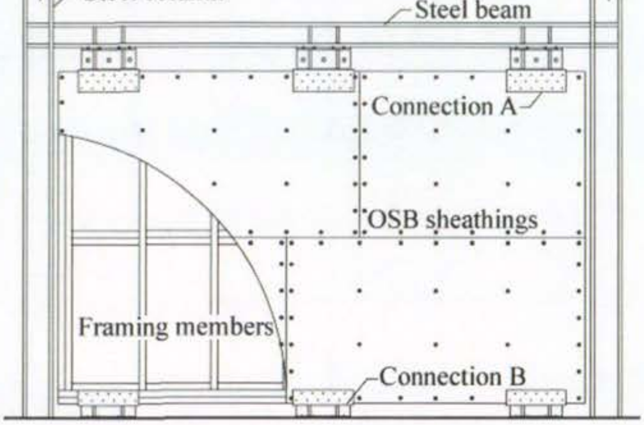

Fig. 1 Steel frame infilled with conventional light-wood frame timber shear wall

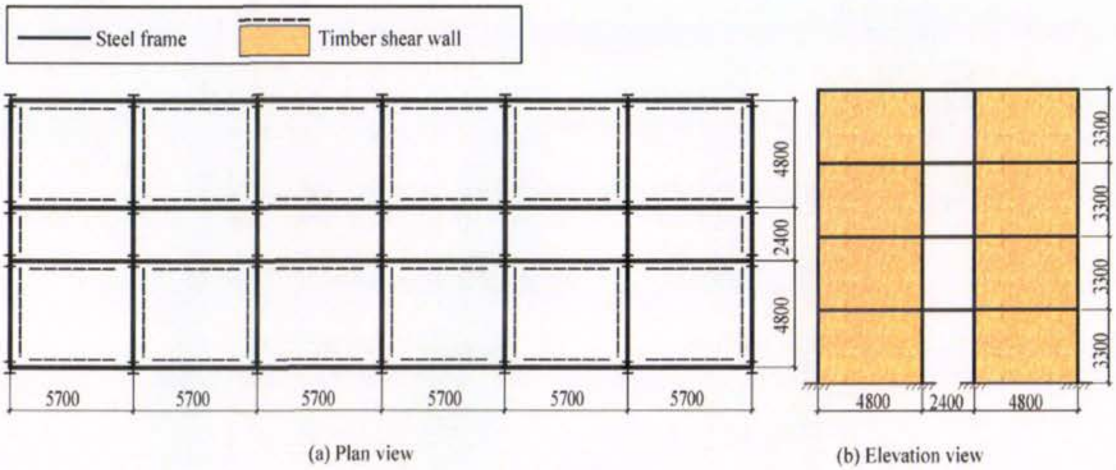

Fig. 2 Plan view and elevation of the prototype building (all dimension are in millimeter)

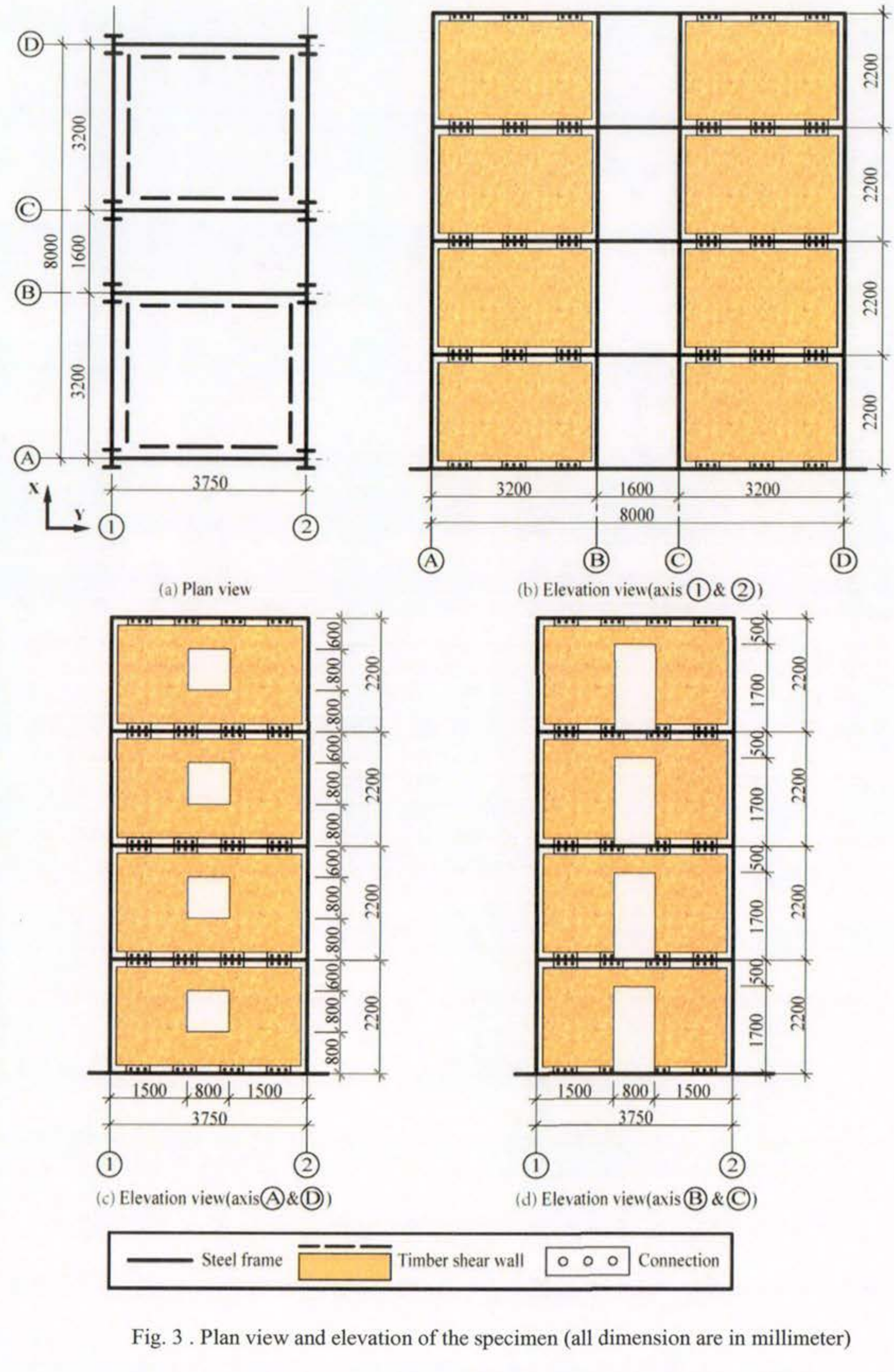

Fig. 3 . Plan view and elevation of the specimen (all dimension are in millimeter)

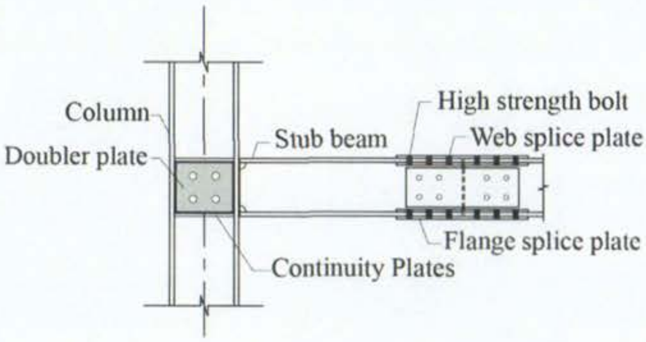

Fig. 4. Bolted spliced joint and panel zone configuration

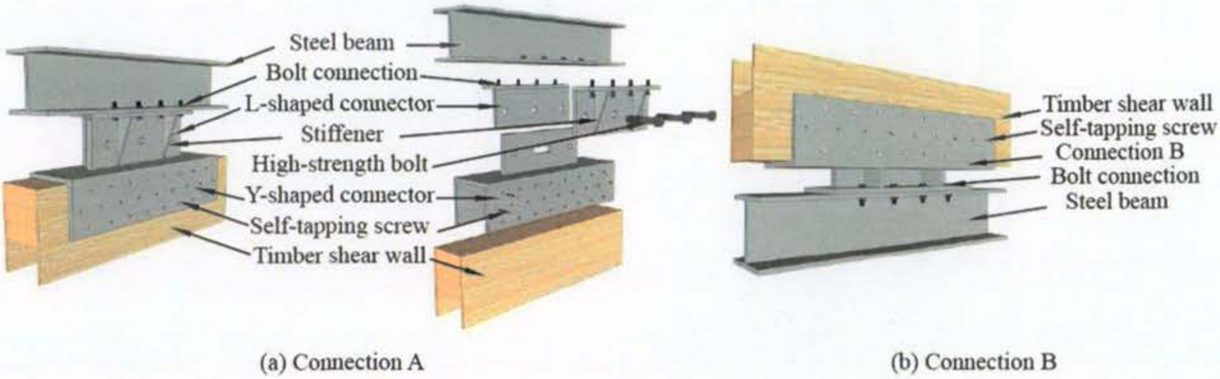

Fig. 5. Frame-wall connections

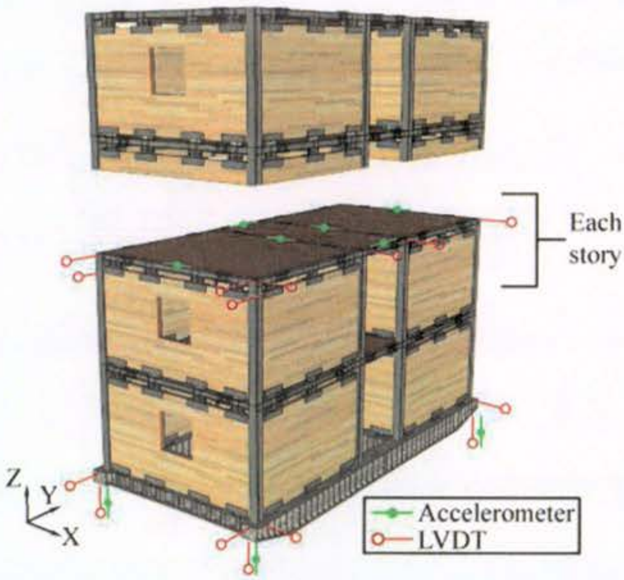

Fig. 6 Arrangement of sensors

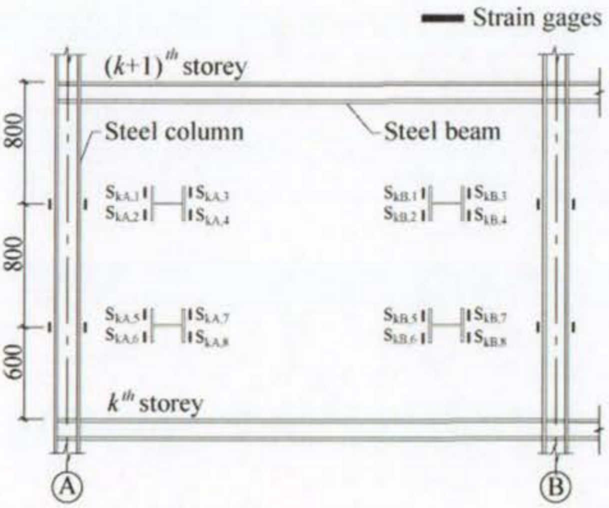

Fig. 7 Arrangement of strain gages

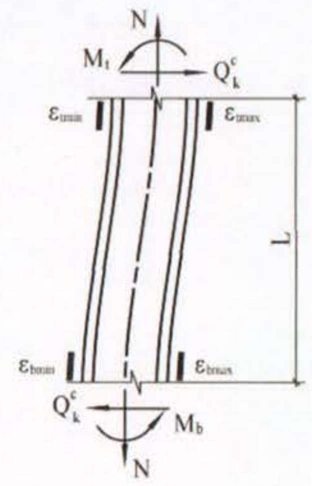

Fig. 8 The method of calculating the shear force in each steel column

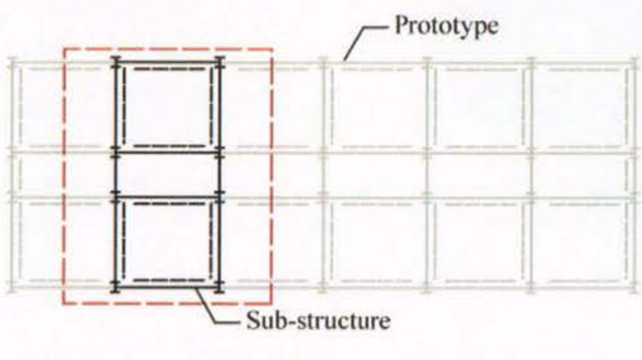

Fig. 9 Tributary area of the sub-structure

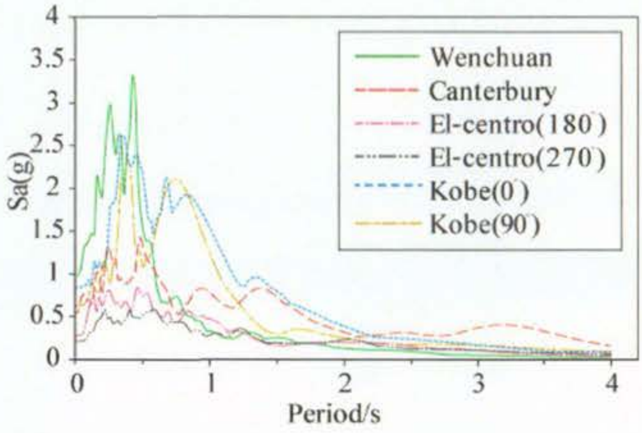

Fig. 10. Unscaled spectral acceleration of the ground motions

Fig. 11. Test specimen

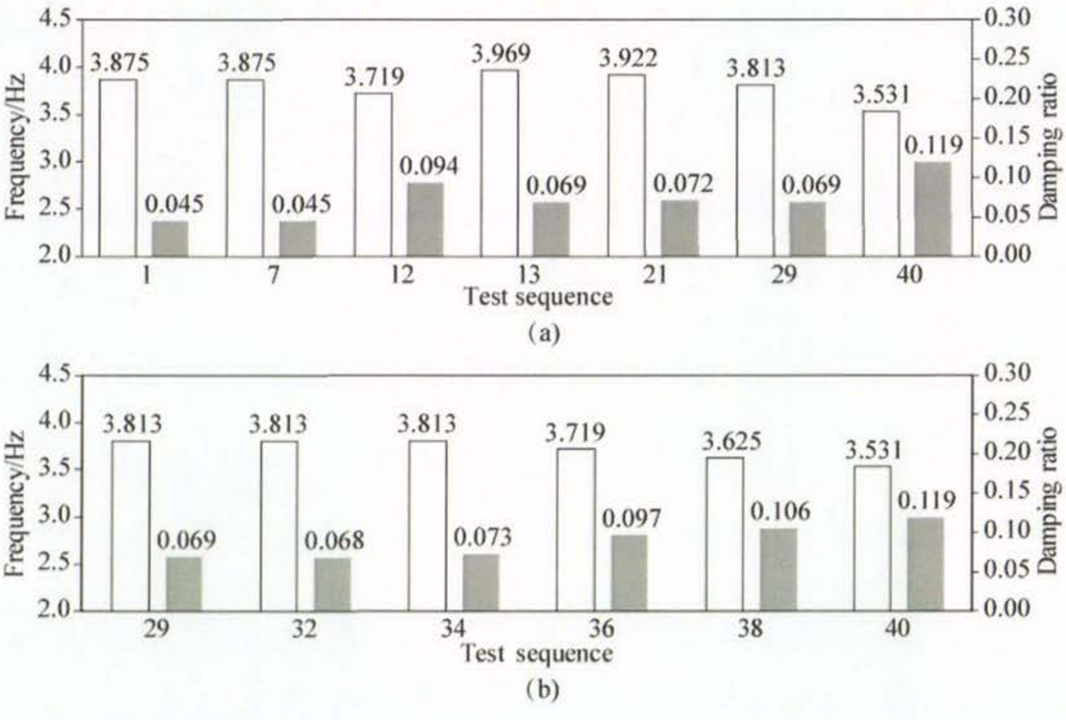

Fig. 12. Fundamental frequency and damping ratio in the X direction

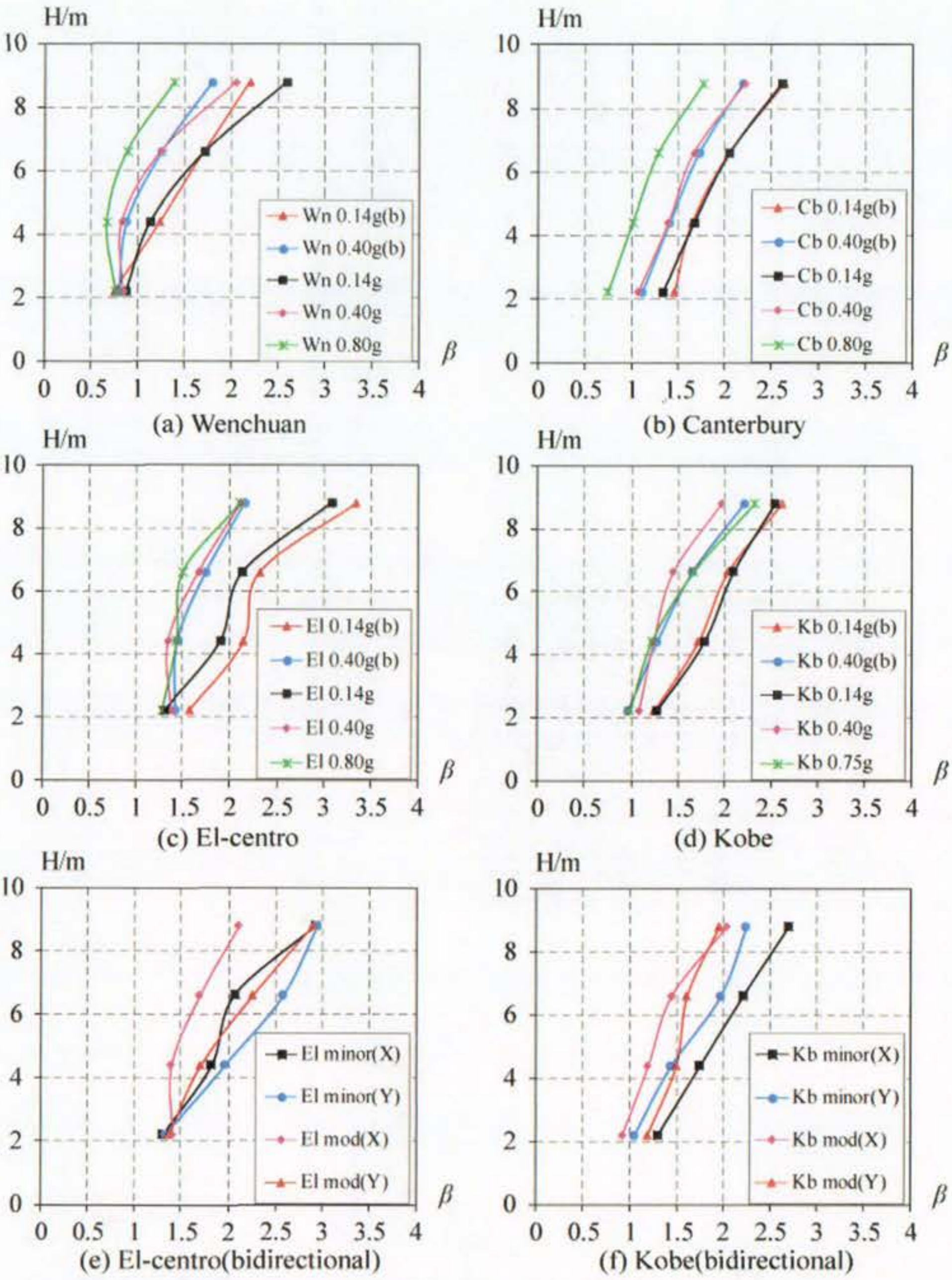

Note: "b" in the legend indicates the seismic excitations were conducted before the specimen was strenghened

Fig. 13. Acceleration amplification factors

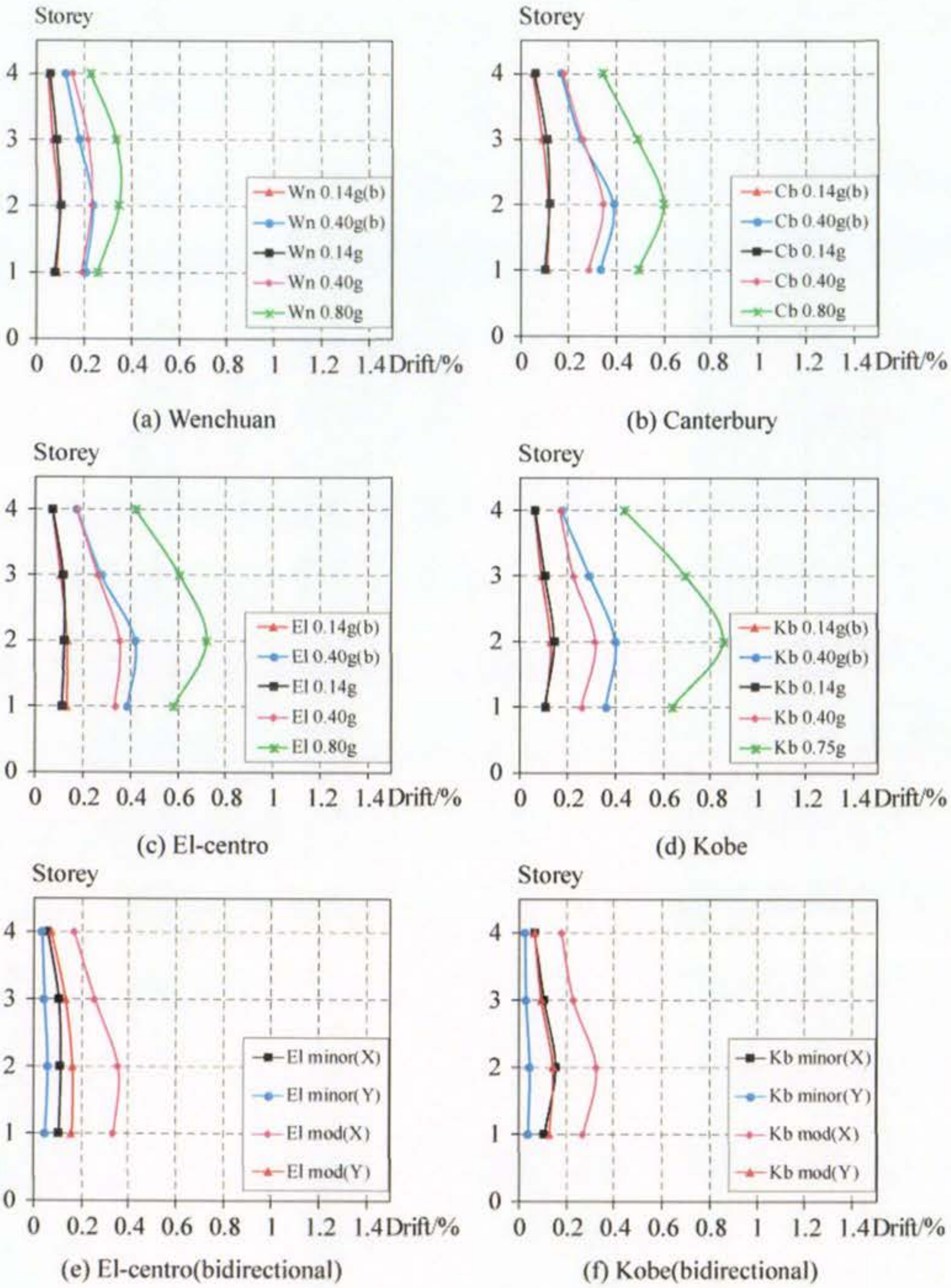

Note: "b" in the legend indicates the seismic excitations were conducted before the specimen was strenghened

Fig. 14. Inter-story drift responses

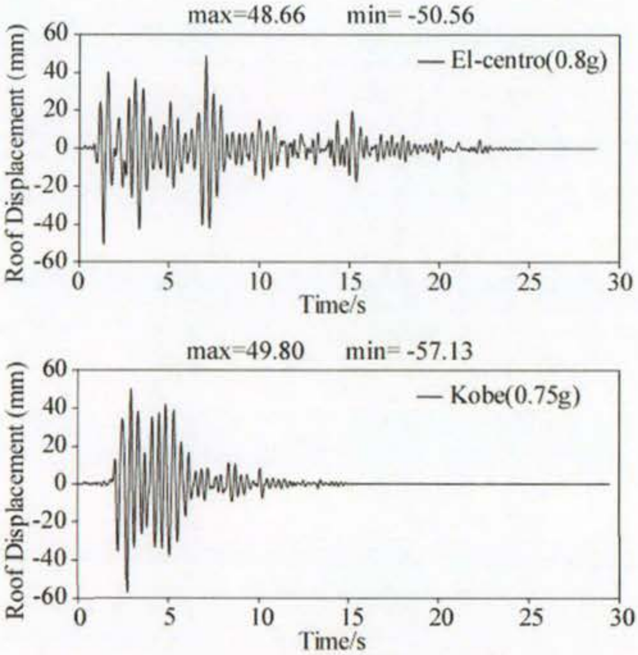

Fig. 15. Roof displacement time history curve

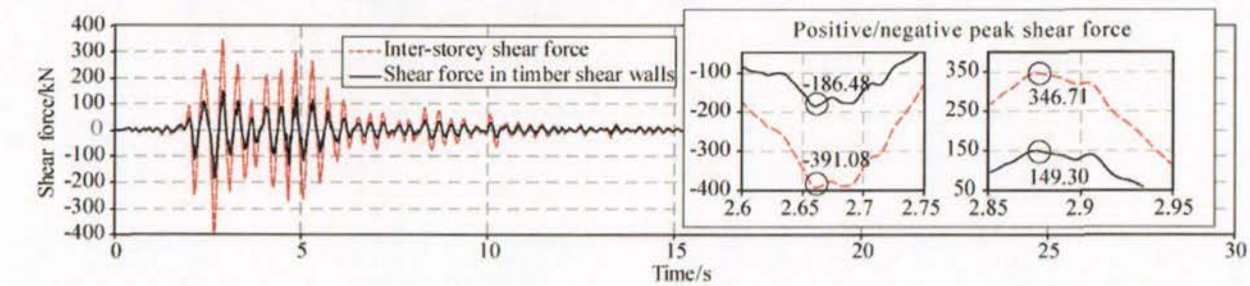

Fig. 16 Shear force in timber shear wall and inter-story shear force

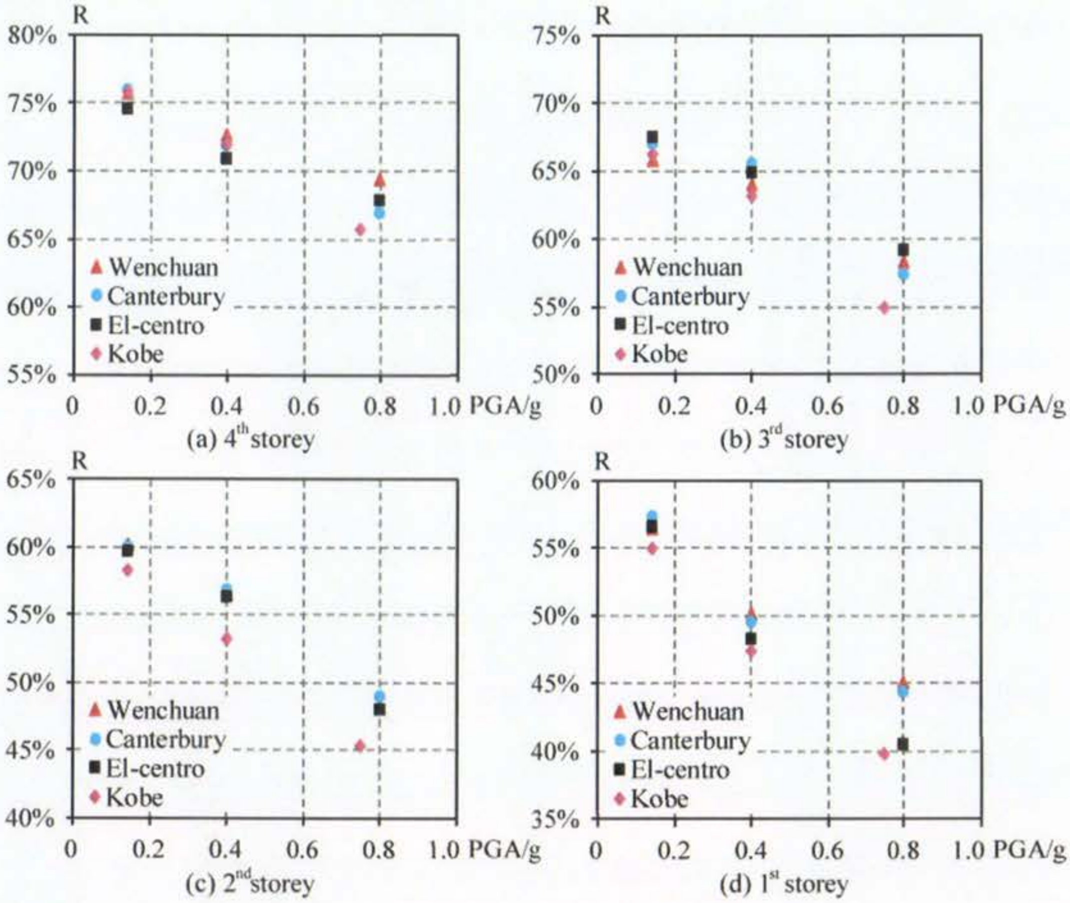

Fig. 17 Peak shear force ratio

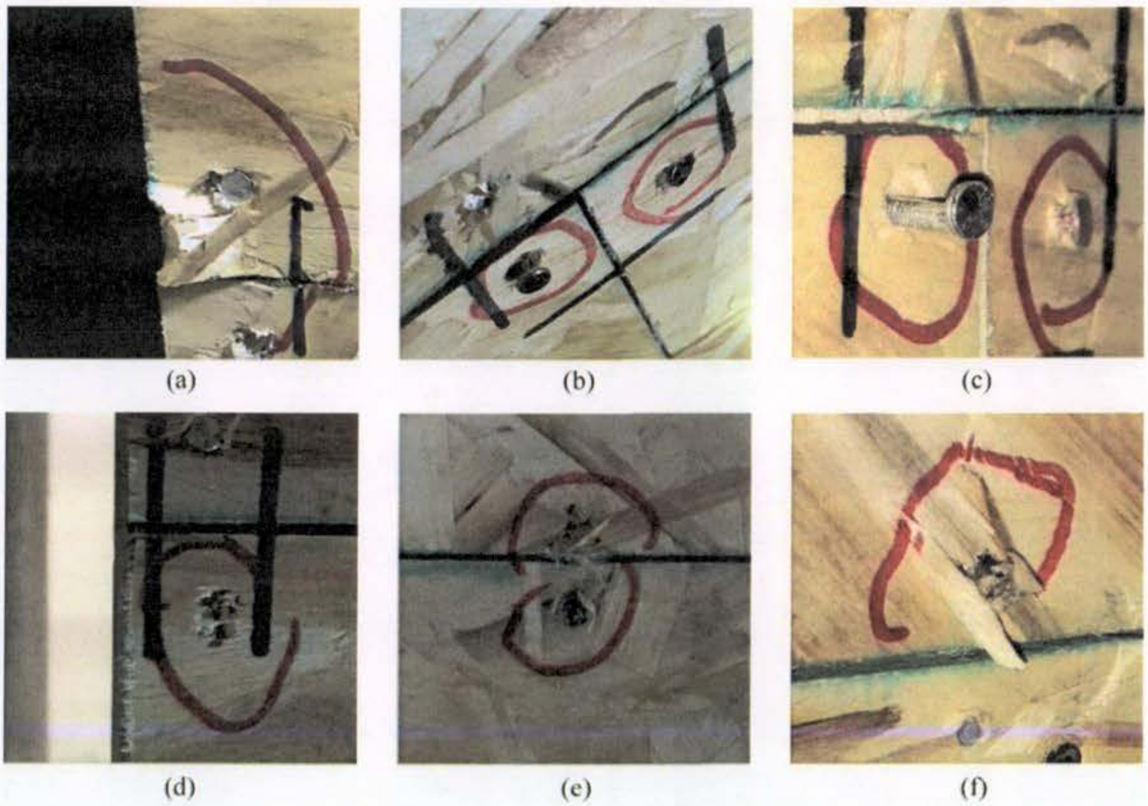

Fig. 18. Typical failures in the timber shear wall

The Press, Christchurch
19 Apr 2017, by Jamie Small

General News, page 7 - 508.00 cm²
Metro - circulation 61,573 (MTWTF--)

ID 760072628 BRIEF EQC(W) INDEX 1

Cheap, quake-safe building tested

JAMIE SMALL

Canterbury University structural timber engineer Dr Minghao Li wants to find cheaper ways to build earthquake-resistant buildings.

His team, including researchers from Tongji University in China, built a replica of a four-storey building out of cheap materials and shook it to see what would happen.

With the help of a $67,000 grant from the Earthquake Commission (EQC) and funding from the Natural Science Foundation of China, Li oversaw the construction of the 8.8 metre building on a "shake table" in Shanghai, China. "Each storey is 2.2m tall. I would say it's two-thirds [of a real building]," Li said.

Constructing large buildings to be earthquake-resistant is expensive – structures often use imported high-grade steel and engineered timber framing. The costs are a barrier to construction for developers looking to make a margin on sales or rental when the building is complete.

Li is using materials readily available in New Zealand - a "hybrid system" of commonly-used steel framing and light structural timber. "The whole idea is to try to combine timber and steel to try and make a stronger system which is able to resist large earthquakes, to try to minimise the damage for mainly multi-storey buildings, mainly for residential applications."

The shake table simulated several earthquakes, including one with ground acceleration 1.4 times stronger than what was detected in the Christchurch Botanic Gardens during the February 2011 earthquake.

Li said the results were promising. "We observed a very small amount of minor damage. So it definitely performed better than a timber-only solution."

He said he hoped cheap hybrid systems could be used soon, but the work was "still in the research stage". "They are not that popular at the moment, because our building standards have not incorporated these type of systems yet."

Case studies would be needed to determine how much money could be saved using hybrid systems, Li said.

"We're confident that it definitely will be much cheaper than using other engineered timber products."

Research at the university to test structural connections and the design of the hybrid concept is ongoing.

"The aim of our project is to feed the findings and outcomes of our research into ongoing and future earthquake strengthening design and builds in New Zealand, to improve building resilience, and keep people safe," Li said.

The research is one of 15 projects that received $1 million in funding from EQC's 2016 Biennial Grants Programme.

The programme is designed to build knowledge about New Zealand's natural disasters. Applications for the 2018 programme open later this month.

"It definitely performed better than a timber-only solution."

Dr Minghao Li

The Press, Christchurch
19 Apr 2017, by Jamie Small

General News, page 7 - 508.00 cm²
Metro - circulation 61,573 (MTWTF--)

ID 760072628 BRIEF EQC(W) INDEX 1

Canterbury University structural timber engineer Dr Minghao Li is working on cheaper hybrid systems of building.

PHOTO: GEORGE HEARD/FAIRFAX NZ